THE APPLICATION OF A FREEZING-SUBSTITUTION METHOD OF FIXATION TO TISSUE CULTURE PREPARATIONS [1]

ARLINE D. DEITCH AND GABRIEL C. GODMAN
Department of Surgery, College of Physicians and Surgeons, Columbia University, New York

SIXTEEN FIGURES

INTRODUCTION

The use of double coverslip preparations for the culture of differentiated tissues has been expanded in recent years by Murray and co-workers (Murray, '51; Pogogeff and Murray, '46; Peterson and Murray, '55). Because of their accessibility to microscopic examination and photography during *in vitro* life and because of their ready availability to fixation and subsequent treatments, such preparations are extremely favorable material for combined cytological and cytochemical researches. In any such study, the initial cytochemical problem concerns the choice of a fixative. The ideal fixative would be one which preserves the cytological details of the cell without inducing visible artefact, while at the same time retaining its important chemical constituents in amounts and distribution comparable to those occurring in the living state. Furthermore, these components should be fixed in such fashion that they can react readily with cytochemical reagents and also be readily extracted chemically and digested enzymatically. The fixative procedure most nearly meeting these requirements is freeze-drying by the Altman-Gersh procedures. However, these procedures as a rule require elaborate and

[1] This investigation was supported in part by a grant from the Jane Coffin Childs Fund for Medical Research and in part by research grant B-105C from the National Institute of Neurological Diseases and Blindness, U. S. Public Health Service.

THE ANATOMICAL RECORD, VOL. 123, NO. 1
SEPTEMBER 1955

relatively costly equipment and need frequent attention by the operator. Because of these factors they have not come into routine cytochemical use. Freeze-drying in a conventional apparatus is particularly ill-suited to tissue culture preparations since only one or two coverslip cultures can be processed at a time.

The use of a variant of the freeze-drying technique has recently been explored by several workers (Lison, '49; Blank et al., '51; Taft, '51; Baud, '52; Bell, '52; Freed, '55; Woods and Pollister, '55). This procedure, mentioned first in a paper by Simpson ('41), is termed freeze-substitution and has been demonstrated to yield results closely comparable to those obtained in the best freeze-drying techniques without entailing expensive or elaborate equipment and without excessive attention from the operator. In this procedure, as in conventional freeze-drying, the tissues are quenched (frozen) with isopentane chilled with liquid nitrogen (Hoerr, '36). Instead of a subsequent *in vacuo* evaporation of water at temperatures of — 30°C. or below, the tissues are dehydrated by being placed in an absolute ethanol bath at similar low temperatures. Under these conditions, water is dissolved from the tissue and is replaced by chilled alcohol. Woods and Pollister ('55) have shown that frozen-substituted cells resemble closely similar living cells, the only conspicuous change being a loss of certain refringent droplets, presumably neutral fat. It was felt that freezing-substitution offered an excellent answer to the difficulties inherent in the freezing-drying technique and could be adapted readily to the special needs of tissue culture preparations.

MATERIALS AND METHODS

1. Biological materials. Double coverslip lying-drop tissue culture preparations furnished the material for freezing-drying. Chick embryo heart, liver and skeletal muscle and spinal ganglion, new-born rat muscle and human tendon were planted on coverslips in mixtures of chicken plasma, human placental serum, ox-serum ultrafiltrate and 50% chick embryo extract.

In addition, chick embryo heart and skeletal muscle and newborn rat muscle were planted on coverslips in the above mixtures without plasma. The proportions of the planting and feeding mixtures were varied for the different tissues (Murray, '51). The coverslip cultures were washed in Simms X-7 balanced salt solution and fed with placental serum, ultrafiltrate and embryo extract two or three times a week. Cultures were grown for periods from 5 days to a month. Prior to freezing, they were washed for 15 minutes or less in Ringer-Locke solution.

2. Freezing. The apparatus needed for freezing the cultures was extremely simple (fig. 2). A small Dewar flask was used as the container for liquid nitrogen: Pint-sized, wide-mouthed vacuum flasks were found to be particularly suitable. A 60 cm^3 beaker containing isopentane (2-methyl butane, Eastman Organic Chemicals, practical grade) was clamped to a small ring stand and lowered gradually into the liquid nitrogen. To control the degree of chilling, the beaker was raised and lowered in the liquid nitrogen. The isopentane was maintained in a partly-frozen condition throughout the period of freezing the cultures, ensuring a freezing temperature of approximately —190°C. (Hoerr, '36). A Born section lifter with perforated nickel silver spoon (A. H. Thomas Company) was used to stir the isopentane vigorously just prior to quenching a culture. Each culture in turn was well drained of all excess moisture, picked up with a pair of cover glass forceps and dropped quickly into the isopentane where it was allowed to fall against the metal spoon. After 15 to 30 seconds, the spoon was raised, the culture removed with a pair of *cold* cover glass forceps and transferred very rapidly to the dehydrating chamber or to a storage bath.

3. Storage of frozen cultures. Although the frozen coverslip cultures might be transferred from the chilled isopentane directly to the dehydration chamber, it was found more convenient to accumulate them as they were frozen in a storage bath. This consisted of a Chen coverslip staining rack with room for 12 coverslips (A. H. Thomas Company) placed in

a beaker of absolute ethanol and chilled by a surrounding layer of powdered dry ice (fig. 2). The alcohol storage bath was maintained at a temperature of — 78°C. during the time in which all the cultures were washed, drained and frozen.

4. Dehydration. A diagram of the dehydration chamber and the surrounding cryostat is shown in figure 1. A Chen coverslip staining rack (D) rests in 150 ml of chilled absolute ethanol in the bottom of a 600 ml tall-form Pyrex beaker (dye pot) (C). The rack is wedged securely into position with two short pieces of Tygon plastic tubing to prevent tipping. The beaker is corked and a low-temperature thermometer extends down along the side of the coverslip rack. The lip of the Pyrex beaker rests on a cork ring (I), which in turn rests on the lip of a two-liter stainless steel beaker (B). The steel beaker contains a low-temperature regulating bath which is cooled by resting on a layer of dry-ice snow (E) contained in a 4-liter Dewar flask (A). The sides of the steel beaker are insulated with a ring of cotton batting wrapped in gauze (J). The width of the latter is adjusted to allow the steel beaker to slip down into the Dewar flask and maintain constant contact with the dry ice as the latter evaporates. Six inches of dry ice at the bottom of the Dewar flask were sufficient for a dehydrating run of 4 to 5 days.

When all the coverslip cultures were frozen, they were transferred very rapidly with *cold* forceps from the storage bath to the coverslip rack in the chilled 100% ethanol dehydrating bath. The top of the Pyrex beaker and the stainless steel beaker were then covered tightly with plastic film to prevent dilution of the alcohol baths by ice formed from moisture in the atmosphere.

The Dewar flask and its contents were placed on a slowly-rotating shaker which served to gently mix its fluid contents and prevent a pronounced temperature gradient in the dehydrating bath.[2] The shaker consisted of a low-speed motor ($3\frac{1}{2}$rev./min.) driving a wooden turntable (fig. 2). A low wood

[2] The use of the shaker apparatus was suggested by Mr. L. Moriber, Columbia University.

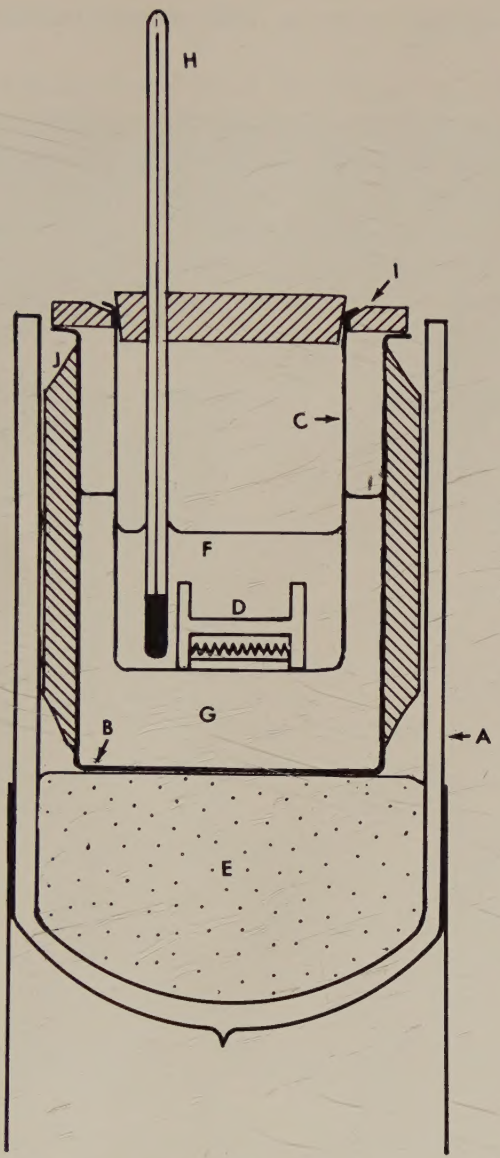

Fig. 1 Diagram of freeze-substitution apparatus for coverslip tissue-culture preparations: A 600 ml Pyrex beaker (C) rests on a cork ring (I) which in turn rests on the rim of a two-liter stainless steel beaker (B). The latter is covered with a layer of insulating material (J) and rests on a bed of dry ice snow (E) in the bottom of a 4-liter Dewar flask (A). The frozen coverslip cultures are placed in a Chen coverslip staining rack (D) in a bath of chilled absolute ethanol (F). A low temperature thermometer (H) projects down by the side of the coverslips. A bath of chilled ethyl oxalate or chilled 85% alcohol (G) is contained within the steel beaker.

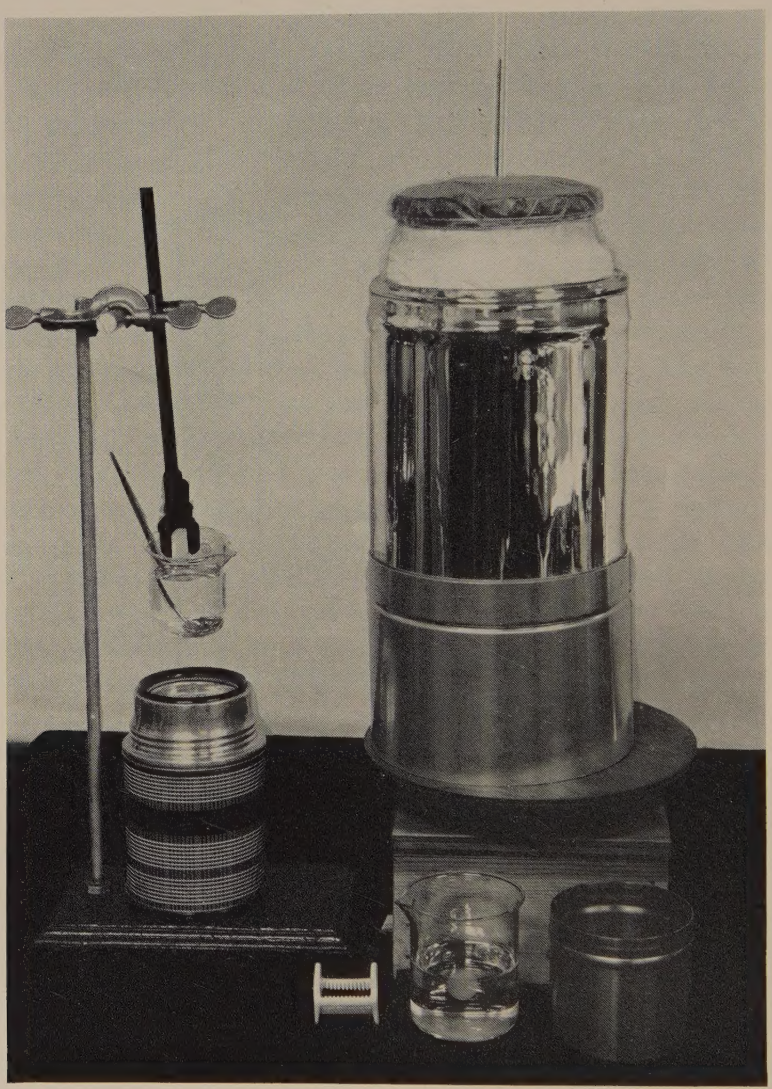

Fig. 2 The entire apparatus needed for freeze-substitution of coverslip cultures: To the left, the freezing assembly, to the right the dehydrating chamber and surrounding cryostat placed on the low-speed turntable shaker, and below, the components of the low-temperature storage bath.

strip was taped under the foot of the shaker and the Dewar flask was placed eccentrically on the turntable. As the turntable revolved, the Dewar flask was tilted to and fro. The Dewar flask and its contents were then left without further attention for the duration of a two to 4 day run.

In the earlier preparations, the low-temperature regulating bath in the cryostat consisted of ethyl oxalate (Mendelow and Hamilton, '50) which maintained this apparatus at temperatures between —30°C. and —40°C.[3] In later runs, lower dehydrating temperatures were achieved with mixtures of alcohol and water (Woods and Pollister, '55). A bath of 85% alcohol was used to maintain the apparatus between —40° and —50°C. No differences were detectable between cultures dehydrated for two or 4 days with the cryostat maintained between —40°C. and —54°C. and the shorter time was adopted in the later experiments. No attempts were made with still shorter times of dehydration.

5. Fixation and subsequent treatment. As Hoerr ('36), Bell ('52) and others have pointed out, the proteins of frozen-vacuum dried tissues retain a large part of their original solubility. That this is true also for frozen substituted tissues has been emphasized by Freed ('55) and Woods and Pollister ('55). The latter have advised fixation of frozen-substituted tissues with hot alcohol, a procedure which has been followed in this study. After dehydration in chilled alcohol, the cultures were routinely put directly into 85% alcohol at 60°C. for two hours and then dehydrated, mounted in Schillaber's oil of refractive index 1.460 and examined under the phase-contrast microscope.

After the cultures had been studied under phase-contrast, they were rehydrated and stained with one of the following procedures: Regaud's iron haematoxylin, dilute Harris' haematoxylin used in progressive fashion, or the azure B method of Flax and Himes. ('51).

[3] The higher temperature refers to the initial temperature of the dehydrating bath. Within two days the temperature usually dropped about 10 degrees.

For comparison, several cultures were fixed by 2% osmic acid for three to 5 minutes followed by a short rinse in distilled water and then 10% buffered neutral formalin for an additional 5 to 10 minutes (Ornstein and Pollister, '52). The cultures were then washed in running water, dehydrated, studied under phase-contrast, and subsequently stained and reexamined.

OBSERVATIONS

The quality of fixation obtained with the freezing-substitution method is shown in plates 1 and 2. Low power observations of the cultures reveal that muscle sarcoblasts, nerve cells and fibers, epithelial sheets and tubules and "fibroblasts" are all preserved in excellent condition. Heart and skeletal muscle are maintained as long fibers stretching considerable distances through the culture (figs. 3, 12, and 14), with the typical nodal swellings and multiple nuclei of these forms being well demonstrated (fig. 14). Cultures of spinal ganglia reveal Nissl material to be distributed in characteristic flocs and masses (figs. 4, 13). The more dense peripheral accumulations of Nissl substance can be resolved into finely granular structures. The kidney culture (fig. 5) shows excellent preservation of the spatial relationships of the elaborate system of tubules formed *in vitro*. Fibroblastic outgrowths from skeletal and heart muscle cultures (fig. 6) show the delicate filamentous cytoplasmic processes appearing in old cultures of these tissues.

In all these preparations, nuclear contents (nuclear sap) appear quite homogeneous (figs. 10–14) and similar to material which has been fixed by the osmic-formol procedure. Nucleoli frequently are shown to have a mulberry-like structure (figs. 9, 10, and 13) which is often seen in living cells and in osmic-fixed preparations. Mitochondria appear as thin rods and filaments, lipid vacuoles are round and smooth (figs. 9–11), and chromosomes appear as plump rods (figs. 15 and 16). Intracellular ice crystal artefact, which would be manifest as irregularly-shaped vacuoles and granular or fibrous-

appearing protoplasm is absent in good preparations. It is particularly instructive to compare intracellular detail in an osmic-formol fixed culture with that in a companion culture fixed by freezing-substitution: In figure 9 such a comparison is presented; the nuclei, nucleoli, and mitochondria appear quite similarly preserved in both procedures. The lipid droplets are, however, osmicated and preserved in the osmic-formol fixed culture, while they appear as empty round holes in the frozen-substituted culture.

The most evident artefact to be observed in these preparations is demonstrated in figures 6 and 7. This is the crazing or cracking that occurs at the time of quenching the culture. As figure 7 demonstrates, the initial very rapid shrinkage of extracellular fluids results in broad cracks which cut the culture up into irregular polygons. Cells, especially long cells such as muscle fibers, may often be snapped in two by this effect. The cells adhering to the coverslip are usually not affected by the cracking and may be seen, out of focus, in figure 7 traversing the clear cracks or channels. Despite this marked, predominantly extracellular artefact, the cells in the islands do not show any particular evidence of intracellular artefact as can be demonstrated by a high power view of the culture in figure 7, taken in an area near a crack (fig. 8). That this cracking occurs at the time of freezing the culture with chilled isopentane can be demonstrated by first quenching a culture and then placing it in formalin vapor. The fixed culture will be seen to have these cracks, most prominent around the explant and less frequent in the thinner regions of the clot. Cultures grown in thin plasma mixtures show this defect to a lesser extent, while cultures planted in fluid medium without plasma show the least amount of cracking (fig. 6).

DISCUSSION

The quality of fixation of tissue culture preparations by freezing-substitution is excellent and compares favorably with the best histological and cytological fixation. One must remark the smooth and even appearance of the nuclear sap, the

excellent preservation of mitochondrial rods; in fact, the lack of loss of cell structures with the exception of the purely lipid inclusions which are dissolved by xylene used in preparing the slides for phase-contrast microscopy. Treatment with xylene would, of course, also extract lipids from conventional frozen-dried preparations.

Simpson ('41) noted that materials prepared by the freezing-substitution method showed "a quality of fixation in most respects exactly comparable with frozen-dried tissues." Yet, Simpson regarded freezing-substitution as giving essentially a chemical fixation with proteins precipitated in a denatured state. However, both Freed ('55) and Woods and Pollister ('55) have noted the necessity of treating frozen substituted animal and plant tissues with hot alcohol in order to prevent extraction of tissue proteins by aqueous solvents, indicating that at least part of the proteins of frozen-substituted material are not actually fixed. While some protein denaturation may occur in alcohol at low temperatures, freezing-substitution obviously cannot be regarded as being the equivalent of fixation by alcohol at room temperature, since as is well known alcohol fixation may lead to coarse protein precipitation, shrinkage, dissolution and disruption of cell contents. In addition, Freed has observed that in the process of freezing-substituting the frog tadpole pancreas, the chilled alcohol gradually replaces the tissue water over a period of several days, beginning in the outer layer of the tissue piece. The author concludes that "it seems safe to regard the freezing-substitution process as a special case of freeze-drying. The solvent or denaturant effect of the substituting medium is possibly the same as that which it would have when applied to the dry tissue."

Two technical details of the method ought to be stressed at this time: The first is with respect to the need for rapid handling of the frozen cultures: In the earlier preparations, a certain amount of ice crystal artefact was observed in cells of some of the cultures. It was noteworthy that this commonly was more prominent in the thinner peripheral areas than in the thicker central area. Frequently, one sector of a culture

showed the artefact to an excessive degree. It became obvious that the artefacts were due to allowing the culture time in which to warm up in the period of transferring it from the freezing to the dehydrating baths. The occurrence of the poorly-preserved sector was due to handling the culture with warm forceps. A second detail of procedure which ought to be emphasized is the need for draining the cultures of all excess moisture, since it is apparent that the thinner cultures freeze better and with less cracking artefact than do thicker, more water-laden cultures. The cracking of the plasma clot which occurs on quenching the cultures is, however, not peculiar to this material since Hoerr ('36) and other workers have also noted cracking of tissue pieces upon quenching, which they ascribe to a decrease in volume when ice is formed at low temperature.

SUMMARY

A method is described for freezing-substituting (i.e., freezing-drying without vacuum dehydration) double coverslip tissue culture preparations with simple and inexpensive equipment. The results obtained are of excellent cytological quality showing good preservation of cell processes, mitochondria, nuclei and nucleoli without apparent shrinkage or distortion. The apparatus is described, the procedure outlined and possible sources of artefact discussed. The technique shows promise as a routine cytochemical procedure.

Grateful acknowledgment is made to Dr. Margaret R. Murray and the members of her laboratory for their advice and generous assistance.

LITERATURE CITED

Baud, C. A. 1952 La fixation "par substitution". Bull. Micr. Appl. Ser. 2, *2:* 158–160.

Bell, L. G. E. 1952 The application of freezing and drying techniques in cytology. Internat. Rev. Cytol., *1:* 35–63.

Blank, H., P. L. McCarthy and E. D. Delamater 1951 A non-vacuum freezing dehydration technique for histology, autoradiography, and microbial cytology. Stain Technol., *26:* 193–197.

FLAX, M. H., AND M. H. HIMES 1952 Microspectrophotometric analysis of metachromatic staining of nucleic acids. Physiol. Zool., *25:* 297–311.

FREED, J. J. 1955 Freeze-drying techniques in cytology and cytochemistry. Lab. Invest., *4:* 106–122.

HOERR, N. L. 1936 Cytological studies by the Altmann-Gersh freezing-drying method. Anat. Rec., *65:* 293–317.

LISON, L. 1949 Sur la fixation histochimique du glycogene. C. R. Soc. Biol., Paris, *143:* 115–116.

MENDELOW, H., AND J. G. HAMILTON 1950 A new technique for rapid freezing and dehydration of tissues for histology and histochemistry. Anat. Rec., *107:* 443–451.

MURRAY, M. R. 1951 Tissue culture procedures in medical installations. In *Methods in Medical Research*, ed. by M. B. Visscher, The Year Book Publishers, Chicago, *4:* 211–216.

ORNSTEIN, L., AND A. W. POLLISTER 1952 Applications of phase microscopy in cytology and electron-micrography. Trans. N. Y. Acad. Sci. Ser. 2, *14:* 194–199.

PETERSON, E., AND M. R. MURRAY 1955 Myelin sheath formation in cultures of avian spinal ganglia. Am. J. Anat., *96:* 319–356.

POGOGEFF, I. A., AND M. R. MURRAY 1946 Form and behavior of adult mammalian skeletal muscle in vitro. Anat. Rec., *95:* 321–336.

SIMPSON, W. L. 1941 An experimental analysis of the Altmann technique of freezing-drying. Anat. Rec., *80:* 173–189.

TAFT, E. B. 1951 The problem of a standardized technique for the methyl green-pyronin stain. Stain Technol., *26:* 205–212.

WOODS, P., AND A. W. POLLISTER 1955 A ice-solvent method of drying frozen tissue for plant cytology. Stain Technol., *30:* 123–131.

PLATES

PLATE 1

EXPLANATION OF FIGURES

The following photomicrographs are of frozen-substituted tissue culture preparations. Cultures were grown with plasma unless otherwise indicated.

3 Skeletal muscle fibers, new-born rat, 21 days *in vitro*. Azure B, yellow filter. × 240.

4 Spinal ganglion cells, chick embryo, 9 days *in vivo*, 21 days *in vitro*. Azure B, yellow filter. × 240.

5 Kidney, showing tubule formation, chick embryo, 7 days *in vivo*, 6 days *in vitro*. Harris haematoxylin, yellow filter. × 240.

6 Fibroblasts, new-born rat muscle grown without plasma. Iron haematoxylin, yellow filter. × 720.

7 Liver, chick embryo, planted in a heavy plasma clot, showing considerable cracking. Azure B, yellow filter. × 120.

8 A high power view of the same culture to show well-preserved liver epithelial cells. × 720.

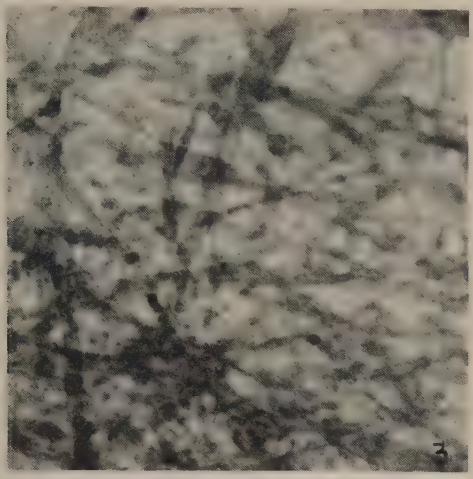
3

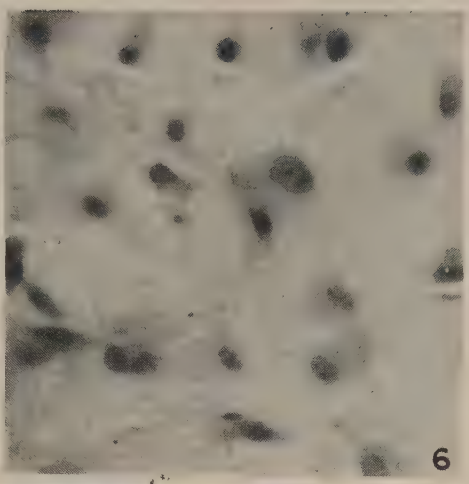
6

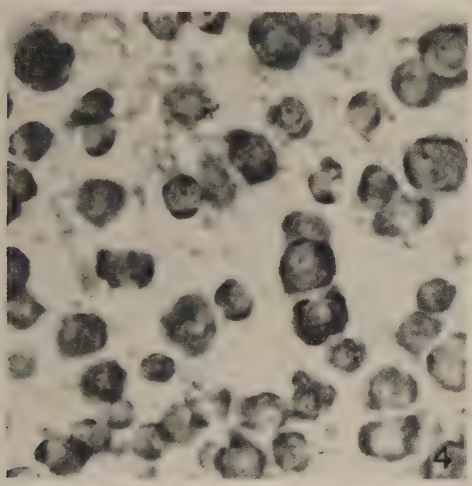
4

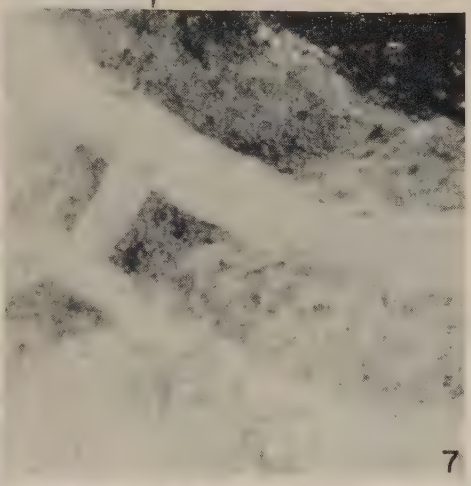
7

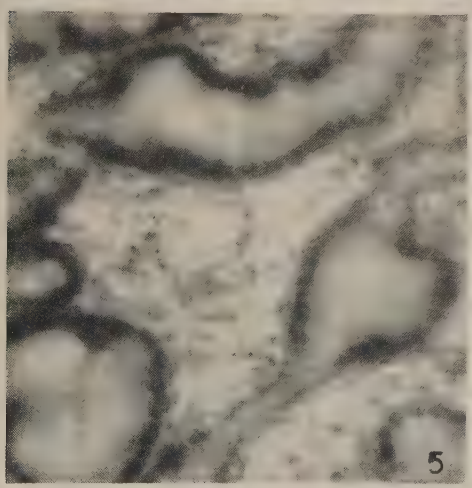
5

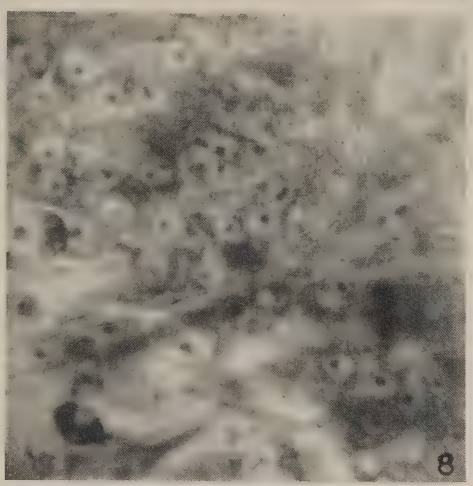
8

PLATE 2

EXPLANATION OF FIGURES

The following photomicrographs, with the exception of 9 A, are of frozen-substituted tissue culture preparations. Cultures were grown with plasma unless otherwise indicated.

9 A comparison of osmic-formol and frozen-substituted cultures with phase-contrast microscopy, unstained chick heart fibroblasts grown without plasma. × 1200. A. Osmic-formol fixation. B. Frozen-substituted. Arrows indicate mitochondria.

10 Chick heart fibroblasts, grown without plasma, stained to show mitochondria. Iron haematoxylin, Wratten 58 filter. × 720.

11 Rat muscle fibroblasts, grown without plasma, stained to show mitochondria. Iron haematoxylin, Wratten 58 filter. × 1080.

12 Rat muscle sarcoblasts, showing smooth contours of the fiber and homogeneous preservation of nuclei and cytoplasm; pyknotic myoblasts also appear, 27 days *in vitro*. Harris haematoxylin, yellow filter. × 720.

13 Chick spinal ganglion cells showing discrete Nissl particles, 21 days *in vitro*. Azure B, Wratten 58 filter. × 720.

14 Chick muscle sarcoblasts, grown without plasma showing smooth contours of fiber and characteristic accumulations of nuclei. Harris haematoxylin, yellow filter. × 720.

15 Mitoses in fibroblasts of chick cartilage culture grown without plasma. A. Unstained, phase-contrast, × 720. B. Harris haematoxylin, × 1080.

16 Mitoses in fibroblasts of rat muscle culture. Azure B. × 1080.

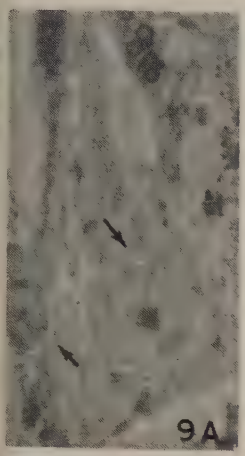
9A

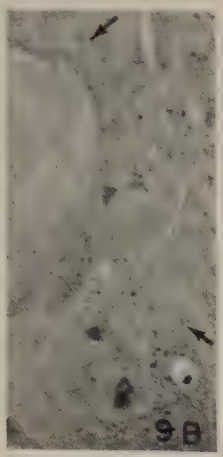
9B

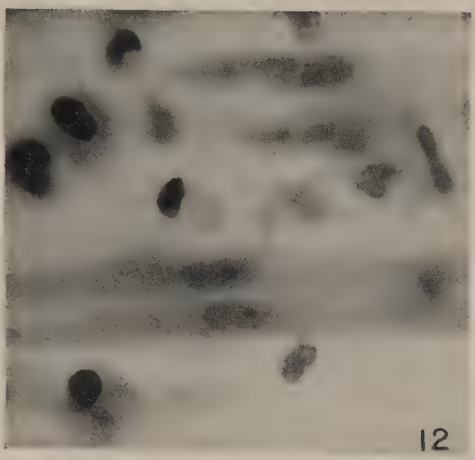
12

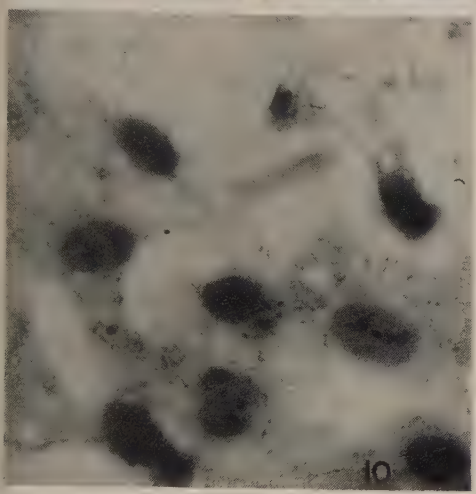
10

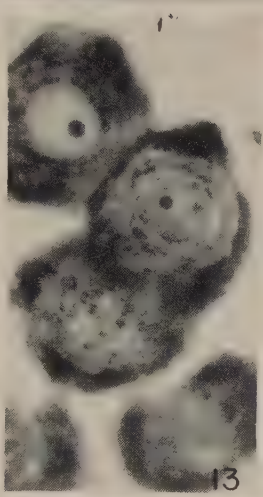
13

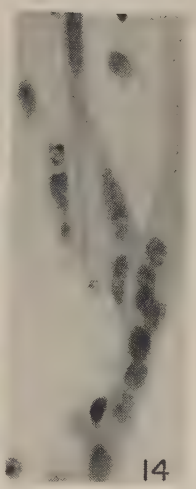
14

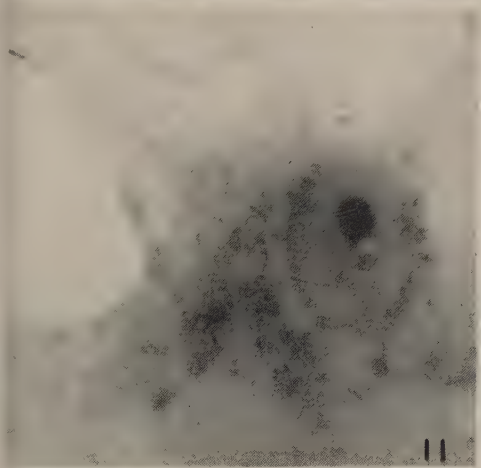
11

15A

15B

16

CYCLIC CHANGES IN THE THYROID AND INTERRENAL GLANDS OF THE VIVIPAROUS LIZARD, XANTUSIA VIGILIS[1]

MALCOLM R. MILLER
Department of Anatomy, Stanford University, Stanford, California

EIGHT FIGURES

INTRODUCTION

The study of the endocrine gland cycles of Xantusia vigilis is particularly interesting because of some unusual features of the life history. Unlike most Southern California reptiles, this lizard has no extended period of winter inactivity, has more gradually occurring gonadal changes, and is viviparous with a three month period of gestation. Details of the gonadal and pituitary gland cycles and the general life history pattern have been published (Miller, '48a, '48b, '51, '54). The present study concerns the seasonal histological changes occurring in the thyroid and interrenal glands.

MATERIALS AND METHODS

Over 200 adult animals of both sexes were collected at approximately two week intervals from June, 1952 through August, 1953 in the Mojave Desert near Palmdale, California. At least 4 individuals of each sex were studied for each date of collection. All animals were sacrificed as soon as possible after capture.

Because of the very small size of the thyroid gland, a block of tissue including the ventral half of the esophagus, the trachea, and the underlying musculature was removed and fixed. As the thyroid gland usually lies just at or slightly

[1] This investigation was supported in part by a research grant from the National Institutes of Health, Department of Health, Education and Welfare.

cephalic to the upper end of the shoulder girdle, a block of tissue extending from the mid-sternal region to the middle portion of the trachea always includes the thyroid gland.

Tissues were fixed in Susa's, Bouin's, Dawson's (formol-sublimate), or acetic osmic bichromate, paraffine embedded, serially sectioned at 5 μ, and stained with Heidenhain's azan. Thyroid follicle cell heights were determined by measuring the lowest and highest cells from each of 10 follicles selected at random from each thyroid gland.

Both adrenal glands together with the gonads were excised and fixed in acetic osmic bichromate, washed, paraffine embedded, and serially sectioned at 5 μ, and stained with Heidenhain's azan. Due to the easily determined seasonal histological differences in the extent of the interrenal tissue, no quantitative measurements were made.

OBSERVATIONS

General life history pattern. In the Antelope Valley of the Mojave Desert, Xantusia vigilis is active throughout the year. In the late summer and fall (August-December), this area is dry and food is less abundant. Although the days are cool during late December, January, and February, the warming of the fallen Joshua logs by the sun permits some continuous daily activity. During the spring months (March-June) food is abundant and growth rapid. During the hot summer months (June-August) activity apparently becomes nocturnal.

After mating (June), the testis is quiescent until late August when a new spermatogenetic cycle begins. Spermatogenic changes occur throughout the fall and winter and are succeeded by spermiogenesis in April and May. Ovulation usually occurs in the latter part of June or in very early July and a three month period of gravidity follows. Most females carry one young in each oviduct and give birth to two (occasionally one or three) young in late September or early October. Ovarian growth occurs slowly throughout the year, but massive yolk deposition takes place in the 4 to 6

weeks preceding ovulation (late May and June). For details of the life history and reproductive cycle see Miller, '48a, '51, '54.

The thyroid gland. The thyroid gland of Xantusia vigilis is an unpaired structure extending transversely across the neck just ventral to the trachea and esophagus at the level of the cephalic end of the ventral portion of the shoulder girdle (fig. 3). The lateral tips of the gland extend somewhat caudally giving the entire gland a slightly bowed shape. As has been described for other lizards, the thyroid gland is contained in a large lymphatic space. This is only apparent, however, if the entire head, neck, and thorax are sectioned. Each lateral tip of the gland receives a short arterial branch (thyroid artery) which arises near the origin of the internal carotid artery. In the median portion, paired vessels branch from the tracheal arteries and enter the dorsal surface of the gland. Small veins drain from the median portion of the thyroid into the right internal jugular. Unlike that in other lizards, the thyroid gland is not enveloped in adipose tissue. The connective tissue capsule is very thin but well supplied with capillaries.

The follicles comprising the gland of which there are 40–50 are mostly spherical, but some are irregular tube-like structures. Interfollicular or parafollicular groups of cells are infrequent. In both gross and microscopic characteristics, the thyroid gland of Xantusia corresponds closely to that described for most other lacertan species by Pischinger ('36) in Bolk's Handbuch.

Seasonal changes in the thyroid gland (figs. 1 and 2). During the fall (October-December) the thyroid gland is most inactive in both sexes. The follicles are relatively large in diameter (100–125 μ), the colloid is dense and usually basophilic, the follicular epithelium is flattened (7–8 μ), and the cytoplasmic and nuclear volume minimal (figs. 4 and 7). At this time most follicles contain occasional erythrocytes and numerous eosinophilic granulocytes in various stages of degeneration within the colloid (fig. 4). "Intrafollicular

bleeding'' as a normal occurrence has been described only in fishes (Bargmann, '39 in von Möllendorff's Handbuch p. 60). Eggert ('35) found intrafollicular granulocytes in various species of Lacerta, and Dimond ('54) describes them in Chelydra, but neither mentions the presence of erythrocytes. That ''intrafollicular bleeding'' occurs when the epithelium

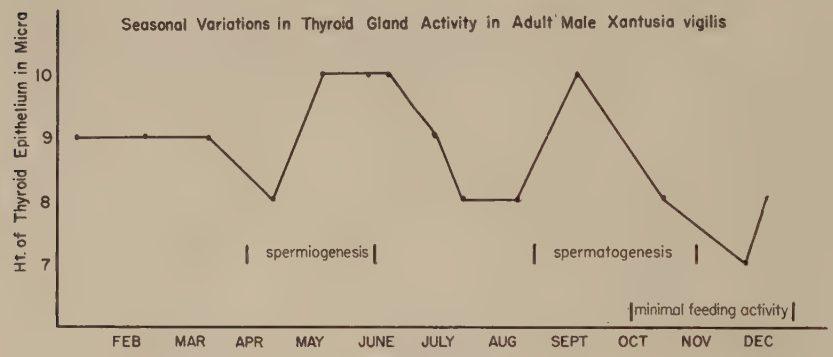

Figure 1

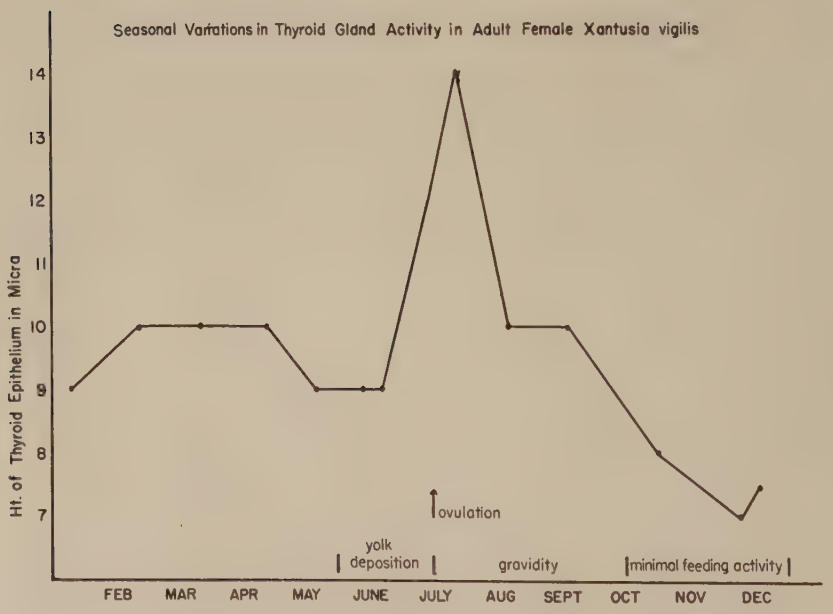

Figure 2

is low and inactive corroborates Bargmann's idea ('39 in von Möllendorff's Handbuch p. 60) that the bleeding process occurs as a result of epithelial thinning. In Xantusia erythrocytes and eosinophilic granulocytes were seen in the colloid following any period of thyroid hyperactivity when there was a sudden thinning of the thyroid epithelium. Mitoses of the follicular epithelium occur especially during more active phases, but are noticeably present during the late fall as though the follicles were being repaired for the coming late winter and early spring upsurge of activity.

In late December thyroid activity increases and during the winter and early spring (late December-early April) the thyroid gland is moderately active. The follicular diameter decreases to 60–75 μ, the colloid is less dense, and the thyroid epithelium increases to an average of 10 μ in height in the female and 9 μ in the male (fig. 5). Increase in thyroid activity at this time is probably associated with both greater feeding activity and cooler temperatures.

In April and early May the testis undergoes rapid spermiogenetic maturation and the sex accessories enlarge. Courting and copulation occur in early June (one to four weeks prior to ovulation). Yolk deposition begins in mid-May and continues through to late June when ovulation occurs.

The male thyroid gland shows a slight decline in activity in mid-April and then an increase during the time of spermiogenesis and copulation (April-early June, figs. 6 and 8). Shortly after copulation (early June) the male thyroid gland decreases in activity, the epithelial height decreases to 7–8 μ, and considerable intrafollicular granulocytes appear.

At the time of rapid yolk deposition in the female, the thyroid gland becomes hyperactive and by late June the follicles are relatively small (40–50 μ in diameter), the colloid is thin and acidophilic, and the epithelium averages 12 μ in height. During the time of ovulation and early gestation (late June-early July) the thyroid gland attains its peak of

activity, the epithelium reaching an average of 14 μ in height with some cells becoming 18–20 μ high.

After the second to third week of gestation, the female thyroid gland undergoes a gradual decline in activity. At the time of parturition (late September-early October), the follicles increase in size (75 μ in diameter), the colloid becomes more dense, and the epithelium an average of 9 μ in height.

In late August and September at the time of spermatogenetic recrudescence, the male thyroid epithelium increases in height to 10 μ. Following parturition in the female and early fall spermatogenesis in the male, the thyroid glands of both sexes become relatively inactive, the follicles expand to 100–125 μ in diameter, the colloid becomes more basophilic and dense, intrafollicular erythrocytes and granulocytes appear, and the follicular epithelium decreases to a minimum average height of 7 μ.

The interrenal tissue. The anatomy and histology of the adrenal gland of Xantusia has been described (Miller, '52). Because of the minute size of the adrenals in this species, it is not feasible to weigh the glands. Variations in interrenal activity are indicated by changes in vascularity, the area of mid-sagittal sections, the width of the cellular cords, the cytoplasmic and nuclear volumes, and differences in the solubility of the cellular lipid content.

Seasonal changes in the interrenal gland. Subtle differences in interrenal activity are difficult to evaluate by histological observations. Large changes in activity, however, are readily apparent. During the late spring and summer (May-August) the interrenal glands are large and vascular. In mid-sagittal section the interrenal area is considerably expanded (1.5 times greater than during the non-breeding season) and the individual cell cords are much wider. Individual cells are taller and wider, and the nuclei more voluminous. Intracellular lipid is more abundant and less soluble in xylene after osmication.

In the female the interrenal tissue is hypertrophic and most active during the time of yolk deposition and the first half of gestation (late May-early August). A state of hyperactivity is not continued throughout the latter half of gestation, however. In the male, the interrenal tissue is largest and apparently most active during late spring at the time of spermiogenesis, the development of the sex accessories, and courtship and copulation. It remains maximally active in the male, however, some 4 weeks after the evacuation of seminal products and the cessation of reproductive activity. In both the male and female, the interrenal glands become less active near the end of July or early August.

For the greater part of the year (August-May), the interrenal tissue in both sexes is considerably less voluminous than it is during the breeding season, the cell cords narrower and the individual cells smaller. No period of winter increase in interrenal activity was observed, although there was marked recrudescence of thyroid gland activity at this time.

DISCUSSION

The thyroid gland cycle. Increase in thyroid gland activity in Xantusia is related both to the reproductive process and to the maintenance of feeding activity during the colder months of the year. The correlation of increased thyroid gland activity with the maintenance of general activity during the colder months has been described in all vertebrates except fishes (see discussion in Miller and Robbins, '55). In reptiles that are inactive during the colder months, the thyroid gland is inactive [Lacerta agilis, L. vivipara, and L. muralis (Eggert, '35) and Chrysemys (Evans and Hegre, '40)], while in those that are winter active the thyroid gland remains active (Anolis carolinensis, Evans and Hegre, '38) and Xantusia.

An increase in thyroid gland activity during the reproductive phase of the life cycle is variable. Both positive and negative correlations have been described in all classes of vertebrates (see discussion in Miller and Robbins, '55). In

Xantusia there is a definite correlation in that the thyroid gland is markedly hyperactive in the female during the period of yolk deposition, ovulation, and the early part of gestation. These observations corroborate those of Evans and Hegre ('38), Evans and Clapp ('40) and Adams and Craig ('51), indicating that greatly increased thyroid activity in lizards is associated with the presence of estrogens.

The thyroid gland in the male, although not nearly as hyperactive as in the female, is more active during the time of final gonad maturation and copulation than it is during the late winter and early spring period of greatest feeding activity and growth.

Eggert ('35) has demonstrated a definite correlation between reproduction and increased thyroid gland activity in Lacerta agilis, L. muralis, and L. vivipara. The ovoviviparous L. vivipara has increased thyroid gland activity extending almost through the period of gravidity (Eggert, '35) which is longer than that observed in Xantusia. It is significant that the only positive correlation between reproductive and thyroid gland activity in fishes occurs in the viviparous Lebistes reticulatus (Stoldt, quoted in Olivereau, '54).

Although the thyroid gland of the female Xantusia is hyperactive at the time of final yolk deposition, ovulation, and early gestation, it declines rapidly in the latter half of gestation and is relatively inactive by the time of parturition. It may be that in the lower vertebrates the stresses of yolk deposition and ovulation are much greater than that of gestation. Eggert ('35) feels that the maintenance of a high thyroid epithelium throughout gestation in L. vivipara is due to the gravid female's habit of lying in the sun and not to an increased metabolic need.

The interrenal gland cycle. Studies of the seasonal variations in the interrenal tissue of reptiles are limited. Fox ('52) states that the interrenal gland of garter snakes (Thamnophis sirtalis) is enlarged during the breeding season. In vertebrates in general, however, there is a close correlation between reproduction and increased adrenal cortical or inter-

renal gland activity (see discussion in Miller and Robbins, '55).

The correlation between reproductive and increased interrenal gland activity in Xantusia is very marked. The interrenal tissue is particularly hypertrophic during the final stages of gonad maturation, the development of the sex accessories, copulation, and the first half of gestation. Apparently the latter half of gestation is not a demanding stress, as the interrenal tissue becomes much less active at this time. The interrenal tissue in the male was also observed not to respond to fall spermatogenesis and testicular recrudescence.

Although the thyroid gland is relatively active in response to feeding activity during the colder winter months, the interrenal tissue does not evidence increased activity at this time.

Pituitary relationships. A previous study of the seasonal histological changes in the anterior pituitary of Xantusia has been made (Miller, '48b). The essential changes in the pituitary gland are an increase in the size of the gland and in the percentage of acidophils and basophils during late spring and early summer. At the time the pituitary study was undertaken (1940), basophilic types were not differentiated and hence no correlations can be made between the relative abundance of cyanophils and fuchsinophils and gonadal and thyroid gland activity. It is significant that the pituitary, thyroid, and interrenal glands all attain their maximum activity during the reproductive phase of the life cycle, but experimental studies will be necessary to extend and clarify interrelationships.

SUMMARY

Xantusia vigilis, a viviparous lizard of the Southern California deserts, does not hibernate during the colder winter months, but feeds whenever it is warm enough. The gonads mature during May and June, ovulation occurs early in July and gestation lasts approximately three months. During the late fall, food is scarce and activity is curtailed.

Histological changes in the thyroid and interrenal glands are closely correlated with the various phases of the life history. The thyroid follicles are largest, the colloid densest and more basophilic, and the follicular epithelium lowest (7 μ) during the dry fall months (August-December). An increase in thyroid gland activity manifested by a decrease in follicle size and an increase in thyroid epithelial height to 9–10 μ occurs during late December and continues through January, February, and March. The increase of thyroid gland activity during the winter is probably related to the fact that the animals are active and feeding during the coldest months of the year.

A further increase in activity of the male thyroid gland in late April, May, and early June is probably related to spermiogenesis, development of the sex accessories, and copulatory behavior. Following evacuation of the testes and seminal ducts by mid-June, the thyroid gland in the male becomes less active until late August and early September when spermatogenesis and testicular recrudescence occur. Following early fall activity in the male, the thyroid gland enters the late fall inactive stage.

The female thyroid gland becomes hyperactive during yolk deposition, ovulation, and early gestation (May–late July). The follicles are small (40–50 μ diameter), the colloid thin and acidophilic, and the epithelium 14–18 μ in height. After the second or third week of gestation, the female thyroid gland becomes less active. By the time of parturition (late September to early October) it is relatively inactive with large follicles and a low follicular epithelium. Increased thyroid gland activity is thus related to both winter activity and reproduction.

The interrenal gland is hyperactive in both sexes during the time preparatory to reproduction and for a time coincident with the first half of gestation (late May–early August) in the female, but for more than a month after the cessation of reproductive activity in the male. What stimulus maintains the post-reproductive hyperactive gland in the male is not

known. At this time the interrenal gland is larger, more vascular, and the cells and nuclei more voluminous. During the remainder of the year the interrenal gland is not hyperactive but more subtle changes such as occur in the thyroid gland are not histologically manifest. Increase in interrenal gland activity is thus definitely correlated only with the preparatory phases of reproductive activity.

ACKNOWLEDGMENTS

The author wishes to extend his appreciation to Mr. and Mrs. Robert V. Miller for aid in the collection of specimens, to Marilyn E. Robbins, Doris Wurster, and Ellen Brennan for technical assistance, and Mr. Frank Barrett for the photographs.

LITERATURE CITED

Adams, A. E., and M. Craig 1951 The effects of antithyroid compounds on the adult lizard, Anolis carolinensis. J. Exp. Zool., *117:* 287–316.

Bolk, L., E. Göppert, E. Kallius and W. Lubosch 1936 Handbuch der vergleichende Anatomie der Wirbeltiere. *3:* 299–300. Urban u. Schwartzenberg, Berlin.

Dimond, Sr. M. T. 1954 The reactions of developing snapping turtles, Chelydra serpentina serpentina (Linné), to thiourea. J. Exp. Zool., *127:* 93–117.

Eggert, B. 1935 Zur Morphologie und Physiologie der Eidechsenschilddrüse. I. Das jahreszeitliche Verhalten der Schilddrüse von Lacerta agilis L., L. vivipara Jacq., und L. muralis Laur. Zeit. f. wiss. Zool., *147:* 215–263.

Evans, L. T. 1940 Endocrine relationships in turtles. Endocrinology, *27:* 144–148.

Evans, L. T., and M. L. Clapp 1940 The effects of ovarian hormones and seasons on Anolis carolinensis. II. The genital system. Anat. Rec., *77:* 57–75.

Evans, L. T., and E. Hegre 1938 The effects of ovarian hormones and seasons on Anolis carolinensis. I. The thyroid. Anat. Rec., *72:* 1–9.

Fox, W. 1952 Seasonal variations in the male reproductive system of Pacific Coast garter snakes. J. Morph., *90:* 481–554.

Miller, M. R. 1948a The seasonal histological changes occurring in the ovary, corpus luteum, and testis of the viviparous lizard, Xantusia vigilis. Univ. Calif. Publ. Zool., *47:* 197–224.

———— 1948b The gross and microscopic anatomy of the pituitary and the seasonal histological changes occurring in the pars anterior of the viviparous lizard, Xantusia vigilis. Univ. Calif. Publ. Zool., *47:* 225–246.

MILLER, M. R. 1951 Some aspects of the life history of the Yucca Night Lizard, Xantusia vigilis. Copeia, 1951, pp. 114–120.

———— 1952 The normal histology and experimental alteration of the adrenal of the viviparous lizard, Xantusia vigilis. Anat. Rec., *113:* 309–324.

———— 1954 Further observations on reproduction in the lizard, Xantusia vigilis. Copeia 1954, pp. 38–40.

MILLER, M. R., AND M. E. ROBBINS 1955 Cyclic changes in the thyroid and interrenal glands of the urodele amphibian, Taricha torosa (Triturus torosus). Anat. Rec., *122:* 79–104.

v. MÖLLENDORFF, W. 1939 Handbuch der mikroskopischen Anatomie des Menschen. *6:* p. 60. Julius Springer, Berlin.

OLIVEREAU, M. 1954 Hypophyse et glande thyroide chez les poissons. Étude histophysiologique de quelques corrélations endocriniennes, en particulier chez Salmo salar L. Ann. de L'Inst. Oceanographique, *29:* 95–296.

PLATE 1

EXPLANATION OF FIGURES

The tissues in figures 3 and 5 were fixed in Bouin's and the others in Susa's. All were stained with Heidenhain's azan.

3 Cross section through the root of the neck showing the transversely placed unpaired thyroid gland lying below the trachea medially and the esophagus laterally and above the muscles overlying the clavicles. × 30.

4 Male sacrificed November 11, 1952 showing large dense colloid filled follicles, flattened epithelium and intrafollicular eosinophilic granulocytes. × 200.

5 Female sacrificed February 11, 1953 showing moderate sized follicles, thinner colloid, and higher epithelium. This is the condition of a winter active gland. × 200.

6 Male sacrificed May 27, 1953 showing smaller follicles, diminished colloid, and a high epithelium. This is characteristic of breeding hypertrophy in the thyroid gland. × 200.

7 Female sacrificed December 10, 1952 showing low flattened epithelium characteristic of the winter inactive thyroid gland. × 400.

8 Male sacrificed May 27, 1953 showing tall epithelium characteristic of breeding hypertrophy. Note the mitoses. × 400.

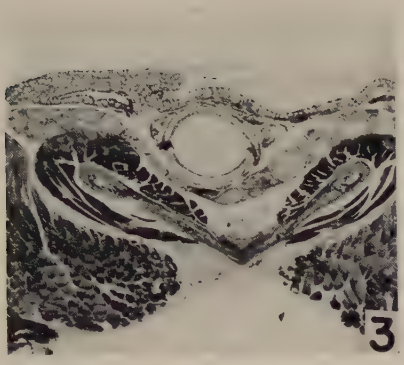
3

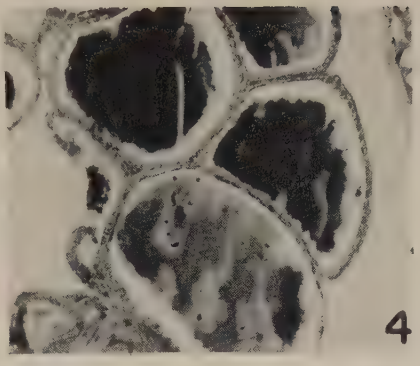
4

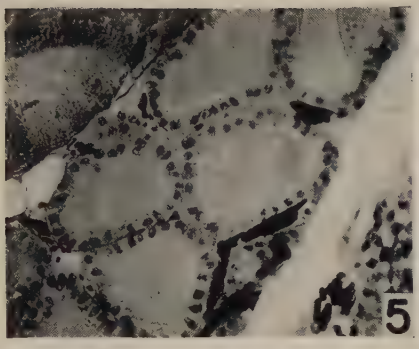
5

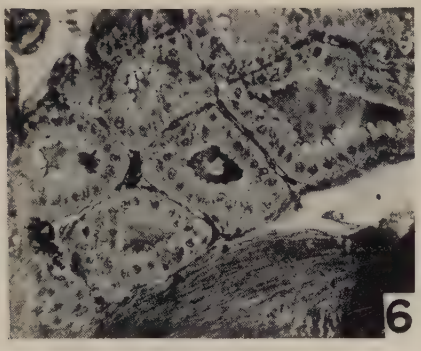
6

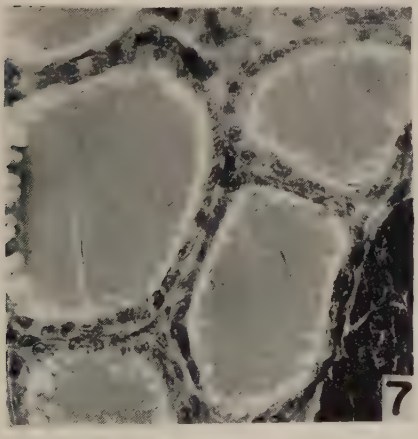
7

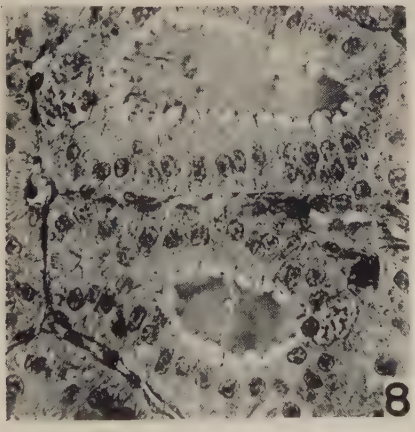
8

ELECTRON MICROSCOPY OF THE PLACENTA OF THE RAT [1]

GEORGE B. WISLOCKI AND EDWARD W. DEMPSEY

Department of Anatomy, Harvard Medical School, Boston, Massachusetts, and Department of Anatomy, Washington University, School of Medicine, St. Louis, Missouri

SEVENTEEN FIGURES

Grosser ('08, '09) divided the chorio-allantoic placentas of eutherian mammals into 4 principal types, basing his classification on the number of layers separating the maternal and fetal blood streams. According to his scheme, the Lagormorpha (rabbits), Myomorpha (rats, mice) and Histricomorpha (guinea-pigs) possess hemochorial placentas in which the chorion, initially composed of cytotrophoblast, becomes later transformed into syncytial trophoblast. Subsequently, Mossman ('26, '37) submitted evidence that in rabbits, rats, mice and guinea-pigs late in gestation, the syncytial trophoblast itself disappears, so that the placental barrier becomes reduced for the most part merely to endothelium lining the fetal capillaries. On this basis, he proposed adding a "hemoendothelial" placenta to the types proposed by Grosser. Although Hard ('46), Wislocki, Deane and Dempsey ('46) and Amoroso ('52) have admitted the possibility of the correctness of Mossman's view, they have pointed out that evidence is inconclusive.

With the development of the electron microscope a means is at hand to investigate further the detailed structure of various types of placentas. We have initiated such a program and have studied the placenta and fetal membranes of the rat

[1] This investigation has been aided in part by grants (C-2174, and G-3298) from the United States Public Health Service, National Institutes of Health.

on the 15th, 17th and 21st days of gestation. It may be stated briefly that electron microscopy has revealed that the rat's placenta is hemochorial and not hemoendothelial in character, its labyrinth possessing throughout gestation a complete layer of trophoblast. Moreover, this layer consists of individual trophoblastic cells (cytotrophoblasts) and not of syncytial trophoblast as has been heretofore believed. An abstract of these findings has been published (Dempsey and Wislocki, '53). The results on rat's placentas were extended and partially confirmed by examination of the placenta of a rabbit on the 28th day of gestation.

MATERIAL

The material consisted of the placentas of three albino rats (Sprague-Dawley strain) killed by concussion on the 15th, 17th and 21st days of gestation. Blocks of tissue were removed from the chorio-allantoic placenta and from the visceral wall of the yolk sac in the region of the endodermal villi. The parietal wall of the yolk sac including Reichert's membrane was obtained on the 15th day. Small bits of these tissues were placed promptly in fixative, consisting of 1% osmic acid buffered with Ringer's solution and veronal to pH 7.5. These specimens were fixed for 4 hours at room temperature, washed briefly in three changes of distilled water and dehydrated in 70%, 95% and absolute ethanol. They were then infiltrated with methacrylate monomer (three parts butyl methacrylate and one part methyl methacrylate) for three hours in three changes of the plastic mixture. Finally, they were transferred to no. 3 gelatin capsules which were filled with the plastic monomer to which benzoyl peroxide had been added as a catalyst (13.5 mg. catalyst per millimeter plastic). The plastic was allowed to set slowly overnight at room temperature, after which polymerization was completed in 24 hours in an incubator at 45°C.

After embedding, the gelatin capsules were removed by soaking in warm water. The glassy-hard blocks were trimmed for sectioning under a low-power binocular dissecting micro-

scope. They were then placed in the chuck of a modified rotary microtome (Geren and McCulloch, '51; Dempsey and Lansing, '53) and sections were cut at thicknesses of .025 to 0.1 μ. The thicker sections proved best for cellular topography whereas the thinner sections permitted the best resolution of fine detail, such as the double layer of the nuclear membrane and the detailed internal structure of mitochondria. The sections were floated and spread upon a 30% acetone solution, lifted upon collodion-coated copper-mesh grids, dried and examined in an RCA electron microscope type EMU2C at initial magnification of 1000 to 6000 diameters. The photographic negatives exposed at these magnifications were subsequently enlarged as desired.

For purposes of ordinary histological and cytological examination, blocks of the same placentas were fixed in Zenker's acetic acid fluid, Orth's fluid, Rossman's fluid and Heidenhain's susa fluid. These blocks were embedded in paraffin and 5 μ sections were cut. These were deparaffinized and stained with eosin and methylene blue, Gomori's chrome alum-hematoxylin and phloxine, Masson's trichrome stain and by McManus' periodic acid-Schiff procedure.

The chorio-allantoic placenta of a rabbit on the 28th day of gestation was similarly prepared and compared with the rats' placentas.

OBSERVATIONS

The electron micrographs of the rat's placentas, which illustrate this paper demonstrate the finer structure and arrangement of the tissues separating the maternal and fetal blood streams in the chorio-allantoic placenta and the nature of the wall of the yolk sac so clearly that no lengthy description is deemed necessary.

Figures 1, 2 and 3 illustrate the topography and cytology of the placental barrier of the rat on the 17th day of gestation and figures 4 and 5 on the 21st day. The places shown are representative of the usual or average appearance of the normal placental labyrinth.

The structure of the placental labyrinth on the 15th day is practically identical with that on the 17th day and hence is not separately illustrated. At full term, on the 21st day of gestation, although the placental barrier has deminished somewhat in width, the number of layers has remained constant.

The most interesting observation is that, at all three stages including the 21st day, the barrier consists typically of two to three overlapping, imbricated sheets of cytoplasm of trophoblastic cells, with the innermost sheet of cells resting upon a basement membrane which intervenes between the trophoblast and the fetal capillaries. The walls of the fetal capillaries possess a separate basement membrane which supports internally the capillary endothelium. Between the basement membrane of the trophoblast and that of the capillary there is a narrow space containing wisps of collagen. Thus, the placental labyrinth appears not only to be completely lined by trophoblast, but the trophoblast is cellular and not syncytial. Moreover, the trophoblastic cells overlap one another forming a laminated membrane. Thus the barrier consists of a succession of two or three flattened trophoblastic cells resting on a basement membrane, lamina of loose connective tissue, and a fetal capillary consisting of a basement membrane lined by endothelium. The trophoblastic cells, basement membranes and endothelial cells are labelled in a number of electron micrographs.

In the electron micrographs the individual trophoblastic cells appear frequently to have been slightly pulled apart, thus revealing their independence and separate individuality. Nevertheless, in certain places the cells resist separation because of the presence of small cytoplasmic pegs or protuberances on the cells which fit into corresponding pockets in the cytoplasm of adjacent cells, a cytological arrangement which would appear to contribute to the stable union of the thin cytoplasmic sheets. In figure 2 several such places are indicated by arrows.

The bodies and nuclei of the respective cells are recognizable at intervals, located seemingly in nodal territories in the trophoblastic lamellae. The cell bodies are relatively large and contain as a rule one, but occasionally two, large nuclei situated side by side. The cytoplasm surrounding the nuclear area is rich in ergastoplasm which often assumes the appearance of threads or skeins. These cytoplasmic structures, encountered in electron micrographs, are the equivalents of cytoplasmic basophilic substance of stained cells in light microscopy and represent ribonucleoprotein. Besides the skeins of ergastoplasm situated mainly in the perinuclear region, the trophoblast displays two other cytoplasmic constituents in the electron microscope. The first of these is mitochondria which are scattered widely throughout the cells. The second is fat droplets which are located mainly in the cytoplasm of the innermost trophoblasts which rest upon the basement membrane.

The surfaces of the outermost trophoblastic cells forming the confining walls of the maternal blood channels may be relatively smooth or possess irregularities varying from small cytoplasmic protuberances to anastomosing threads and strands of cytoplasm which project variously into the blood lacunae. Thus the surfaces have a variably scalloped or festooned appearance. Sundry such cytoplasmic projections are visible in the electron micrographs (figs. 1 to 5).

Reichert's membrane has been identified in the electron microscope, especially in the portion of the parietal wall of the yolk sac which is attached to the surface of the chorioallantoic placenta. Reichert's membrane appears as a broad sheet of substance possessing a faint fibrillar texture (figs. 6, 7). On its internal surface, but easily detached from it, is the layer of parietal endodermal epithelial cells. Only remnants of these remain attached in the electron microscope preparations.

The wall of the visceral yolk sac in the villous region is readily identifiable. Here the most prominent feature is the visceral endodermal epithelial cells. These constitute a single

layer of columnar cells resting upon a narrow basement membrane and protruding apically into the lumen of either the yolk sac or uterus, depending upon the stage of development (figs. 8, 12). The outer or apical surface is studded with short irregular microvilli (figs. 8, 10, 12). In occasional places between the villi the cytoplasm of the cell surface appears to be invaginated in the form of minute tubular pockets extending into the cytoplasm (fig. 10). The nuclei are basally situated, with a wide expanse of cytoplasm between the nucleus and the cell surface. Immediately beneath the microvilli there is often a clear zone relatively devoid of differentiated material (fig. 12). Beneath this, in turn, is a zone which is relatively rich in mitochondria and small vacuoles which merges with a broad outer zone of the cell cytoplasm containing numerous large vesicles of variable size (figs. 10, 11). It is possible that some of the vesicles arise by a cutting off or separation of the tubular invaginations mentioned above. The vesicles contain greyish material and some darker particles. Mitochondria are scattered between the vesicles. Deeper still in the cells and extending down and around the nuclei are large fields of uniformly stippled material which represents glycogen (fig. 8). In the cytoplasm just above and lateral to the nucleus are coils and skeins of material recognizable as ergastoplasm. In favorably cut sections some of this ergastoplasm is related to a cytocentrum located in a supranuclear position. Beneath the nucleus, down to the basement membrane, there is a relatively narrow zone in which mitochondria, ergastoplasm and glycogen are discernible.

Between the dome-shaped surfaces of adjacent cells there are often relatively deep notches into which microvilli project (fig. 8). Between the adjacent sides of the cells, extending down to the basement membrane, one occasionally discerns irregular, narrow clefts (fig. 12). Whether these spaces are artifacts or physiological in nature is uncertain. Between the majority of the cells clefts are lacking (fig. 8).

The bases of the cells rest upon a narrow basement membrane (figs. 8, 9). The stroma also contains mesenchymal fibroblasts and capillaries.

The inner surface of the visceral layer of the rat's yolk sac is formed of a stout, continuous basement membrane which is clothed by flattened serous cells of the exocoelomic cavity. Wislocki and Padykula ('53) called this membrane the "serosal basement membrane" and compared it on the basis of various histochemical reactions with Reichert's membrane from which it differed in some respects. With the electron microscope it is revealed as a stout membrane which is not as wide as Reichert's membrane, is more open textured and consists of a felt work of wavy lines which appear to be fine bundles of collagen (fig. 13). The mesothelial cells lining the exocoelome appear to be directly attached to the serosal basement membrane. Moreover, they are surprisingly rich in cytoplasm which contains an unexpected quantity of ergastoplasm indicative of the presence of ribonucleoprotein (fig. 13).

The placental labyrinth of a rabbit was examined on the 28th day of gestation for comparison with the rat's placenta. The findings were similar, suggesting that its placental labyrinth consists also of trophoblastic cells which overlap one another to form a thin sheet constituting a hemochorial placental barrier (figs. 14, 15).

DISCUSSION

The major results of this study indicate that the chorioallantoic placenta of the rat throughout gestation possesses a placental barrier which is composed of (1) two or three, thin, overlapping sheets of cytoplasm of individual trophoblastic cells, (2) a basement membrane supporting the trophoblast and (3) the wall of a fetal capillary consisting of a basement membrane bearing a lining of overlapping endothelial cells. Thus the placental barrier is not hemoendothelial, but hemochorial in character, and is also cellular instead of syncytial.

Upon reexamining the labyrinth of the rat's chorio-allantoic placenta at the end of gestation with the light microscope, the difficulty of establishing whether the placental barrier is hemochorial or hemoendothelial is at once apparent (figs. 16, 17). However, Hard ('46) argued that, since alkaline phosphatase forms a continuous layer within the labyrinth of the guinea pig's placenta and appears to be confined to the trophoblastic syncytium, the labyrinth must be hemochorial in structure throughout gestation. But, Wislocki et al. ('46), studying various rodents including the rat, concluded that although the enzyme was abundantly present in the placental barrier, it gave no clue as to which placental layer it was associated with. The present observations with the electron microscope appear to prove conclusively that trophoblast persists in the placental barrier, in the rat throughout gestation and probably also in the rabbit, as revealed by electron microscope. Its continued presence would favor the supposition advanced by Hard that alkaline phosphatase is located in the trophoblastic layer.

The fat droplets, mitochondria and ergastoplasm encountered in the trophoblast of the rat's chorio-allantoic placental barrier coincide in amount and distribution with comparable organelles recognizable in the placenta with the light microscope (Wislocki et al., '46; Wislocki, '55). The fat droplets are localized in the innermost cytotrophoblastic cells adjacent to the fetal stroma. The ergastoplasm of the electron microscope and the cytoplasmic basophilia of ordinary histological preparations are confined principally to the cytoplasm around the nuclei and are attributable to the presence of ribonucleoprotein. The mitochondria after both procedures are numerous and widely dispersed in the cell cytoplasm. The interlocking protuberances and concavities uniting the surfaces of adjacent trophoblastic cells are not visible in the light microscope, but comparable structures have been described in hepatic cells with the electron microscope by Fawcett ('54).

In a previous paper on the electron microscopy of the visceral yolk-sac epithelium of the guinea pig, Dempsey ('53)

interpreted the structural complexities of the free border and apical cytoplasm of the cells — especially the microvilli; surface invaginations and vacuoles — as cellular specialization which enhance absorption. The cells of the rat's vitelline epithelium exhibit a complex internal structure similar to that described by Dempsey for the guinea pig and hence the interpretations offered for the one would appear to be applicable to the other. However, there is one difference, in that the changes in the mitochondria suggestive of degeneration, described by Dempsey in the guinea pig, are not encountered in the rat's vitelline epithelium. This difference is ascribable probably to the fact that gestation is relatively brief in the rat (21 days), compared to the guinea pig (68 days), so that degenerative age changes in the yolk sac have relatively little time in which to express themselves in the former. The large and small vacuoles encountered in the distal ends of the epithelial cells in the electron micrographs coincide in number, size and distribution with the periodic acid-Schiff stained droplets described and illustrated previously by Wislocki and Padykula ('53). This coincidence suggests that the yolk sac is actively engaged in the absorption of a mucopolysaccharide or glycoprotein from the uterine cavity.

In a previous paper (Wislocki and Padykula, '53) the histological and histochemical properties of Reichert's membrane and of the "serosal basement membrane" in the rat's yolk sac were compared and certain differences noted. Reichert's membrane stained intensely with the periodic acid-Schiff reagents, whereas the serosal membrane was less strongly stained. With the electron microscope, differences between the two membranes are also evident. The serosal basement membrane is composed of a loose meshwork of fibers resembling collagen, whereas Reichert's membrane is characterized by a feltwork of poorly defined wavy bundles in which the typical pattern of collagen is not clearly apparent. The interpretation might be offered that the ground substance, which must be responsible for the strong periodic

acid-Schiff reaction of Reichert's membrane, is so dense that it overshadows and obscures the pattern of the fibrous protein, probably collagen, forming the basis of the membrane.

SUMMARY

Rat's placentas of 15, 17 and 21 days of gestation were examined with the electron microscope. The chorio-allantoic placenta of the rat throughout gestation possesses a placental barrier which is composed of (1) two or three, thin, overlapping sheets of cytoplasm of individual trophoblastic cells, (2) a basement membrane supporting the trophoblast and (3) the wall of a fetal capillary consisting of a basement membrane bearing a lining of endothelial cells. Thus the placental barrier is not hemoendothelial but hemochorial in character, and the trophoblast is also cellular instead of syncytial in structure.

The cytoplasm of the trophoblastic cells contain numerous mitochondria, and fat droplets are characteristically present in the innermost cell layer. Ergastoplasm is abundant in the thicker nuclear regions of the cells. The sheets of cytoplasm of the trophoblasts are united in many places by cytoplasmic surface protuberances which fit into corresponding cups or depressions of adjacent cells.

The structure of the epithelium of the visceral wall of the yolk sac and of Reichert's membrane is described and illustrated.

The appearance of the chorio-allantoic placenta of a rabbit examined on the 28th day of gestation suggests that it is also hemochorial rather than hemoendothelial in structure.

LITERATURE CITED

Amoroso, E. C. 1952 Placentation. Marshall's Physiology of Reproduction. 3rd ed., A. S. Parks, Editor. *2:* 127 Longmans, Green. N. Y.

Dempsey, Edward W. 1953 Electron microscopy of the visceral yolk sac epithelium of the guinea pig. Am. J. Anat., *93:* 331–364.

Dempsey, E. W., and A. I. Lansing 1953 Improved knife-holder for thin-sectioning with rotary microtomes. Proc. Soc. Exp. Biol. and Med., *82:* 253–256.

DEMPSEY, E. W., AND G. B. WISLOCKI 1953 Electron microscopy of the rat's placenta. Anat. Rec., *117:* 581–582.

FAWCETT, DON W. 1954 Cytological observations on liver with the electron microscope. Anat. Rec., *118:* 422–423.

GEREN, BETTY B., AND DAVID MCCULLOCH 1951 Development and use of the Minot rotary microtome for thin sectioning. Exp. Cell Res., *2:* 97–102.

GROSSER, O. 1908 Ueber vergleichende Placentation und die Einteilung tierischer Placenten. Zentralbl. Physiol., *22:* 198–199.

———— 1909 Vergleichende Anatomie und Entwicklungsgeschichte der Eihäute und der Placenta. Wien und Leipzig. Wilhelm Braumüller.

HARD, W. L. 1946 A histochemical and quantitative study of phosphatase in the placenta and fetal membranes of the guinea pig. Am. J. Anat., *78:* 47–77.

MOSSMAN, H. W. 1926 The rabbit placenta and the problem of placental transmission. Am. J. Anat., *37:* 433–497.

———— 1937 Comparative morphogenesis of the fetal membranes and accessory uterine structures. Contrib. Embryol. Carneg. Instn., *26:* 129–247.

WISLOCKI, G. B. 1955 The cytology and histochemistry of the placenta. Allen's Sex and Internal Secretions, 3rd edition, edited by E. W. Dempsey. The Williams and Wilkins Co., Baltimore.

WISLOCKI, G. B., H. W. DEANE AND E. W. DEMPSEY 1946 The histochemistry of the rodent's placenta. Am. J. Anat., *78:* 281–346.

WISLOCKI, G. B., AND H. A. PADYKULA 1953 Reichert's membrane and the yolk sac of the rat investigated by histochemical means. Am. J. Anat., *92:* 117–152.

PLATE 1

EXPLANATION OF FIGURES

1 Electron micrograph of the labyrinth of a rat's chorio-allantoic placenta (17th day of gestation). Three cytoplasmic layers are seen intervening between a maternal blood space (m.b.s.) and the basement membrane (b.m.) and endothelium (en) of a fetal capillary containing an erythrocyte. × 9000.

2 Electron micrograph of the placental membrane of a rat's chorio-allantoic placenta (17th day of gestation). Three layers of trophoblast intervene between the maternal blood space (m.b.s.) and a fetal capillary which is lined by endothelial cells (en) which rest on a basement membrane (b.m.). Small projections of cytoplasm are visible which fit into corresponding pockets in adjoining sheets of trophoblast (arrows). × 9000.

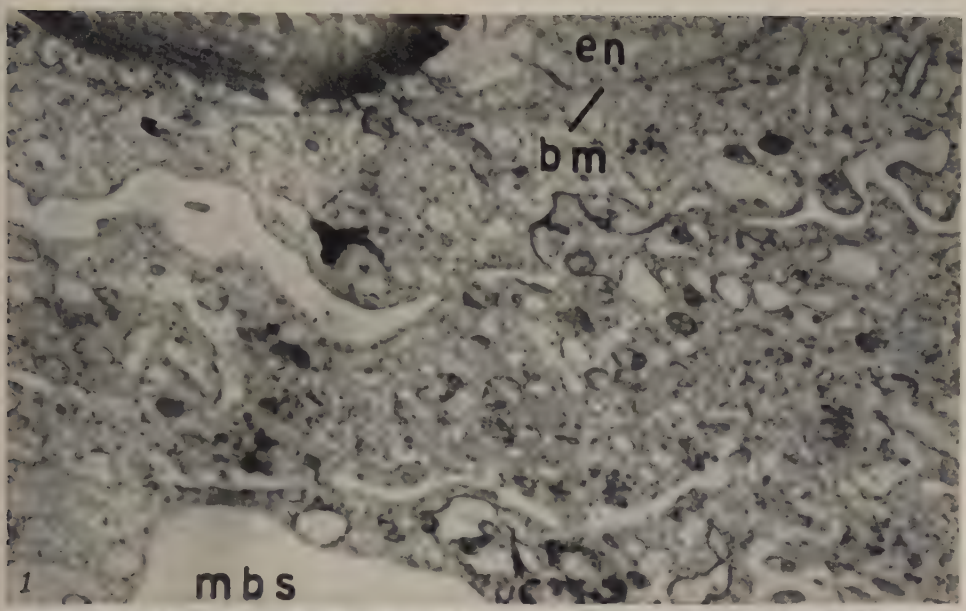
en
bm
mbs
1

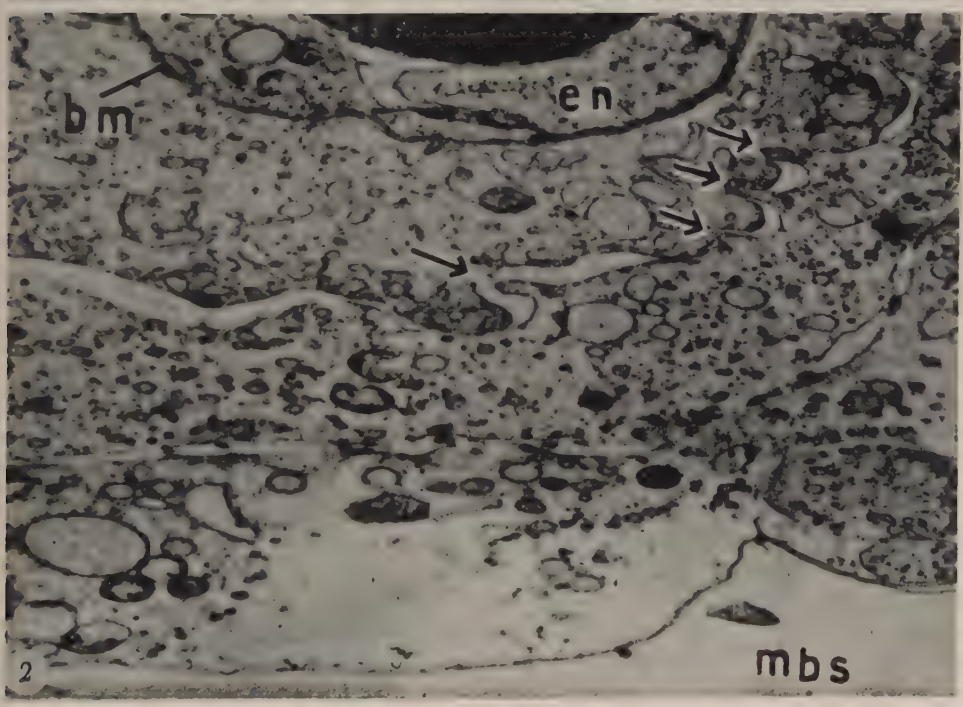
bm
en
mbs
2

PLATE 2

EXPLANATION OF FIGURE

3 Electron micrograph of the placental membrane of a rat (17th day of gestation) showing the cell bodies and nuclei of two trophoblasts. In the cell cytoplasm, many ovoid mitochondria and skeins of ergastoplasm are visible. A fetal capillary (f.c.) and maternal blood space (m.b.s.) are visible, separated by several sheets of trophoblast. B.m., the basement membrane of the fetal capillary. × 6000.

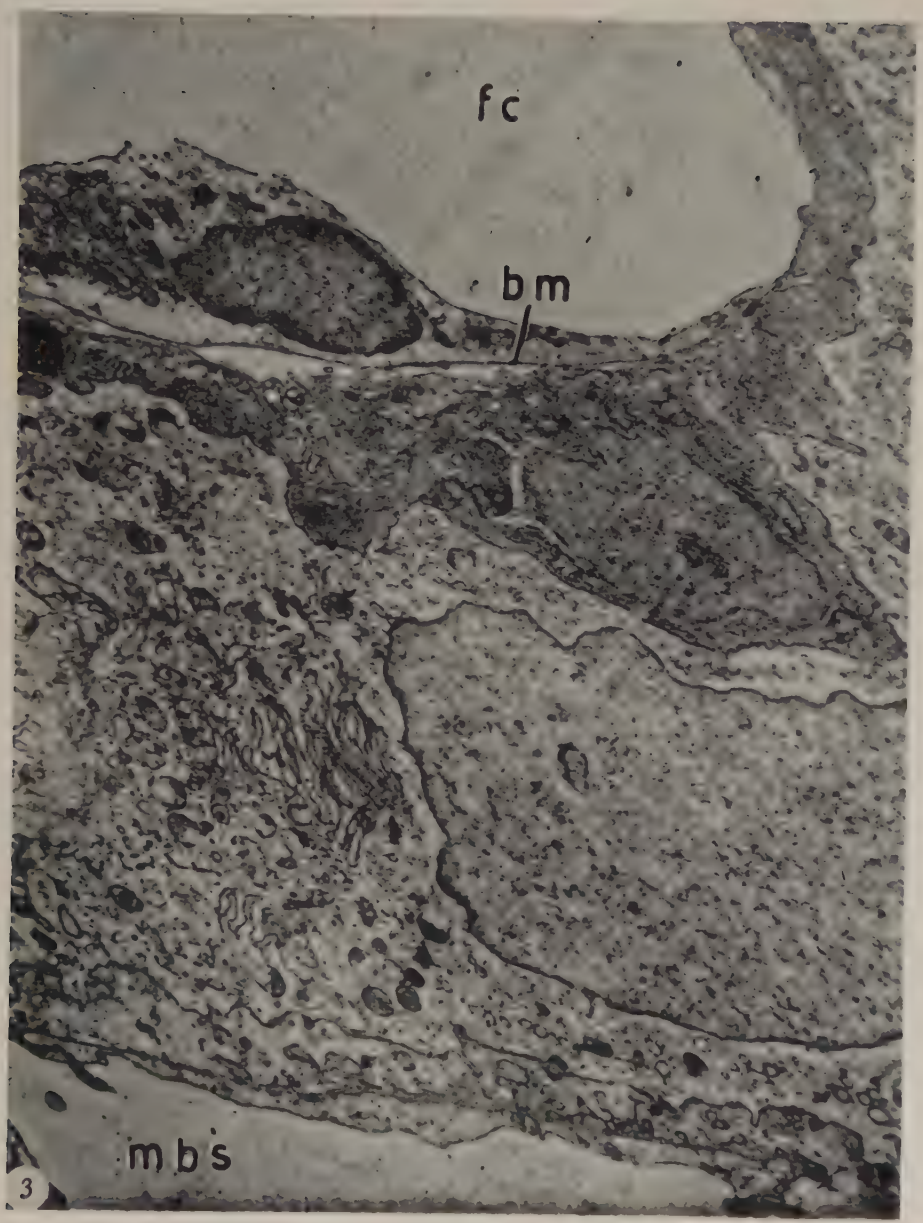
fc
bm
mbs
3

PLATE 3

EXPLANATION OF FIGURES

4 Electron micrograph of a rat's placental labyrinth at full term (21st day of gestation), illustrating a fetal capillary (f.c.), maternal blood spaces (m.b.s.) and the intervening tissue consisting of endothelium, a basement membrane, and several sheets of trophoblastic cytoplasm. × 6000.

5 Electron micrograph of a rat's placental labyrinth at full term, showing a maternal blood space (m.b.s.) a fetal capillary (f.c.) with its endothelium (en) and basement membrane, and three intervening sheets of trophoblast. × 9000.

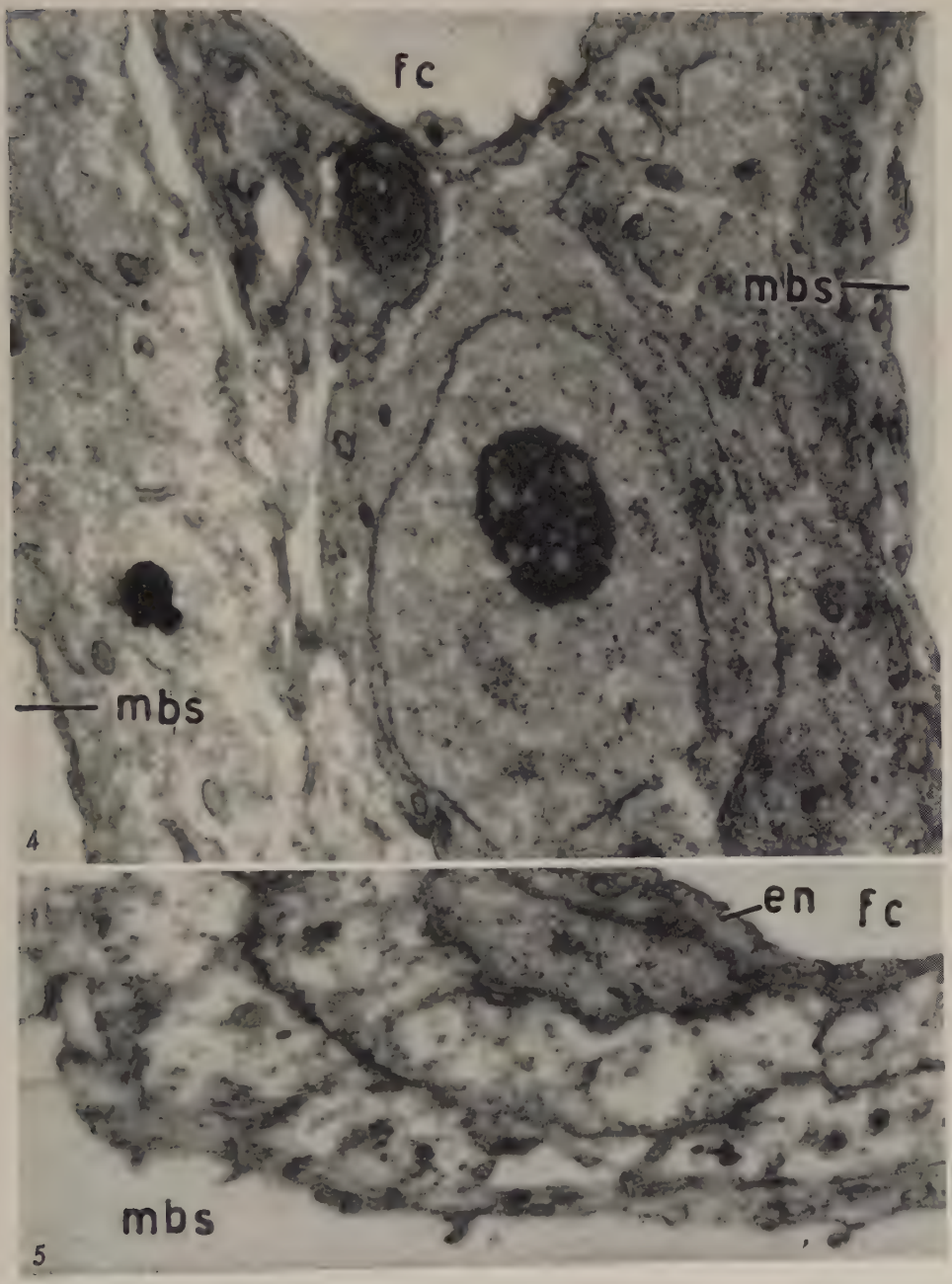
fc
mbs
mbs
4
en
fc
mbs
5

BOSTON
APR
MEDICAL LIBRARY

PLATE 4

EXPLANATION OF FIGURES

6 Electron micrograph of a portion of Reichert's membrane (15th day of gestation). The parietal endodermal epithelium has been torn off of the inner surface of the membrane, but on the outer (upper) surface the cytoplasm of a trophoblastic giant cell is adherent to it. At the right, erythrocytes may be seen in a maternal blood space. × 3000.

7 Higher power micrograph of a portion of Reichert's membrane. The indistinct, wavy texture of the membrane is apparent. Its appearance should be compared with that of the serosal basement membrane shown in figure 9. At the bottom of the figure, some processes of the parietal endodermal epithelium are adherent to the membrane. × 20,000.

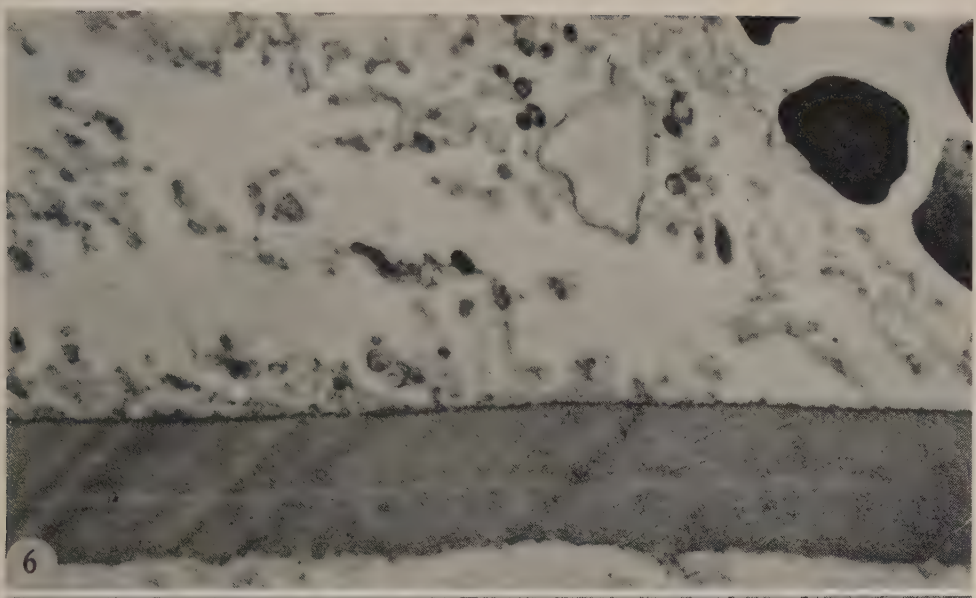
6

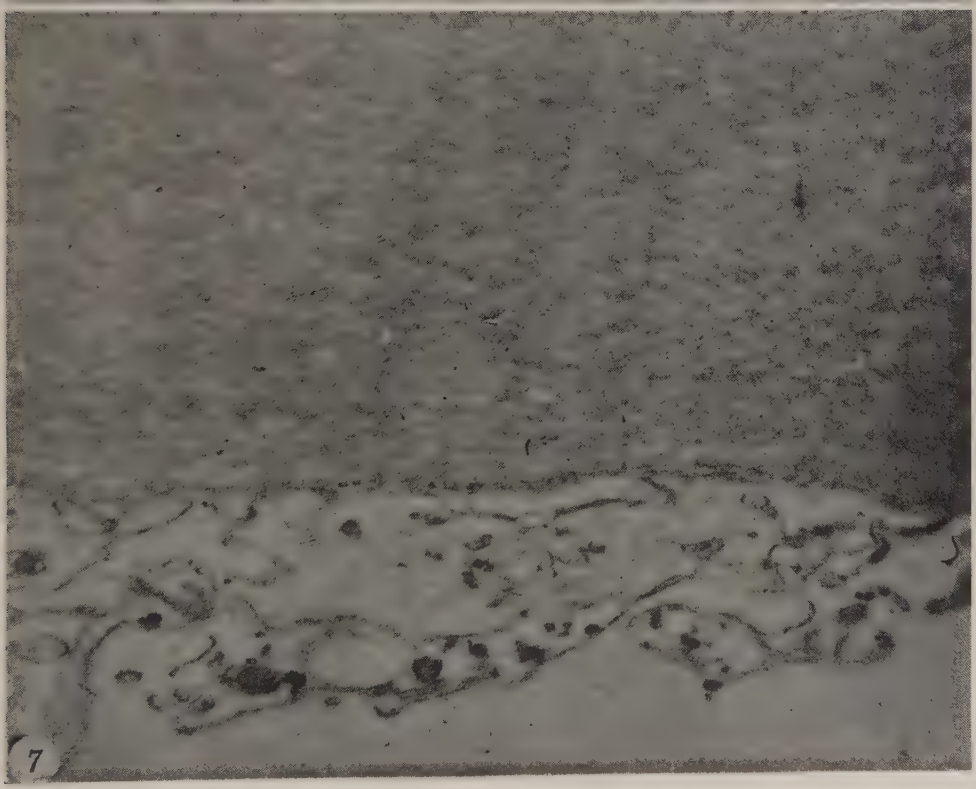
7

PLATE 5

EXPLANATION OF FIGURES

8 Electron micrograph of several epithelial cells of the visceral wall of the yolk sac (21st day of gestation). The cells rest upon a narrow basement membrane beneath which is fetal stroma containing a mesenchymal fibroblast. Short, irregular microvilli are visible on the distal surfaces of the cells. The cytoplasm contains vacuoles, mitochondria, glycogen and ergastoplasm. × 6000.

9 Higher power of the basal portion of an epithelial cell and the basement membrane (b.m.) on which it rests. The indistinct, amorphous character of the membrane is evident. Immediately beneath the membrane small bundles of fibrils resembling collagen are visible; these appear to join the membrane. The texture of their basement membrane should be compared with that of Reichert's membrane (figs. 6 and 7). The associated bundles of fibrils resemble the appearance of the bundles comprising the much thicker serosal basement membrane with which many of them are connected (fig. 13). × 18,000.

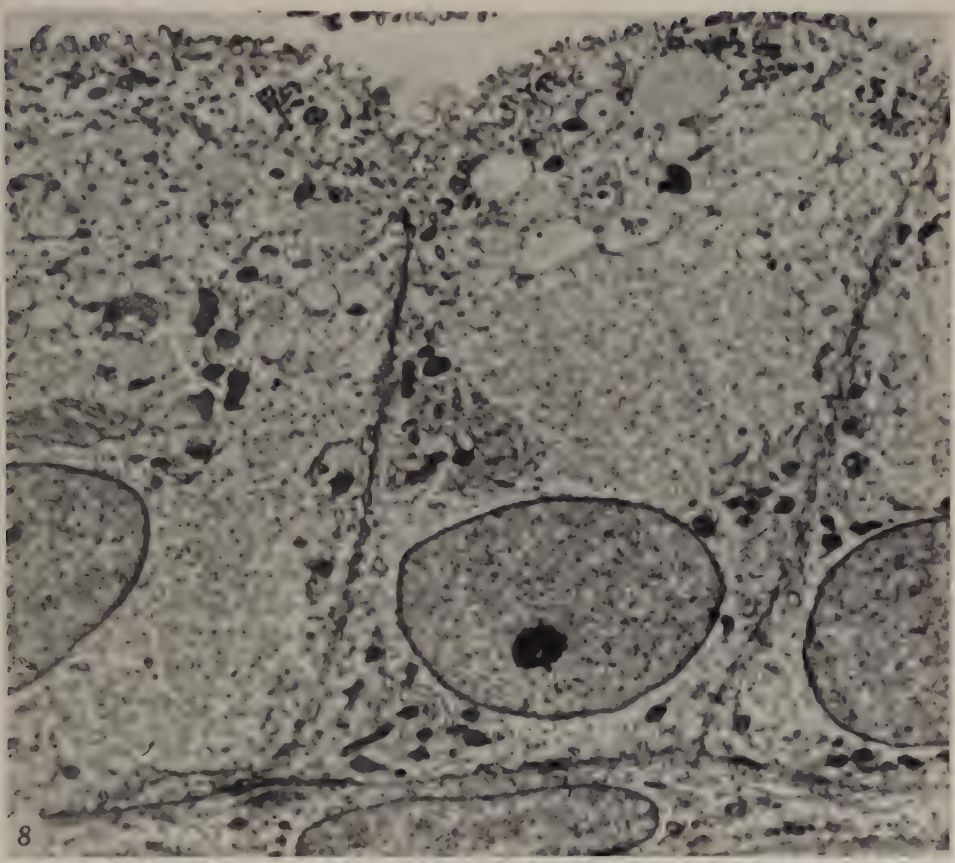
8
bm
9

PLATE 6

EXPLANATION OF FIGURES

10 A micrograph of a portion of the distal end of an epithelial cell, illustrating the microvilli, the invaginations into the cytoplasm, the small vesicles close to the surface and the larger ones somewhat deeper in. ×20,000.

11 The distal part of an epithelial cell containing numerous mitochondria and small and large vesicles (15th day of gestation). × 20,000.

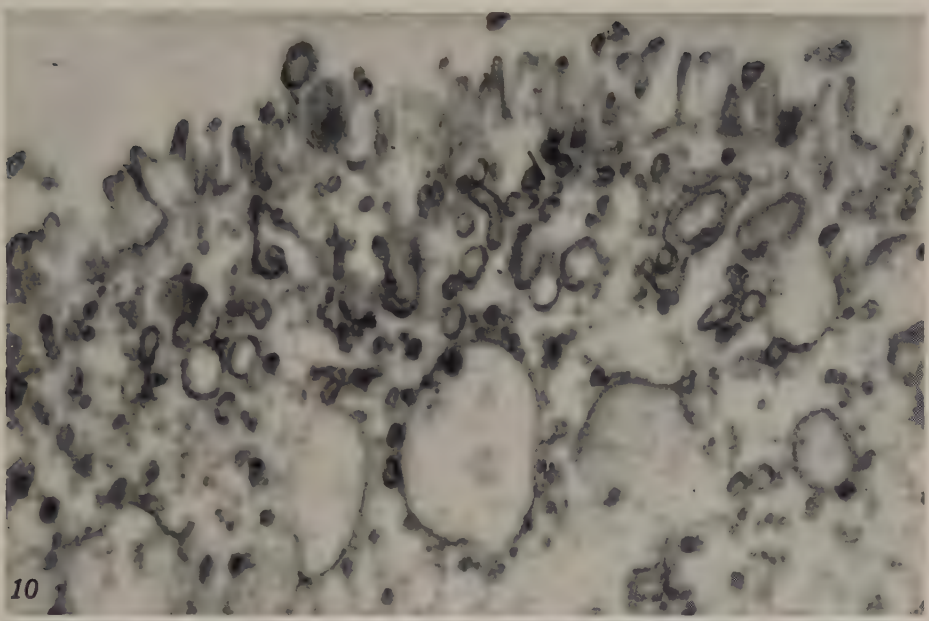
10

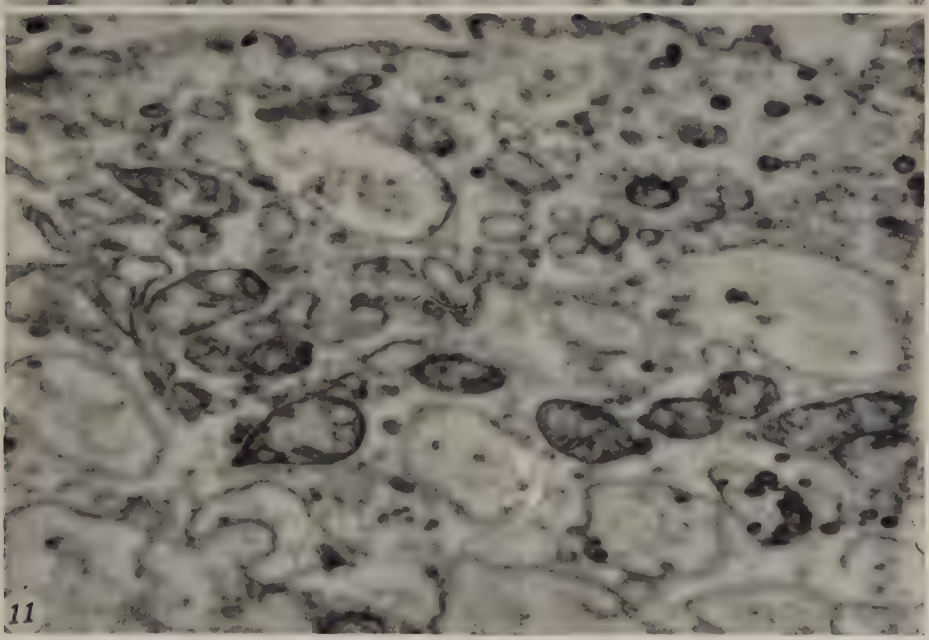
11

PLATE 7

EXPLANATION OF FIGURE

12 More epithelial cells showing a notch between two neighboring cells and narrow, irregular clefts between the sides of the cells (21st day of gestation). A narrow clear zone is visible beneath part of the surface cap of microvilli. × 10,000.

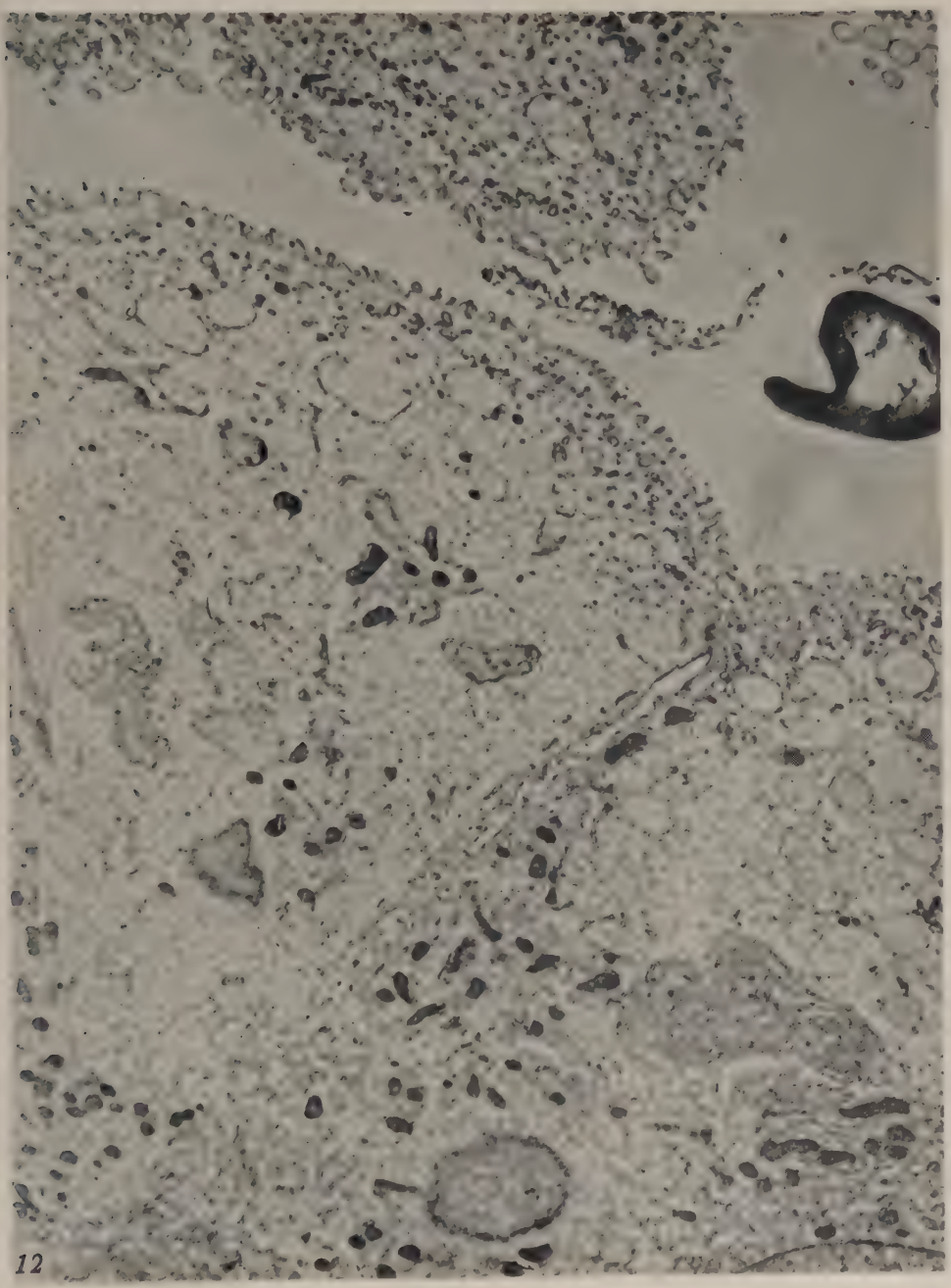
12

PLATE 8

EXPLANATION OF FIGURE

13 The serosal basement membrane of the visceral wall of a rat's yolk sac (17th day of gestation). The fibrillar texture of the membrane, resembling collagen, is apparent. Adherent to the membrane is a mesothelial cell lining the exocoelome, with a considerable amount of ergastoplasm visible in its cytoplasm. Running off toward the upper right corner is a bundle of fibers which becomes continuous with the basement membrane of the epithelial cells. × 10,000.

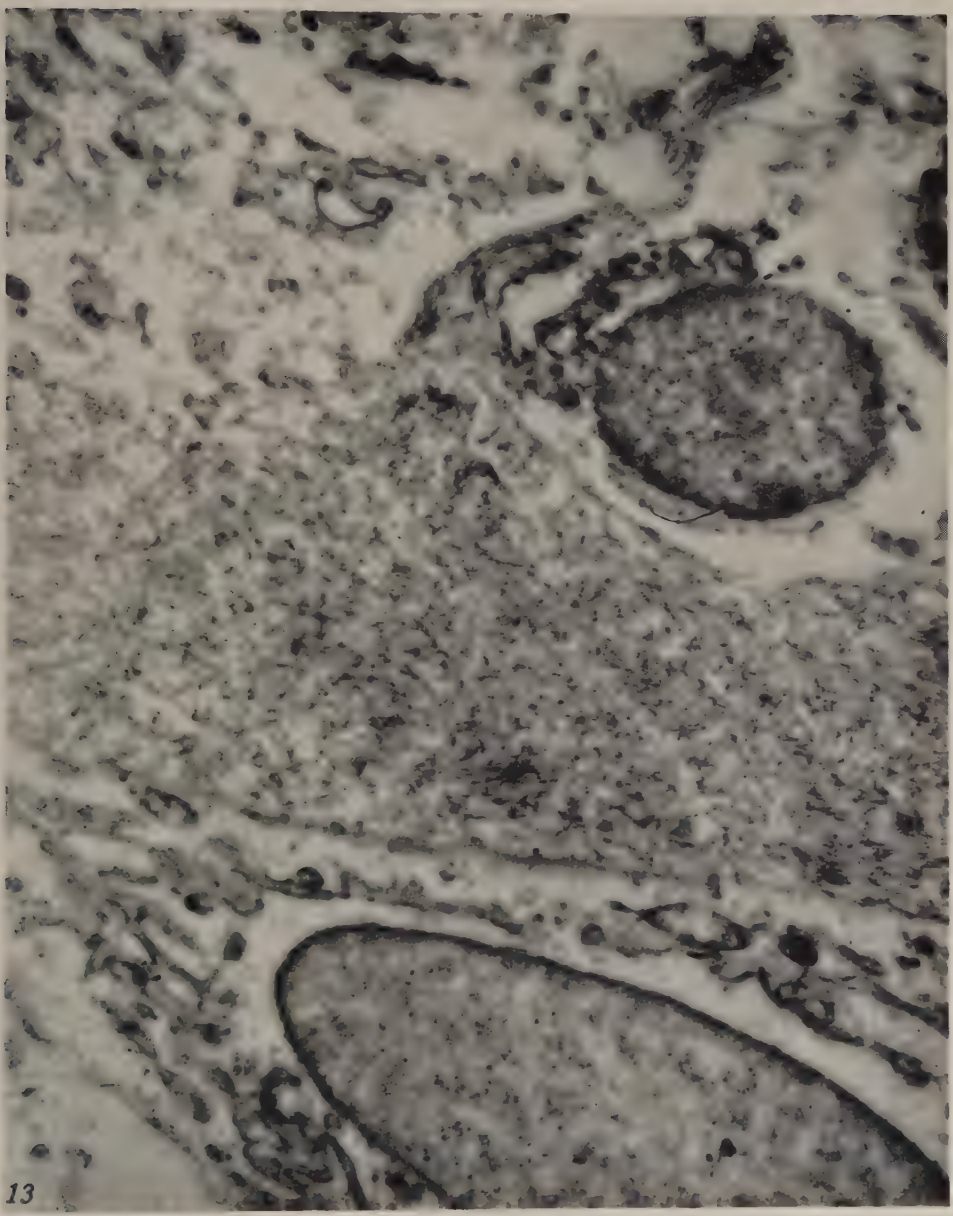
13

PLATE 9

EXPLANATION OF FIGURES

14 Electron micrograph of the labyrinth of a rabbit's placenta on the 28th day of gestation, showing a maternal blood space (m.b.s.), separated by two thin sheets of trophoblast from the basement membrane (b.m.) and the endothelium (en) of a fetal capillary (f.c.). × 9000.

15 Higher power of a typically thin portion of a rabbit's labyrinth, separating maternal from the fetal blood spaces. The fetal capillary (f.c.) is at the top of the figure. The fetal endothelium, (en) basement membrane (b.m.) and trophoblastic cytoplasm intervenes between the capillary lumen and the maternal blood space (m.b.s.). × 30,000.

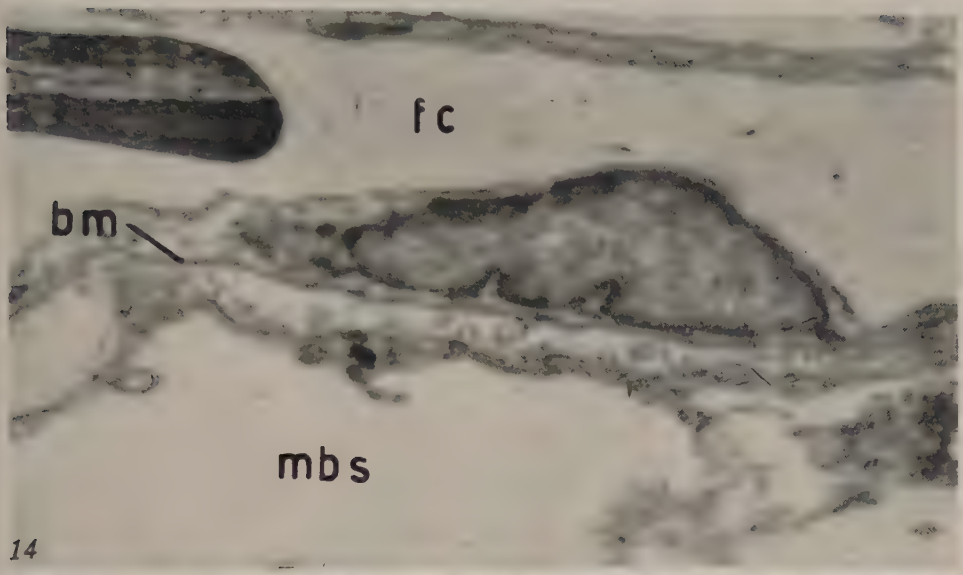

14

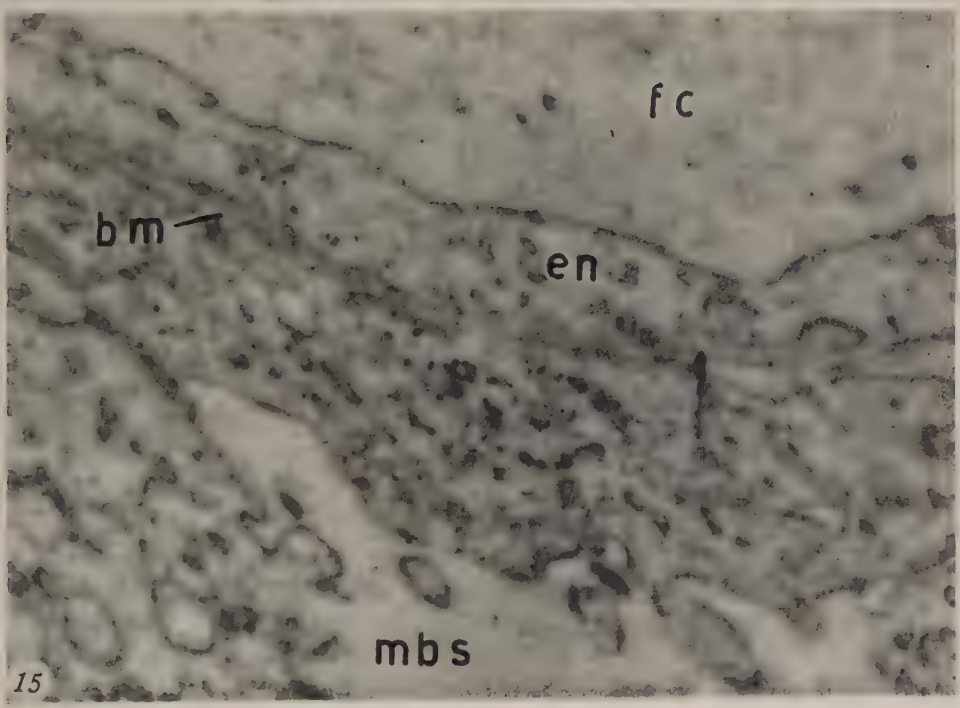

15

PLATE 10

EXPLANATION OF FIGURES

16 The labyrinth of a rat's placenta on the 21st day of gestation, drawn at high magnification with the light microscope, showing the ill-defined character of the placental layers separating the maternal blood spaces (m) from the fetal capillaries (f). Masson's triacid stain.

17 The labyrinth of a rat's placenta on the 21st day of gestation, viewed at high magnification with the light microscope. Stained with chrome alum-hematoxylin and phloxine. Again observe the ill-defined appearance of the placental membrane. M, maternal blood space; f, fetal capillary. Three large trophoblastic cells are visible.

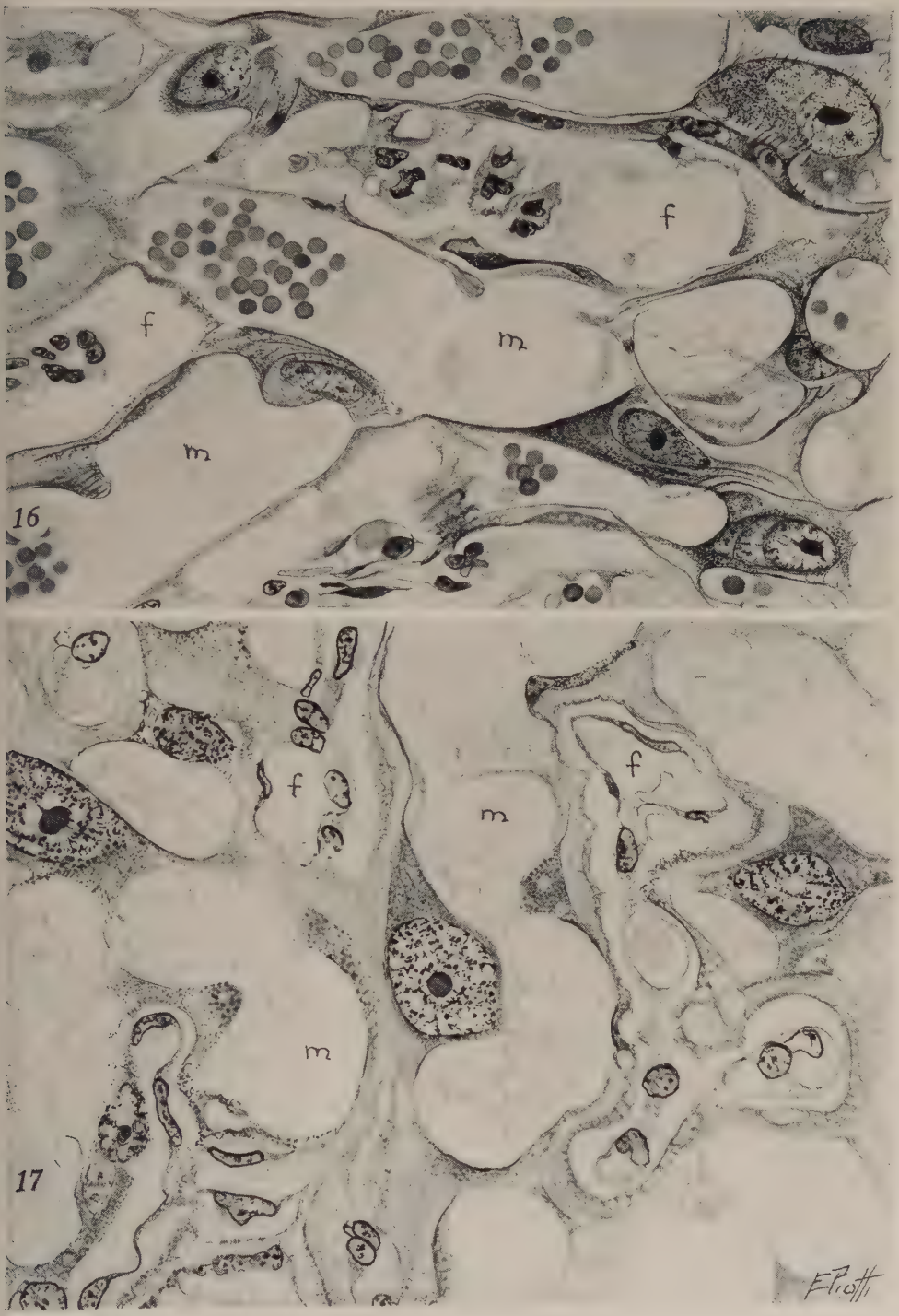
f
f
m
m
16
f
f
m
m
17
E. Pratt

NERVE FIBERS IN THE AREA POSTREMA OF CAT, RABBIT, GUINEA PIG AND RAT[1]

C. D. CLEMENTE[2] AND V. L. VAN BREEMEN
Departments of Anatomy, University College London, England, and University of Colorado School of Medicine, Denver, Colorado

FIFTEEN FIGURES

INTRODUCTION

The area postrema is a highly vascular but small region of the brain stem situated at the level of the obex in the floor of the fourth ventricle. This area can easily be identified from the surrounding medulla and is composed principally of blood vessels and parenchymal cells whose cytoplasmic processes attach to vascular walls. It has been said that in the human neurons exist in the area postrema (Wilson, '06; Cammermeyer, '47), and Cammermeyer felt that these neurons contained a "melanin-like pigment." King ('37), on the other hand, concluded that neurons did not exist in the area postrema of adult cats, stating further that nerve fibers were only rarely seen and that the area postrema did not have neural connections with other regions in the brain.

It was first shown by Wislocki and Putnam ('20, '24) that the area postrema became vitally stained after the systemic administration of trypan blue of Prussian blue dyes. In this respect this region differed from most other areas of the brain but was similar to the supraoptic crest, the neurohypophysis and the hypophysial stalk, the intercolumnar tubercle (Putnam, '22) or subfornical organ (Pines, '26) and

[1] A preliminary report of this work was presented before the Physiological Society of Great Britan, March 26, 1954. J. Physiol., *124*, 23 P.

[2] Bank of America-Giannini Foundation Fellow, Present Address: Department of Anatomy, University of California at Los Angeles School of Medicine, Los Angeles 24, California.

the pineal body. This property of selective permeability in the central nervous system has led to a general acceptance of the existence of a blood-brain barrier.

Although the function of the area postrema has not been established, it is of interest to note that Ranson and Billingsly ('16) recorded marked and immediate depressions of blood pressure upon direct faradic stimulation of this area in cats. On the other hand, stimulation only 3 mm away from the area postrema (at the apex of the ala cinerea or the fovea inferior) resulted in a marked elevation of blood pressure. King ('37), claiming that nerve fibers were only rarely seen in the region, was "certain that the effect on the blood pressure obtained in cats by Ranson and Billingsly through stimulation of the area postrema could not have resulted from nerve impulses arising in this area." Cammermeyer ('47) favored the view that the cellular elements of the area postrema were neurosecretory in nature while Wislocki and Leduc ('52) suggested that the area postrema represented a "thickened specially differentiated portion of the subependymal plate," and agreed with King that the predominant cells were related to ependymal spongioblasts.

Recently it has been repostulated that a central coordinating region for emesis exists in the dorsal medulla (Borison and Wang, '49; Wang and Borison, '50). From electrical stimulation and ablation studies, it has been concluded that the "vomiting center" is located at the dorsolateral border of the lateral reticular formation, including the tractus solitarius and its nucleus. It was also felt that the area postrema may be associated with a "chemotrigger mechanism" initiating the vomiting response (Borison and Brizzee, '51; Brizzee and Borison, '52).

Most interpretations on the functional significance of the area postrema have been suggestive of some neural mechanism, and yet the existence of nerve fibers in the region has not been thoroughly established. For this reason the areae postremae of several species of animals have been studied

by silver staining methods, and the present communication reports the anatomical findings.

MATERIALS AND METHODS

Histological observations were made on adult cats, rabbits, guinea pigs and rats. Animals were sacrificed by perfusion with physiological saline followed by 10% formalin according to the method of Koenig, Groat and Windle ('45). After perfusion, the brain stem containing the intact area postrema was dissected, and further fixation was carried out in different ways. Some tissues were allowed to remain in formol-saline for 48 hours, while others were placed in absolute ethanol or Carnoy's fixative for 6 to 12 hours. Tissues were embedded in paraffin and cut serially at 8 μ. General observations such as location, size and relationships of the area postrema were made on sections stained with hematoxylin and eosin, while a modification of the Holmes' ('42) slide silver technique was used for nerve fiber staining. The Holmes' technique gave the finest results in preparations perfused with formol-saline and hardened in Carnoy's fixative. The modification (suggested by R. W. Guillery) involved heating the hydroquinone-sodium sulfite reducing solution to about 50°C. The reducing process required two to three minutes. Other cytological stains used in this study included the buffered thionin technique (Windle, Rhines and Rankin, '43) and the iron hematoxylin nuclear stain.

OBSERVATIONS

Distinguishable from the surrounding brain stem by its rich vascularity and loose structure, the area postrema in the cat is located in a slightly different position from that in the rabbit, guinea pig and rat. In the cat the area postrema is bilateral and projects as two small symmetrical masses of tissue from the ventrolateral walls into the fourth ventricle, just rostral to the obex in the medulla (fig. 2). It varies in length from approximately 1.3 to 1.6 mm and, continuing

caudally to the obex, the two "horns" of tissue converge at the midline forming a V-shaped organ (fig. 1).

In the rabbit, guinea pig and rat the area postrema is not bilateral, but is situated in the midline and forms the dorsal wall over the central canal just caudal to the extent of the fourth ventricle (figs. 1, 3, 7). In this position it overlies the alae cinereae and is bounded by the hypoglossal nuclei, the dorsal nuclei of the vagal nerves and the nuclei of the solitary tracts. In the rabbit the area postrema is about 0.6 to 0.8 mm in length, whereas in the guinea pig and the adult rat it extends for approximately 0.5 mm.

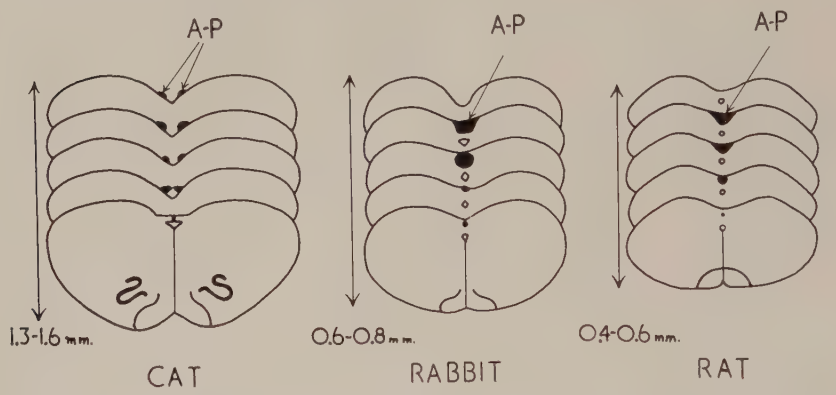

Fig. 1 A diagrammatic representation of the location of the area postrema (A-P) in the brain stem of cat, rabbit and rat. Note the bilaterality of the structure in the cat.

As the ependymal lining of the fourth ventricle continues over the area postrema, a morphological transition becomes apparent in the ependymal cells. The characteristic ciliated border is lost and the ependymal cells are no longer columnar, but assume a more cuboidal shape (fig. 15). The cell bodies of one characteristic cell type in the area postrema of the cat, the glialoid cell, vary in shape and size. These cells, however, have oval-shaped nuclei of consistent size (5 to 7 μ in diameter) which are markedly similar to the nuclei of the ependymal cells (figs. 14, 15). Elongated cytoplasmic extensions of the

glialoid cells attach to the walls of blood vessels. These modified ependymal cells exist in greatest numbers throughout the area postrema of the cat.

A second cell type, less numerous than the glialoid cell, can usually be identified in the area postrema of the cat. Although the cell bodies resemble small neurons seen in the medullary regions immediately surrounding the area postrema, and the cytoplasm contains thionin chromophilic material, argyrophilic fibers cannot be seen originating from these cells. Nevertheless, these cells have been called neurons (Brizzee and Neal, '54).

The area postrema of the cat, rabbit, guinea pig and rat was found to be richly innervated. Tissues impregnated by the Holmes' sliver technique revealed nerve fibers varying in diameter from one to 8 μ. The fibers formed a pathway between the surrounding medulla and the area postrema in every animal studied, regardless of the species. At the lateral aspects of the organ fascicles of nerve fibers assembled to form discrete tracts (figs. 4, 5, 6, 8, 9). On serial sections the fibers could be traced to the nearby nuclei of the solitary tracts and the dorsal nuclei of the vagal nerves. However, it could not be ascertained that the fibers arose from these areas. It seemed certain that the fibers did not arise from within the area postrema.

Upon entering the area postrema the fibers became dispersed and coursed freely among the parenchymal cells (figs. 10, 13, 14), often dividing into several branches. Some terminated on the walls of blood vessels (figs. 4, 5, 6), while others ended in intimate contact with the parenchymal cells (figs. 12, 13, 14). No specialized terminals could be found.

Many of the nerve fibers contained argyrophilic nodular swellings. These were not of uniform size or spacing and often three or 4 were seen along a short course of nerve (figs. 11, 12). The nodules occurred more frequently on fibers coursing within the area postrema, although a few were seen also on the axons in the lateral tracts.

COMMENT

In every mammal in which information is available on the subject, the area postrema exists as a highly vascular region in the dorsal medulla. Its position and size vary slightly in different species. Generally it can be said to lie in the floor of the fourth ventricle near the obex. The functional significance of this area has given rise to much speculation, and indeed anatomists have not even been able to agree on the types of cells that exist in this region. It is generally believed, however, that the main cell type in the area postrema is a neuroglial element, possibly derived from ependyma, and containing the staining characteristics of the protoplasmic astrocyte. Wilson ('06) described neurons in the area postrema of humans, whereas King ('37) not only stated that neurons were lacking in the area postrema of cats, but also that the region was devoid of nerve fibers and neural connections. Since King's work, however, Cammermeyer ('46) described nerve fibers in the area postrema of the human and Borison and Brizzee ('51) described them in the cat. Both felt that probably there were neural connections with other medullary areas.

The observations reported here clearly confirm those of Borison and Brizzee ('51) and more recently Brizzee and Neal ('54) on the existence of nerve fibers in the area postrema of the cat. Furthermore, it has been shown that the area postrema of the rabbit, guinea pig and rat contain an abundant innervation and that the nerve fibers enter the area postrema at a comparable point in each of the 4 species studied. Within the organ the fibers course among the parenchymal cells and terminate on cell surfaces and on blood vessel walls in a manner suggesting (1) a true secretomotor glandular innervation or (2) an afferent or receptor phenomenon associated with either the vascular system or the parenchymal cells of the area postrema on the one hand and some other region in the medulla on the other. No conclusive evidence exists to indicate which mechanism the described nerve fibers serve, nor has it been established whether the

nerves are motor or sensory. Experimental methods must be employed to determine the site of origin of these fibers. It seems quite certain, however, that the nerve fibers do not arise from within the area postrema, but enter the lateral aspect of the organ from elsewhere in the central nervous system.

SUMMARY

The morphology of the area postrema has been studied in cats, rabbits, guinea pigs and rats by various staining methods. Silver impregnated material revealed many nerve fibers within the area postrema. Fascicles of fine unmyelinated fibers and thicker fibers entered the lateral aspects of the area postrema from adjacent bulbar regions. Within the area postrema the fibers were seen to course freely among the parenchymal cells and to terminate on the walls of blood vessels and on parenchymal cell surfaces. The functional significance of these neural elements in the area postrema is yet to be established.

ACKNOWLEDGMENT

The authors acknowledge with thanks the technical assistance of Messrs. R. Ansell and J. Armstrong from the Department of Anatomy, University College, London, England.

LITERATURE CITED

Borison, H. L., and K. R. Brizzee 1951 Morphology of emetic chemoreceptor trigger zone in cat medulla. Proc. Soc. Exp. Biol. and Med., *77:* 38–42.

Borison, H. L., and S. C. Wang 1949 Functional localization of central coordinating mechanism for emesis in cat. J. Neurophysiol., *12:* 305–313.

Brizzee, K. R., and H. L. Borison 1952 Studies on the localization and morphology of the chemoreceptor trigger (C.T.) zone in the area postrema of the cat. Anat. Rec., *112:* 13–14 (Abstract).

Brizzee, K. R., and L. M. Neal 1954 A reevaluation of the cellular morphology of the area postrema in view of recent evidence for a chemoreceptor function. J. Comp. Neur., *100:* 41–61.

Cammermeyer, J. 1947 Is the human area postrema a neuro-vegetative nucleus? Acta Anat., *2:* 294–320.

Holmes, W. 1952 A new method for the impregnation of nerve axons in mounted paraffin sections. J. Path. and Bact., *54:* 132–136.

King, L. S. 1937 Cellular morphology in the area postrema. J. Comp. Neur., *66:* 1–22.

Koenig, H., R. A. Groat and W. F. Windle 1945 A physiological approach to perfusion fixation of tissues with formalin. Stain Tech., *20:* 13–20.

Pines, J. L. 1926 Über ein bisher unbeobachtetes Gebilde im Gehirn einiger Säugetiere: Das subfornicale Organ des III Ventrikel. J. f. Psychol. u. Neur., *34:* 186–193.

Putnam, T. J. 1922 The intercolumnar tubercle, an undescribed area in the anterior wall of the third ventricle. Johns Hopkins Hosp. Bull., *38:* 181–182.

Ranson, S. W., and P. R. Billingsly 1916 Vasomotor reactions from stimulation of the floor of the fourth ventricle. Studies in vasomotor reflex arcs III. Am. J. Physiol., *41:* 85–89.

Wang, S. C., and H. L. Borison 1950 The vomiting center: A critical experimental analysis. Arch. Neur. and Psychiat., *63:* 928–941.

Wilson, J. R. 1906 On the anatomy of the calamus region in the human bulb; with the account of the hitherto undescribed "nucleus postrema." J. Anat. (London), *40:* 210–241, 357–386.

Windle, W. F., R. Rhines and J. Rankin 1943 A Nissl method using buffered solutions of thionin. Stain Tech., *18:* 77–86.

Wislocki, G. B., and E. Leduc 1952 Vital staining of the hematoencephalic barrier by silver nitrate and trypan blue, and cytological comparisons of the neurohypophysis, pineal body, area postrema, intercolumnar tubercle and supraoptic crest. J. Comp. Neur., *96:* 371–414.

Wislocki, G. B., and T. J. Putnam 1920 Note on the anatomy of the areae postrema. Anat. Rec., *19:* 281–286.

———— 1924 Further observations on the anatomy of the areae postremae. Anat. Rec., *27:* 151–156.

PLATES

PLATE 1

EXPLANATION OF FIGURES

2 In this figure is shown the area postrema (AP) in a cat and its relation to the 4th ventricle (IV). Note the many blood vessels (bv) in this highly vascular structure. The outlined region in the upper right is shown in higher magnification in figure 5. Holmes' silver method, magnification × 60.

3 Here is shown the area postrema (AP) of a rat. It is seen to lie in the floor of the 4th ventricle (IV). The ventral boundary of the area postrema is designated by the arrows, and the outlined region in the upper right is shown in higher magnification in figure 6. Holmes' silver method, magnification × 60.

4 The arrows indicate a blood vessel in the area postrema of a rat and show nerve fibers terminating on and in the vicinity of the blood vessel. Holmes' silver method, magnification × 300.

5 This figure shows a detail of the outlined region in figure 1. The area postrema (AP) is seen to contain a large number of nerve fibers, many of which can be traced from the medulla (on the right) and which often terminate on blood vessel walls (arrows). Holmes' silver method, magnification × 360.

6 This shows a detail of the outlined area in figure 2. The rat, similar to the cat (fig. 5), shows fibers entering the area postrema from the surrounding medulla and terminating on the walls of blood vessels (arrow). Holmes' silver method, magnification × 360.

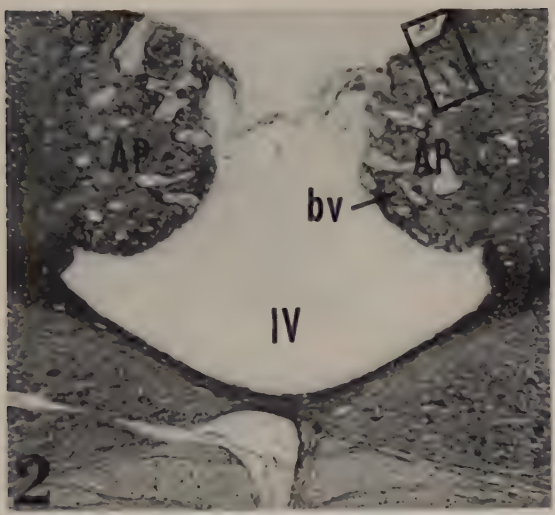
AP
AP
bv
IV
2

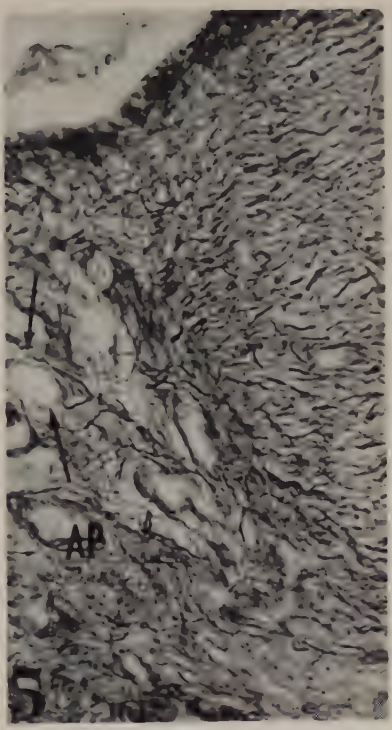
AP
5

IV
AP
3

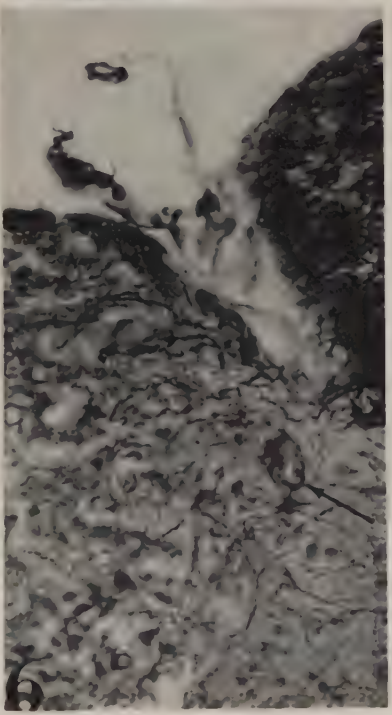
6

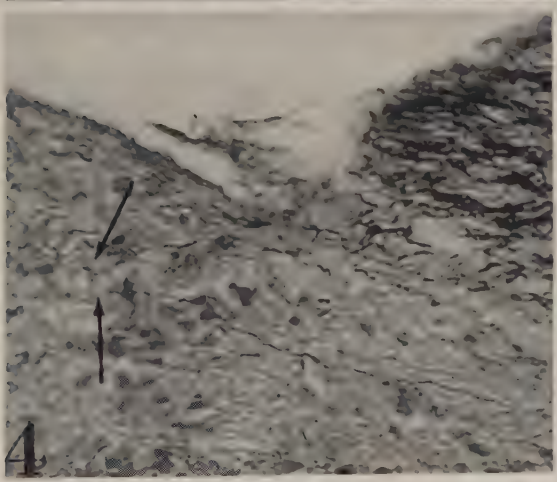
4

PLATE 2

EXPLANATION OF FIGURES

7 The three arrows indicate the extent of the area postrema in this section of the medulla in a guinea pig. The outlined areas (a, b and c) are shown in higher magnification in figures 8, 9 and 10 respectively. Bodian silver method, magnification × 60.

8 A detail of the outlined region (a) in figure 7. Here can be seen nerve fibers (nf) appearing as a compact bundle connecting the area postrema (to the right) and the medulla (to the left). Blood vessels (bv) are also designated. Bodian silver method, magnification × 360.

9 A detail of the outlined region (b) in figure 7. This shows an area comparable to figure 8, but on the opposite side of the area postrema and again illustrates similar bundles of fibers (nf) entering the area postrema from the surrounding medulla. Bodian silver method, magnification × 360.

10 A detail of outlined region (c) in figure 7. Note the intimacy with which the nerve fibers (nf) course amongst the glialoid cells (gc), often terminating on cell surfaces. Bodian silver method, magnification × 360.

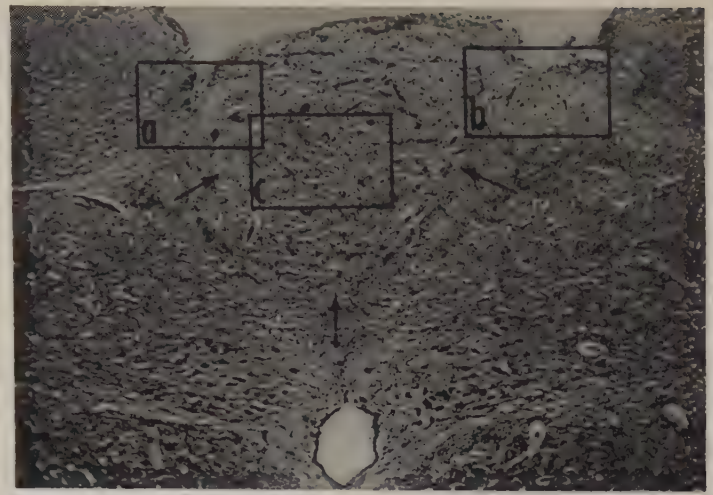
a
b
c

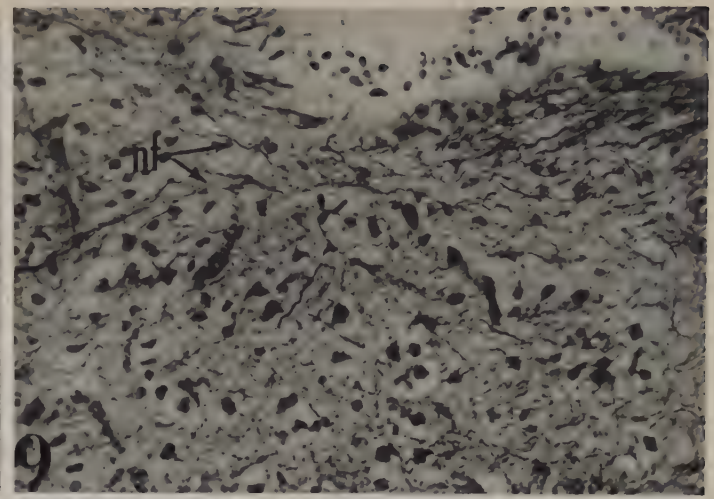
nf
9

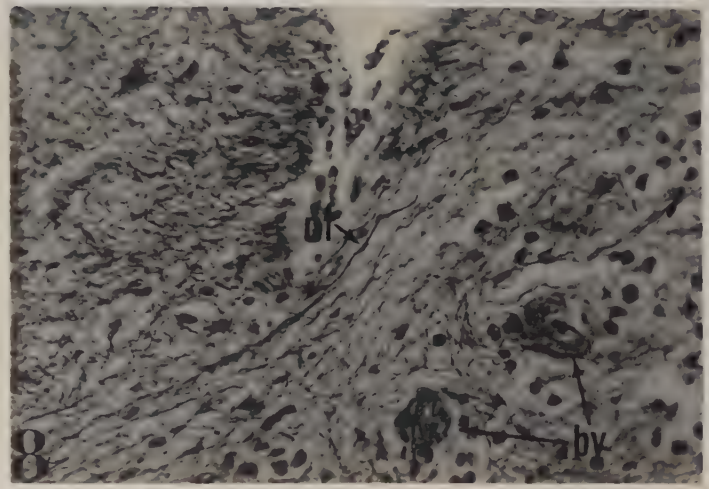
of
bv
8

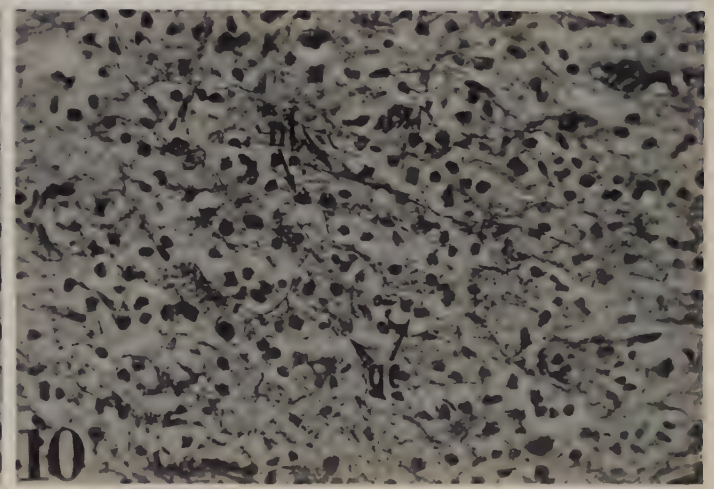
nf
gc
10

PLATE 3

EXPLANATION OF FIGURES

11 This figure illustrates under high magnification a nerve fiber in the area postrema of a rat showing the argentophilic nodules (n) which were often seen along the course of nerve fibers in this region. Holmes' silver method, magnification approximately × 850.

12 A high magnification photomicrograph of the area postrema of a cat showing a large nerve fiber with nodules (n) and the glialoid cells. Holmes' silver method, magnification approximately × 430.

13 Glialoid cells (gc) are seen with nerve terminals (t) ending directly on the cell walls. The nucleus and the cytoplasm of the cells are not in perfect focus with the nerve terminals. Holmes' silver method, magnification approximately × 850.

14 This photomicrograph shows a cluster of glialoid cells (surrounded by arrows) in the area postrema of the cat and an abundant number of nerve fibers coursing within the cell cluster. This typifies the general histologic structure throughout the area postrema of the cat. Holmes' silver method, magnification × 450.

15 Here is illustrated the region of transition between the ependymal cells (ep) lining the 4th ventricle (IV) and the glialoid cells (gc) of the area postrema (AP). Note that the ependymal cells lose their ciliated border and become flattened. Note also the similarity in size and impregnation of the nuclei in the glialoid cells of the area postrema and the ependymal cells. Holmes' silver method, magnification × 450.

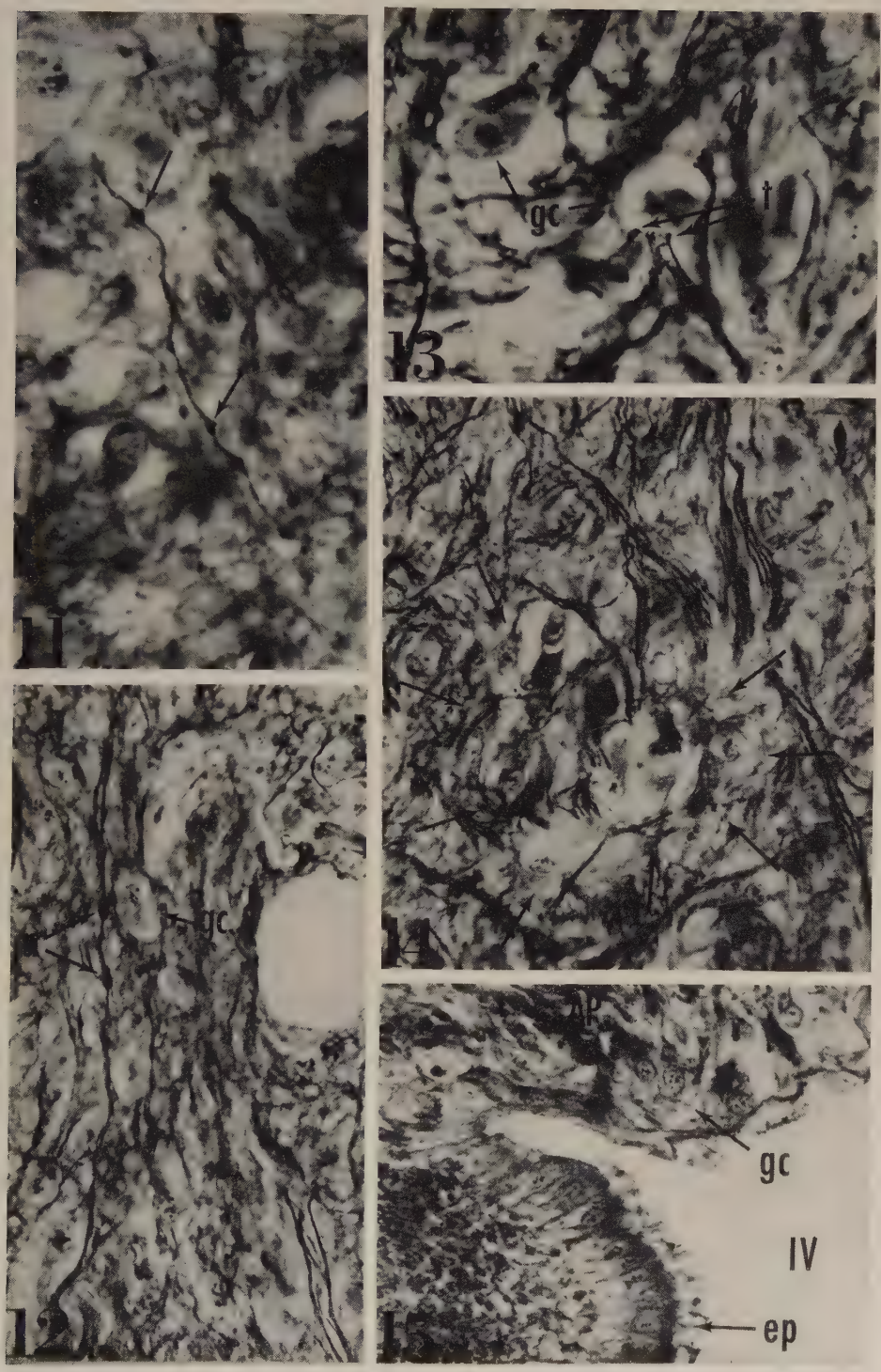
gc
gc
AP
gc
IV
ep

MORPHOGENETIC STUDIES OF THE RABBIT

XII. ORGAN SIZE IN RELATION TO BODY WEIGHTS IN ADULTS OF SMALL SIZED RACE X [1]

HOMER B. LATIMER
Department of Anatomy, University of Kansas
AND
PAUL B. SAWIN
Roscoe B. Jackson Memorial Laboratory, Bar Harbor, Maine

The extensive use of the rabbit as a laboratory animal in bacteriology, physiology, pathology and in laboratory dissections (Bensley, '45) seems to justify a more complete quantitative analysis of its anatomy. This study supplies 33 weights and linear dimensions of the major parts and organs of the body in a genetically synthesized race of rabbits of small adult body size.[2]

Intensive study of the body weight in the rabbit was initiated by MacDowell ('14) and Castle ('22). In 1932 Hammar published a monumental study on the postnatal growth of the native Swedish rabbit, including body weight and both gross and microscopic details of many of the organs. In the same year Allanson studied the postnatal growth of the hypophysis, using mixed races of rabbits obtained from dealers. Brown et al. ('26) published a study of body and organ weights of 645 adult male rabbits from various races,

[1] This investigation was supported (in part) by research grants from the American Cancer Society on the recommendations of the Committee on Growth of The National Research Council, and the National Cancer Institute of the National Institutes of Health, Public Health Service.

[2] This race has been closely bred by sib, parent-offspring and when necessary cousin matings for approximately 18–20 generations. Continuous sib-matings were not successful in the early generations without rigid selection to maintain reproductive capacity. These animals are taken from the subsequent 2nd, 3rd, and 4th generation of brother-sister matings.

as supplied by dealers. Levine et al. ('41) have weighed 14 systems and organs from male New Zealand white rabbits. Body weight and weights of 7 organs in Flemish Giant rabbits are given by Crile and Quiring ('40); and Sawin and Crary ('51) have studied the racial differences in the size of the gall bladder in several inbred races of rabbits.

The lengths of the long bones in the rabbit were studied by Castle ('22) and the skeletal parts have been studied more recently by Sawin and his co-workers (Sawin, '45, '46a, '46b; Hull, '47; Crary and Sawin, '49 and Tanner and Sawin, '53). Some quantitative information on individual organ weights in the rabbit is available in the data on control animals in various experimental studies but these usually include but a few specimens and often race and body weight are not given. A further study of the weights and percentage weights of the systems and organs in this important animal in a genetically controlled race is needed.

This study is part of a broader program aimed at differentiation of influences, both genetic and environmental, which affect growth and development of a mammalian species manifesting patterns of growth in many ways comparable to man.

Reports on detailed studies of the parts of the digestive system and the influence of the dwarf gene (Greene, '40) carried by this race are reserved for later communications. The weights of the parts of the brain have been reported (Latimer and Sawin, '55).

MATERIALS AND METHODS

The group of rabbits used in this study consisted of 50 males and 50 females of inbred race X, and varied in age from about 5 months to over two years. They were descended from Castle's small sized race and outcrossed in 1936 to include the dwarf gene. Fifteen males and 20 females carried this dwarf gene in the heterozygous condition and the effects of this dwarf gene upon the various organs will be reported in a later communication. They were raised at the Roscoe B.

Jackson Memorial Laboratory and delivered by railway express for dissection in Kansas. During the three to 4 days enroute, they subsisted upon hay and carrots supplied at packing time. Each animal was weighed just before it was shipped and immediately after its arrival in Kansas. The range of weight shrinkage enroute varied from 2.67 to 20.56% (average 9.40) for the males and from 2.11 to 20.46% (average 10.24) for the females. This loss was recovered rapidly, usually in one to three days.

The steps in the dissection are listed and described in chronological order. All parts of the rabbits were kept in moist chambers to avoid drying, when not actually being worked upon.

As soon as they had regained their shipping weight, the rabbits were weighed and sacrificed with chloroform. Immediately after death they were laid on a table with the right side down and the total length (nose to tip of tail) and the body length (nose-anus) were measured with a flexible steel tape graduated in millimeters. In both of these measurements the tape followed the contour of the body along the mid-dorsal line, using the ischial tuberosity as the landmark for the caudal end of the nose-anus length. These measurements were followed by a series of 15 linear measurements made with a vernier caliper reading to 0.1 mm. All readings were made to the nearest millimeter. These linear measurements are not included in this report.

The integument, including the ears and the toe nails, was removed with as little subdermal fat as possible and weighed.

The head was severed from the body by an incision starting at the dorsal base of the skull and passing ventrad, close to the base of the skull, between the occipital condyles and the atlas and cephalad to the larynx, thus severing the brain from the cord at the level of the upper root fila of the first cervical nerve. The fore limbs were removed by first palpating the tip of the coracoid process, then carrying the incision just distal to this process and inwards to the capsule of the shoulder joint. Then the humerus was easily separated from

the glenoid cavity of the scapula. The two hind limbs were removed by an incision passing close to the ilium and along the ventral side of the os coxa and pubis, thus exposing the capsule of the hip joint.

The fat deposits of ventral abdomen, scapular, inguinal and neck regions and from the dorsal part of the abdominal cavity and the thorax were removed as encountered, placed in the moist chamber and weighed when all had been assembled. In some animals the kidneys and suprarenals were almost completely imbedded in fat. Some fat remained diffusely distributed between the various muscles and in other places and this constitutes a certain amount of error.

The thyroid gland and contents of the chest cavity were exposed by a midline incision from the larynx along the ventral side of neck to sternum and then passing to each side of the sternum through the costal cartilages. The infrahyoid muscles were displaced laterally and the thyroid gland removed. The lungs and heart were raised from the thoracic cavity by separating the trachea from the esophagus and lower end of the larynx and incising the phrenic nerves, vagi and blood vessels on the right side first and then on the left, including the aorta. The trachea and bronchi are included in the weight of the lungs. Considerable loose connective tissue, fat and the thymus found in the neck and thoracic inlet were removed as completely as possible. The cavities of the heart were opened and the contained blood washed out and then the heart was dried with paper toweling and placed in the moist chamber. All vessels were severed close to the heart.

The organs of the abdominal cavity were removed, freed of fat, the blood vessels cut as close as possible to the organ and then put in watch glasses in the moist chamber. The diaphragm was incised and the symphysis pubis split so that the entire digestive tube could be removed and weighed together with its contents. It was then divided into its parts or regions, the length of each measured and the contents removed by "milking" them from the parts of the tube.

The sum of the lengths of the parts before removing the contents is the length of the digestive tube, and the sum of the weights of these parts after removal of the contents is the weight of the empty digestive tube. The difference between this weight and the weight of the tube and its contents is the weight of the contents. The eyeballs and the harderian glands were removed and put in the moist chamber.

After all of the organs had been removed, the remaining blood vessels and fat were removed and the trunk, head and the two pairs of extremities were all weighed together. Then each part was taken, one at a time, and all of the muscles were removed. The weight of the skeleton and central nervous system subtracted from the weight of the musculature, skeleton and central nervous system is the weight of the musculature. It was easier to keep the individual parts from drying than to keep the musculature from drying until it could all be weighed.

The brain, spinal cord and hypophysis were next removed. Their weight subtracted from the combined weight of the skeleton and the central nervous system is the weight of the ligamentous skeleton. The ligamentous skeleton was soaked over night in water with a small amount of powdered soap and the following day was cooked in a solution of washing powder until the bones could easily be separated. Any remaining bits of muscle or ligaments were removed and the bones with the cartilages were allowed to drain on paper toweling until all excess water had been removed. The moist cartilaginous skeleton was then weighed.

The entire rabbit, its major parts, the integument and the entire digestive tube and its contents were all weighed to the nearest gram on a laboratory balance sensitive to 0.1 gm. The smaller organs were weighed on an analytical balance sensitive to 0.1 mg. The larger organs were weighed only to the nearest milligram and the smaller organs to 0.1 mg. All weighings on the analytical balance were made in weighing bottles to avoid loss through evaporation.

The gross body weight is the weight of the entire animal prior to anesthetization. Net body weight is the gross body weight minus the weight of the contents of the digestive tube and the fat. The weights of all paired organs include both right and left organs. All of the measurements are for 50 animals except the lungs and the uteri. One pair of pathological lungs was found in each sex and three females were in very early pregnancy and these uteri were not included.

The empirical formulae in tables 3 and 4 were derived by the method of least squares (Snedecor, '38). The data were arranged first in order of increasing body weight and all individual weights plotted and then these data were grouped by intervals of 200 gm. The average body weight was determined for each of these groups and when the individual organs or parts were being studied, the average organ weight for each group was found and plotted against the gross body weight average. These double averages were used in determining the formulae and also for comparing the observed and calculated averages. Similar groups with a range of body length (nose–anus) of 20 mm were used for the study of the organ weights against nose-anus length. The plotting of the entire group permitted a study of the scatter and distribution of the individual weights.

Weights and linear measurements

The average, standard deviation and the coefficient of variation of the weights and linear measurements of the males and females are shown in table 1. The last column shows the "t" values for the sex differences in the averages.

The females are heavier by 17% and also longer and, as is to be expected, all of the other measurements are greater in the females with only two exceptions, namely, the weights of the integument and harderian glands which are heavier but not significantly so in the males. Sixteen measurements in the females are significantly greater and 13 other measurements are greater but not significantly greater.

TABLE 1

Weights in grams and lengths in millimeters

	50 MALES			50 FEMALES			"t" [1]
	AVERAGE	STAND. DEV.	COEF. VAR.	AVERAGE	STAND. DEV.	COEF. VAR.	
Body weight, gross	1870.0	301.81	16.14	2192.9	459.67	20.96	4.11
Body weight, net	1565.4	244.43	15.61	1734.9	337.3	19.44	2.86
Body leng., nose-tail	528.2	30.8	5.82	546.5	37.2	6.81	2.65
Body leng., nose-anus	454.6	24.1	5.30	478.3	33.7	7.05	4.00
Head	111.8	15.6	13.93	113.8	16.6	14.57	0.62
Trunk	1092.8	178.7	16.36	1329.3	296.5	22.30	4.81
Fore limbs	69.3	12.6	18.13	74.9	16.3	21.72	1.91
Hind limbs	270.3	45.9	16.96	310.7	72.5	23.34	3.30
Integument	238.5	47.0	19.70	236.4	47.2	19.88	0.21
Musculature	874.9	153.8	17.57	1018.1	218.6	21.47	3.75
Skeleton, lig.	170.2	26.7	15.69	183.8	31.9	17.34	2.29
Skeleton, cart.	110.4	17.3	15.69	117.1	20.3	17.35	1.17
Fat	110.1	54.6	49.57	249.9	132.7	53.11	6.83
Digest. tube wgt.	83.114	13.16	15.83	88.485	16.50	18.65	1.77
Digest. tube wgt. contents	195.015	42.61	21.85	208.146	67.28	32.32	1.15
Digest. tube length	3961.6	450.4	11.37	4100.6	485.2	11.83	1.47
Liver	67.867	17.14	25.26	72.107	22.97	31.85	0.33
Pancreas	4.263	1.273	29.87	5.261	1.58	29.99	3.45
Lungs [2]	13.197	6.672	50.56	12.359	5.067	41.00	0.71
Lungs (clear only)	8.015	1.245	15.54	9.070	1.716	18.92	2.66
Heart	4.318	0.710	16.44	4.583	0.889	19.41	1.63
Spleen	0.4899	0.196	40.02	0.5615	0.230	40.89	1.66
Thyroid	0.1203	0.0340	28.30	0.1406	0.0571	40.62	2.32
Suprarenals	0.2959	0.0988	33.40	0.3300	0.1093	33.11	1.62
Hypophysis	0.0270	0.0062	22.92	0.0361	0.0123	34.05	4.63
Gonads	3.613	1.396	38.65	0.422	0.264	62.66	...
Uterus [3]				7.938	3.411	42.96	...
Kidneys	14.897	2.868	19.25	15.970	3.515	22.01	1.65
Bladder, urinary	1.144	0.256	22.38	1.332	0.419	31.46	2.68
Eyeballs	5.032	0.444	8.81	5.487	0.575	10.49	4.38
Harderian glands	1.538	0.492	31.97	1.364	0.411	30.13	1.90
Brain	9.156	0.537	5.86	9.349	0.717	7.67	1.48
Spinal cord	3.925	0.384	9.78	4.292	0.470	10.96	4.23

[1] "t" values above 1.98 are significant at the 5% level and those above 2.63, at the 1% level.

[2] Only 49 animals.

[3] Only 47 animals.

The net body weight is 16% less than gross body weight in the males and 21% in the females. This greater difference in the females is due in large part to the greater amount of fat, which is more than double that found in the males. The contents of the digestive tube is also somewhat greater in the females. The difference between the average lengths of the nose to tip of tail length and the nose-anus length is the length of the tail, which is 74 mm in the males and 68 mm in the females. The lengths of the tail itself were measured in some of the specimens and these measurements were very similar to the tail length derived from the two linear measurements of the body. The ligamentous skeleton is a little over one third heavier than the cartilaginous skeleton due to the loss of blood, the ends of tendons and small pieces of flesh in the process of soaking and cooking the skeleton. It is interesting to see that the testes minus the epididymi are about 9 times the average weight of the ovaries.

The average female rabbit is larger, 30% more variable in gross body weight and 33% more variable in body length (nose-anus). The average of the coefficients of variation for the male rabbits is 21.11% with a range from 5.30 to 50.56%. The similar average for the females is 25.34% with a range of 6.81 to 62.66%. The two lowest coefficients of variation are for the body lengths which are linear, or but one dimensional measurements, and therefore less than the three dimensional measurements of volume or weight. The parts of the central nervous system have low coefficients of variation in these rabbits as in many other animals. The head alone, of the 4 parts of the body, is less variable than the total body weight.

The 4 organs having the maximum variability, but not in the same order in both sexes are: gonads, spleen, fat and lungs, and the uterus in the females. These are all organs which due to various reasons are usually quite variable.

The two lines in table 1, listing "all" the lungs and in the line below, the "clear" lungs only, need some comment. It was found, during the dissections, that the color of the lungs varied, some being pink in color and others dark red, as

though gorged with blood. The condition or color of the lungs was marked on each individual data card at the time of autopsy and only the 28 male and 32 female lungs marked "clear" are included in this second line. The average weight for the "clear" lungs is 39% less in the males and 27% less in the females. All of these lungs were plotted on gross body weight and nose-anus length and the two groups of "clear" and "bloody" lungs were distinctly separate, with no intermingling of the cases. In another series of rabbits, electrocution and nembutal were used as well as chloroform. Nembutal seems to give the best results but these findings will be published later.

As the ovaries were removed, a marked difference in the size and number of ovarian follicules was observed, which contributes to the high variability of this organ. As expected, the thyroid and hypophysis are more variable in the females.

The weights of each of the organs in grams of each rabbit were reduced to percentages of the net body weight and the averages, the standard deviations and the coefficients of variation of the individual percentages are given in table 2. The "t" values for the sex differences of the average percentage weights are given in the last column. In contrast with table 1, where there are but two organs heavier in the males, in this table 15 of these percentages are greater in the males and of these 5 are significantly greater. Ten of these percentages are larger in the females with 5 of these significantly greater.

The 5 parts which are significantly greater when expressed as percentages of net body weight in the males are: head, harderian glands, brain, integument and heart. The greater relative size of the first three of these suggests a certain degree of cephalization in the male rabbit. The greater relative weight of the heart and integument is no surprise, for the males are generally more active than the females and at autopsy one readily notices the greater toughness of skin and connective tissues in the male. The fat shows the greatest sex difference in percentage weight as well as in absolute

weight for the average percentage weight of fat in the females is double that of the males. The hypophysis, as is to be expected, is relatively heavier in the females. Whether measured in grams or as percentages of net body weight, the female rabbit of race X has a larger trunk, more fat, a greater mass of muscles, and a larger hypophysis.

TABLE 2

Percentages of the net body weight

	50 MALES			50 FEMALES			"t" [1]
	AVERAGE PER CENT	STAND. DEV.	COEF. VAR.	AVERAGE PER CENT	STAND. DEV.	COEF. VAR.	
Head weight	7.17	0.36	5.01	6.63	0.49	7.33	6.19
Trunk weight	69.78	2.74	3.92	76.27	4.74	6.22	8.36
Fore limbs	4.42	0.30	6.82	4.29	0.37	8.72	1.90
Hind limbs	17.25	0.96	5.58	17.66	1.33	7.51	1.75
Integument	15.19	1.58	10.42	13.66	1.25	9.17	5.34
Musculature	55.72	2.48	4.46	58.50	3.17	5.41	4.83
Skeleton, lig.	10.92	1.03	9.39	10.66	0.84	7.88	1.37
Fat	7.00	3.02	43.23	14.08	6.00	42.65	7.32
Digest. tube wgt.	5.37	0.90	16.81	5.15	0.70	13.53	1.34
Digest. tube contents	12.55	2.54	20.26	12.10	3.65	30.18	0.70
Liver	4.36	0.99	22.69	4.07	0.97	23.88	1.47
Pancreas	0.271	0.058	21.52	0.305	0.072	23.46	2.60
Lungs, all [2]	0.837	0.388	46.37	0.745	0.363	48.70	1.22
Lungs, clear only	0.523	0.043	8.26	0.500	0.060	11.93	1.66
Heart	0.277	0.024	8.53	0.266	0.029	10.85	2.07
Spleen	0.031	0.011	34.03	0.032	0.011	33.96	0.46
Thyroid	0.00763	0.00157	20.55	0.00802	0.00224	27.97	0.99
Suprarenals	0.0188	0.0054	28.84	0.0193	0.0061	31.85	0.43
Hypophysis	0.00175	0.00041	23.55	0.00207	0.00053	25.52	3.35
Gonads	0.229	0.067	29.13	0.0239	0.0131	54.85	...
Uterus [3]	....	....	....	0.453	0.140	30.96	...
Kidneys	0.958	0.155	16.21	0.927	0.138	14.89	1.04
Bladder	0.073	0.011	14.57	0.077	0.017	22.27	1.36
Eyeballs	0.328	0.047	14.34	0.324	0.048	14.77	0.42
Harderian glands	0.097	0.022	22.75	0.078	0.018	22.98	4.70
Brain	0.596	0.077	12.94	0.554	0.082	14.77	2.66
Spinal cord wgt.	0.255	0.031	12.15	0.253	0.032	12.85	0.41

[1] "t" values above 1.98 are significant at the 5% level and those above 2.63, at the 1% level.

[2] Only 49 animals.

[3] Only 47 animals.

These percentage weights are all less variable in both sexes than the weights in grams, except the percentages of the three parts of the nervous system, and the weight of the empty digestive tube. The male hypophysis is slightly more variable when expressed as a percentage of net body weight. The average of all male coefficients of variation is 17.8% or 16% less than the similar coefficients of the absolute weights of these parts. The average for the females is 20.9% or a reduction of 17% over these weights in grams.

The average weights or lengths of these measurements are given in table 1. However to more accurately estimate these dimensions in rabbits above or below average body weight, empirical formulae have been developed. In table 3 all of the formulae for the males and females are based on gross body weight in grams and in table 4 the formulae are based on nose-anus length measured in millimeters. These formulae all represent straight lines whose slopes increase with body weight or body length and to save space they are not shown. The individual cases, for most of the organs, were moderately scattered around these regression lines.

These formulae are valid only between 1300 and 2400 gm of gross body weight for the males and from 1400 to 3200 gm inclusive, for the females. The formulae in table 4 are valid only between 400 and 500 mm of nose-anus length for the males and between 415 and 530 mm inclusive for the females, except those otherwise designated in the tables. The figures in parentheses following the formulae in both tables are the average percentage deviations of the calculated from the observed averages.

The average percentage deviations are generally small indicating that nearly all of these lines are rather well fitted to the data. Obviously those organs having a wide range of variation could not be fitted with an empirical formula with the same degree of accuracy as those with less variation. Most of the percentage deviations are below 10%. All of the organs with an average percentage deviation over 10% are organs with large coefficients of variation. For example,

TABLE 3

Empirical formulae for estimating the dimensions of the organs and parts of the male and female rab from gross body weight. X represents the gross body weight in grams. Formulae are to be used only within limits given in text

	MALES				FEMALES			
Nose-anus length	= 0.075X	+	314.1	(2.04%)	= 0.053X	+	357.0	(2.19
Head weight	= 0.046X	+	25.0	(2.25%)	= 0.033X	+	40.77	(3.35
Trunk weight	= 0.58X	+	8.0	(0.67%)	= 0.63X	—	48.97	(1.93
Fore limbs wgt.	= 0.036X	+	1.5	(1.24%)	= 0.032X	+	4.37	(4.01
Hind limbs wgt.	= 0.141X	+	5.0	(1.81%)	= 0.13X	+	20.53	(3.49
Integument	= 0.13X	—	4.9	(3.05%)	= 0.093X	+	32.3	(3.51
Musculature	= 0.49X	—	46.1	(1.35%)	= 0.46X	+	8.0	(1.56
Skeleton, lig.	= 0.071X	+	37.52	(2.02%)	= 0.059X	+	53.6	(4.64
Skeleton, cart.	= 0.049X	+	18.643	(1.35%)	= 0.037X	+	35.2	(4.54
Dig. tube empty	= 0.025X	+	36.085	(3.97%)	= 0.023X	+	37.373	(6.47
Contents, dig. tube	= 0.08X	+	43.0	(4.86%)	= 0.071X	+	49.19	(7.74
Dig. tube length	= 0.98X	+	2110	(2.17%)	= 0.79X	+	2359	(3.13
Liver	= 0.035X	—	1.546 [1]	(8.18%)	= 0.031X	+	4.925	(8.38
Pancreas	= 0.0029X	—	1.1248	(9.02%)	= 0.002X	+	0.8755	(2.09
Lungs (clear only)	= 0.0033X	+	1.731	(5.27%)	= 0.0029X	+	2.2239	(8.67
Heart	= 0.002X	+	0.62	(3.29%)	= 0.0015X	+	1.2894	(2.48
Spleen	= 0.00031X	—	0.0829	(5.98%)	= 0.00025X	+	0.0134	(11.06
Thyroid	= 0.000085X	—	0.037	(5.49%)	= 0.000085X	—	0.0415 [2]	(5.34
Suprarenals	= 0.00016X	+	0.0007	(8.13%)	= 0.000079X	+	0.1626	(7.83
Hypophysis	= 0.0000049X	+	0.0176	(5.86%)	= 0.000017X	—	0.0008	(6.25
Kidneys	= 0.0067X	+	2.592	(5.81%)	= 0.005X	+	4.888	(3.81
Gonads	= 0.0029X	—	1.786	(12.83%)	= 0.00045X	—	4.6046 [3]	(16.67
Uterus					= 0.0052X	—	3.2388	(10.89
Bladder	= 0.00058X	+	0.0488	(2.28%)	= 0.00065X	—	0.0842	(6.71
Eyeballs	= 0.00072X	+	3.688	(1.74%)	= 0.00079X	+	3.7736	(1.96
Harderian glands	= 0.00095X	—	0.2842	(4.76%)	= 0.00058X	+	0.0779	(10.46
Fat	= 0.126X	—	118.0	(10.94%)	= 0.21X	—	208.0	(14.91
Brain	= 0.001X	+	7.212	(2.05%)	= 0.0011X	+	6.9119	(2.09
Spinal cord wgt.	= 0.0008X	+	2.435	(1.64%)	= 0.00079X	+	2.5639	(1.64
Spinal cord length	= 0.04X	+	202.0	(0.34%)	= 0.026X	+	230.3	(1.69

[1] For body weight 1500 to 2400 gm only.
[2] For body weight 1400 to 2800 gm only.
[3] For body weight 1800 to 3200 gm only.

TABLE 4

pirical formulae for estimating the weights or lengths of the various parts and organs of the males and females from the body length. X represents the body lengths (nose-anus) in millimeters. Formulae are to be used only within limits given in text

	MALES				FEMALES			
d weight	= 0.59X	—	156.0	(0.35%)	= 0.45X	—	102.0	(3.14%)
nk weight	= 6.85X	—	2014.0	(1.21%)	= 8.4X	—	2679.0	(4.96%)
e limbs wgt.	= 0.44X	—	130.56	(0.65%)	= 0.42X	—	127.0	(4.40%)
d limbs wgt.	= 1.69X	—	498.81	(1.34%)	= 1.7X	—	507.3	(3.81%)
gument	= 1.5X	—	440.1	(3.00%)	= 1.2X	—	341.0	(5.93%)
sculature	= 5.8X	—	1761.0	(1.82%)	= 6X	—	1850.0	(3.07%)
leton, lig.	= 0.97X	—	270.52	(2.12%)	= 0.91X	—	251.63	(3.26%)
leton, cart.	= 0.65X	—	185.34	(2.34%)	= 0.57X	—	155.6	(3.42%)
. tube, empty	= 0.3X	—	51.84	(3.10%)	= 0.43X	—	118.95	(9.17%)
. tube, contents	= 0.97X	—	245.2	(1.76%)	= 1.3X	—	414.4	(8.89%)
. tube length	= 13X	—	1949	(2.36%)	= 13.4X	—	2320	(3.69%)
er	= 0.25X	—	44.679	(6.22%)	= 0.83X	—	334.859 [1]	(3.93%)
ncreas	= 0.029X	—	8.938	(7.44%)	= 0.022X	—	5.352	(7.22%)
gs (clear only)	= 0.04X	—	10.107	(3.16%)	= 0.061X	—	20.404	(6.86%)
rt	= 0.023X	—	6.053	(3.20%)	= 0.021X	—	5.503	(3.71%)
een	= 0.0044X	—	1.4911	(10.22%)	= 0.0046X	—	1.6378	(7.61%)
roid	= 0.0011X	—	0.3794	(5.45%)	= 0.00087X	—	0.2787	(9.59%)
rarenals	= 0.0019X	—	0.5517	(10.01%)	= 0.0013X	—	0.2899	(6.29%)
pophysis	= 0.000069X	—	0.0049	(5.35%)	= 0.00025X	—	0.0835	(6.94%)
neys	= 0.077X	—	19.556	(6.36%)	= 0.093X	—	28.434	(7.07%)
ads	= 0.032X	—	10.879	(6.10%)	= 0.003X	—	0.9886	(8.69%)
rus					= 0.077X	—	28.905 [2]	(10.87%)
dder	= 0.0067X	—	1.9009	(2.91%)	= 0.0083X	—	2.6438	(4.14%)
balls	= 0.0096X	+	0.6749	(0.58%)	= 0.013X	—	0.679	(1.39%)
derian glands	= 0.012X	—	3.923	(1.21%)	= 0.01X	—	3.4286 [2]	(7.04%)
	= 1.21X	—	434.0	(11.12%)	= 1.6X	—	504.0 [2]	(8.55%)
in	= 0.015X	+	2.297	(1.41%)	= 0.016X	+	1.6875	(2.01%)
nal cord wgt.	= 0.011X	—	1.0634	(0.96%)	= 0.013X	—	1.9181	(1.60%)
nal cord length	= 0.5X	+	49.0	(0.28%)	= 0.52X	+	40.0	(0.72%)

[1] From 450 to 530 mm of body length only.
[2] From 430 to 530 mm of body length only.

the weight of the uterus against either body weight or body length has an average percentage deviation of over 10%. Likewise in table 3 the gonads, fat, spleen and harderian glands have average percentage deviations over 10% and all have large coefficients of variation. In table 4 there are but three male organs with deviations over 10% (spleen, suprarenals and fat). In the females, the uterus has the largest percentage deviation (10.87%) and the only one above 10%. These percentage deviations in tables 3 and 4 not only show that the females are less well fitted by these formulae but also reflect the greater variability of the females, and of these specific organs, which due to cyclic or physiological functions, vary a great deal irrespective of the body weight or length. They further show that body length used as abscissae do not give as close an approximation to the observed organ weight as the use of gross body weight.

All of these are simple first degree algebraic formulae, and it is merely necessary to substitute either gross body weight in grams or nose-anus length in millimeters and solve for the estimated weight in grams or length in millimeters of the organ or part. The weights thus obtained will more nearly approximate the weight of an average organ for the respective body weight or body length, unless body weight or body length is very close to the average for the group.

DISCUSSION

A considerable amount of information is available upon the body weights in various races, in backcrosses and in mixed groups of rabbits.

Castle ('31) gives a coefficient of variation for adult body weight of 7.1% for males and 8.3% for females of the small sized race from which race X is derived, and 7.1 and 9.1% respectively, for the large sized race of Checkered Giant origin. MacDowell ('14) gives coefficients of variation for 16 families of rabbits, some of them backcross groups, whose coefficients vary from 5.9% to a maximum of 13.6%, or an average of 9.9%. Levine et al. ('41) give body weights of

10 adult male New Zealand white rabbits, and using these weights a coefficient of variation for the gross body weight of 12.4% was found. Hammar ('32) in his study of postnatal growth of the native Swedish rabbit lists a coefficient of variation of 12.5% for all rabbits, both male and female, in the postpuberal period, and Brown et al. ('26) found a coefficient of variation of 14.9% in 645 male rabbits of mixed breeds as supplied by dealers. The coefficients of variation of 16% for the males and 21% for the females in race X appear large, but some of this variability can be explained by the presence of 15 males and 20 females carrying the dwarf gene (Greene, '40). The effect of this gene on these rabbits is being studied and will be reported in another communication. The normal and dwarf groups separately have a variability of about 14% showing that a part of the variation in these rabbits is genetic.

Coefficients of variation for the live weight in 7 families of inbred guinea pigs (Eaton, '38) ranged from 10.1 to 14.1% and in a random collection of plain alley cats, Latimer ('36) found coefficients of variation of 25.0 for the males and 21.1% for the females. Thus we find these rabbits more variable than Eaton's guinea pigs but not as variable as the cats. Since nothing is said with regard to inbreeding in Castle's original race, it is presumed that the usual procedure among practical rabbit breeders was employed.

Although race X is undoubtedly much more uniform genetically than the material of most studies of this kind, this race still is not isogenic, and since it is not possible to secure large numbers from the same mating it seems likely that a further portion of this variation is also the result of genetic segregation. The coefficients of inbreeding calculated by the method of Cruden ('49) for two of the larger groups of sibs shows a value of approximately 50%.

Two possible sources of the variation in weight of the rabbits of race X have been examined, namely, age and seasonal variation. To test the possible influence of age, the body weights and the weights of several of the organs of

both sexes were plotted against age in days. The range of abscissae was from 130 to 1080 days for the males and from 170 to 1240 days for the females. No trends could be recognized in any of these field graphs, in either sex, since the younger members of the group were fully mature and the older rabbits showed no apparent quantitative effects of senescence. To test the effects of season on the weights of the body, integument and several of the internal organs, the weights in grams and also the percentages of net body weight, were placed in two groups, one for the summer season and the other for the winter months, and the averages were found for these two periods. Most of these rabbits were sacrificed in the cooler months of the year. The skin seems to evidence the greatest reaction to the seasonal influence, being on the average heavier in the winter. There was much individual variation and much intergradation between the two groups when these data were plotted. In a recent paper, Crary and Sawin ('53) show that there is no apparent seasonal effect on the growth of the fur in the angora rabbit. Brown ('29) has studied the seasonal fluctuations of the organ weights in a series of 645 rabbits and he feels that there are seasonal variations. Due to the irregularity of the weights and percentage weights of our rabbits and of their organs, no definite conclusions can be drawn from the present data.

Comparison of the individual organ weights of race X with those of other studies on rabbits shows both similarities and dissimilarities. The percentage weights from 4 papers which give most of the data on organ weights are summarized in table 5. All data are for males except the percentages given by Hammar, which include both sexes, and the percentages calculated from the weights in grams published by Crile and Quiring which are for female rabbits. Some of the percentages were relative to gross body weights and to make comparisons, the percentages of these organs relative to gross body weight for race X are shown in the last column.

This table also shows that the following systems and organs are relatively heavier in race X: integument, mus-

culature, skeleton, fat, all lungs together, hypophysis, kidneys and the brain, while the liver, suprarenals and testes are very much alike in all the groups. The heart, spleen and thyroid are relatively lighter in race X. The first three percentages listed from Hammar, or musculature, skeleton and fat, are relatively much smaller than the same parts in race X. Race X was on the average very fat, but the musculature and skeleton follow the general pattern as usually given for man and most animals (Latimer, '44).

TABLE 5

The percentage values of the various organs and systems as reported by several workers

	PERCENTAGE OF NET BODY WEIGHT			PERCENTAGE OF GROSS BODY WEIGHT		
	Race X	Brown et al.	Levine et al.	Hammar	Crile and Quiring	Race X
Integument	15.2	...	13.4	...	...	12.73
Musculature	55.7	...	52.0	34.2	...	46.69
Skeleton, lig.	10.9	...	8.0	5.1	...	9.15
Fat	7.0	...	...	2.2	...	5.82
Liver	4.36	4.74	3.61	3.4	3.19	3.65
Lungs (all)	0.837	...	0.603	..	0.530	0.700
Heart	0.277	0.287	0.307	..	0.357	0.32
Spleen	0.031	0.056	0.059	..	....	0.0261
Thyroid	0.0076	0.0127	0.0132	0.050	0.0156	0.0064
Suprarenals	0.0188	0.0208	0.0158	..	0.0256	0.0157
Hypophysis	0.00175	0.00155	...	..	....	0.00147
Testes	0.229	0.253	...	0.2	....	0.192
Kidneys	0.958	0.713	0.705	0.6	0.707	0.802
Brain	0.596	0.508	0.32	..	0.392	0.499

Allanson ('32) has studied the increase in weight of the hypophysis during the postnatal growth of 48 male and 31 female rabbits of mixed breeds. Kibler et al. ('42 and '43) have studied the growth of the 4 endocrine glands in a series of New Zealand white rabbits. The weights of the body and all 4 glands are heavier in these New Zealand rabbits. The percentages with reference to gross body weight of hypophysis and thyroid are greater in race X, the percentages of the

suprarenals are very similar in both races and the gonads are relatively larger in both sexes in the New Zealand white rabbits. These data are of course inadequate for final conclusions, but they do seem to point to a distinct cephalization in race X as far as these 4 glands are concerned. The enlargement of the thyroid and hypophysis in race X is also of interest in view of the previous observations on this race (Peck and Sawin, '50).

The percentage weights of the kidneys from 7 male and 7 female rabbits listed by Denzer ('38) are much like the percentages found in this series of rabbits. Schmidt and Ivy ('37) give the weight of the liver as 2.70% of the body weight, but they do not give the number of rabbits used, the body weight or the sex. This percentage is below the average of our series but still within the range of our percentages. Jaffe ('51) gives the body weight and the weight of the pancreas in 6 rabbits but he does not mention the race. Jaffe's rabbits are larger but the weight of the pancreas in race X is 1.8 times heavier than his weights as percentages of the gross body weight. Rous and Robertson ('17) report the spleen weight in an 1800 gm rabbit as 0.6 gm or 0.033% of the body weight which is not far from the average of our group.

Brown et al. ('26) list coefficients of variation for 9 organs, Hammar ('32) for 5, and the coefficients of variation were calculated from the 7 weights given by Levine et al. ('41) and these coefficients are compared with the similar coefficients of race X. Coefficients for 4 organs are represented in three of these groups of rabbits and by comparison race X is the least variable in the weights of the heart, thyroid and suprarenals and is intermediate between the data given by Levine and Brown for the weight of the spleen. The coefficients of the musculature and skeleton are greater in race X than those of Hammar and the fat in race X is less variable than the fat as reported by Hammar. The coefficients of variation of the hypophysis and testes are greater in race X, while that for brain is less than the coefficients listed by Brown et al.

('26). The coefficient variation of 63.35% for the male thyroid as given by Brown is greater than any of the male coefficients of variation in race X or in any of the other groups of rabbits and also slightly greater than the coefficient of 62.66% for the ovaries in race X.

In race X, body length or a single dimensional measurement appears to be the least variable of these values. The brain, spinal cord and eyeballs are also very constant in weight. Of the remaining values, there is a second rather large group which includes the weights of the body, head, trunk, both extremities, integument, heart, musculature, skeleton, kidneys and the weight and length of the digestive tube, all with coefficients of variation ranging from 13 to 19% in the males and from 14 to 23% in the females. All of these organs are rather large and vital parts of the organism. The third group includes the liver, pancreas, spleen, gonads and other endocrine glands which seem to form a group with a range of considerably greater magnitude, or from 25 to 50% in the males and from 30 to 60% in the females. This last group is known to be more strongly influenced by cyclic, physiological and other environmental influences.

With due allowance for variations in numbers of specimens, age, and strains of rabbits used in the previous reports in the literature, all of the American rabbits seem to have much the same proportions in the relative weights of the internal organs.

SUMMARY

Three linear and 30 ponderal measurements were made on 50 male and 50 female rabbits of race X, a race of small adult body size. Body weight is 17% greater in the females and also more variable. In actual weight all of the organs are heavier in the females except the gonads, integument and harderian glands, 16 of the organs being statistically significant. Body length, the weights of the brain, eyeballs and spinal cord, the length of the digestive tube and the weight of

the head are the least variable measurements in both sexes and in the above order of increasing variability.

When expressed as percentages of net body weight, 5 of the organs (head, integument, heart, harderian glands and brain) constitute significantly larger percentages of net body weight in the males and 5 (trunk, musculature, fat, pancreas and hypophysis) are significantly larger in females. All but 5 (integument, skeleton, fat, digestive tube weight and kidneys) are less variable in the males.

Empirical formulae are given, whereby the weights or the linear dimensions may be estimated easily from either gross body weight or nose-anus length. The average percentage deviations of the calculated from the observed values are also given.

Comparison of these values with previous reports in the literature reveals an apparent cephalization in race X in so far as the important glands of internal secretion (hypophysis, thyroid, suprarenals and gonads) are concerned. This is of particular interest in view of the previous evidence of differences in regional growth between this and the New Zealand white races.

LITERATURE CITED

ALLANSON, M. 1932 The growth of the pituitary body in the female rabbit. J. Exp. Biol., *9:* 117–123.

BENSLEY, B. A. 1945 Practical anatomy of the rabbit. Seventh Ed., edited by E. Horne Craigie, Blakiston Co., Philadelphia. pp. 358.

BROWN, W. H. 1929 Constitutional variation and susceptibility to disease. Arch. Int. Med., *44:* 625–662.

BROWN, W. H., L. PEARCE AND C. M. VAN ALLEN 1926 Organ weights of normal rabbits. Second paper. J. Exp. Med., *43:* 733–741.

CASTLE, W. E. 1922 Genetic studies of rabbits and rats. Carnegie Inst. of Wash., no. 320.

———— 1931 Size inheritance in rabbits; the backcross to the large parent race. J. Exp. Zool., *60:* 325–338.

CRARY, D. D., AND P. B. SAWIN 1949 Morphogenetic studies in the rabbit. VI. Genetic factors influencing the ossification pattern of the limbs. Genetics, *34:* 508–523.

———— 1953 Some factors influencing the growth potential of the skin in the domestic rabbit. J. Exp. Zool., *124:* 31–62.

CRILE, G., AND D. P. QUIRING 1940 A record of the body weights and certain organ and gland weights of 3,690 animals. Ohio J. Science, *40:* 219–259.

CRUDEN, D. 1949 The computation of inbreeding coefficients. J. Heredity, *40:* 248–251.

DENZER, H. W. 1938 Masze und Gewichte zur vergleichenden Anatomie und Histologie der Vertebraten-Niere. Tabulae Biol., *15:* 260–332.

EATON, O. N. 1938 Weights and measurements of the parts and organs of mature inbred and crossbred guinea pigs. Am. J. Anat., *63:* 273–295.

GREENE, H. S. N. 1940 A dwarf mutation in the rabbit. J. Exp. Med., *71:* 839–856.

HAMMAR, J. A. 1932 Über Wachstum und Rüchgang, über Standardisierung, Individualisierung und bauliche Individualtypen in Laufe des normalen Postfötallebens. Konstitutionsanatomische Studien an Kaninchen. Zchtr. f. Mik.-Ant. Fors., *29:* 1–540.

HULL, I. B. 1947 Morphogenetic studies in the rabbit. IV. The inheritance of developmental patterns of rib ossification. J. Exp. Zool., *105:* 173–197.

JAFFE, F. A. 1951 A quantitative study of the islets of Langerhans in the rabbit. Anat. Rec., *111:* 109–122.

KIBLER, H. H., A. J. BERGMAN AND C. W. TURNER 1942 Pituitary weight in growing New Zealand white rabbits in relation to live weight. Endocrinology, *31:* 59–62.

———— 1943 Relation of certain endocrine glands to body weight in growing and mature New Zealand white rabbits. Endocrinology, *33:* 250–256.

LATIMER, H. B. 1936 Weights and linear measurements of the adult cat. Am. J. Anat., *58:* 329–347.

———— 1944 The prenatal growth of the cat. XV. The weight of the musculature in the fetal and in the adult cat. Growth, *8:* 205–219.

LATIMER, H. B., AND P. B. SAWIN 1955 The weight of the brain, of its parts and the weight and length of the spinal cord in the rabbit (race X). J. Comp. Neur., in press.

LEVINE, C. J., W. MANN, H. C. HODGE, I. ARIEL AND O. DU PONT 1941 Distribution of body weight in the organs and tissues of the rabbit. Proc. Soc. Exp. Biol. and Med., *47:* 318–321.

MACDOWELL, E. C 1914 Size inheritance in rabbits. Carnegie Inst. Wash., no. 196.

PECK, E. D., AND P. B. SAWIN 1950 Morphogenetic studies of the rabbit. VIII. Genetic variations in the sternum as determined by the interaction of general and of regionally specific growth factors. J. Exp. Zool., *114:* 335–357.

ROUS, P., AND O. H. ROBERTSON 1917 The normal fate of erythrocytes. I. The findings in healthy animals. J. Exp. Med., *25:* 651–663.

SAWIN, P. B. 1945 Morphogenetic studies of the rabbit. I. Regional specificity of hereditary factors affecting homoeotic variations in the axial skeleton. J. Exp. Zool., *100:* 301–329.

SAWIN, P. B. 1946a Morphogenetic studies of the rabbit. II. Evidence of regionally specific hereditary factors influencing the extent of the lumbar region. J. Morph., *78:* 1–26.

———— 1946b Morphogenetic studies of the rabbit. III. Skeletal variations resulting from the interaction of gene determined growth forces. Anat. Rec., *96:* 183–200.

SAWIN, P. B., AND D. D. CRARY 1951 Morphogenetic studies of the rabbit. X. Racial variations in the gall bladder. Anat. Rec., *110:* 573–590.

SCHMIDT, C. R., AND A. C. IVY 1937 The general function of the gall bladder. Do species lacking a gall bladder possess its functional equivalent? The bile and pigment output of various species of animals. J. Cell. and Comp. Physiol., *10:* 365–383.

SNEDECOR, G. W. 1938 Statistical Methods. Collegiate Press. Ames, Iowa, pp. 388.

TANNER, J. M., AND P. B. SAWIN 1953 Morphogenetic studies of the rabbit. XI. Genetic differences in the growth of the vertebral column and their relation to growth and development in man. J. Anat., *87:* 54–65.

SUCCINIC DEHYDROGENASE ACTIVITY IN THE PRE-NATAL AND POST-NATAL RAT HEART [1]

W. GREGORY COOPER [2]
Department of Anatomy, Columbia University, New York, New York

TEN FIGURES

INTRODUCTION

The fact that the atria and ventricles of the pre-natal and post-natal mammalian heart carry different functional loads has led numerous investigators to look for differences between the chambers other than the difference in the number of fibers contained within their walls. Thus, it has been established that the atria and ventricles differ in regard to fiber size, histological structure, intrinsic contraction and conduction rates and concentration of various chemical constituents. Little has been done in the way of an analysis of the enzymes present in the different chambers of the heart of the developing and mature mammalian heart.

The role of the succinoxidase complex of enzymes in the maintenance of the energy-producing apparatus for the contractile process of muscle has been established. The intracellular structures which provide the framework for the proper functioning of this complex of enzymes are now known to be the mitochondria (Hogeboom, Schneider and Pallade, '48; Harman, '50; Harman and Feigelson, '52c). Sippel ('54) studied succinoxidase activity in the embryonic rat ventricle with special reference to a possible correlation between the increase in succinoxidase activity and the development of cardiac function.

[1] Supported, in part, by grant H-1221-c, administered by W. M. Copenhaver, from the National Heart Institute, United States Public Health Service.

[2] Present address: c/o Department of Anatomy, University of Colorado, School of Medicine, Denver 20, Colorado.

The development of histochemical techniques utilizing tetrazolium salts (in the presence of sodium succinate) as indicators of succinic dehydrogenase activity has made it possible to carry out parallel studies in which both the level and the site of enzyme activity can be determined by similar methods. In this study a modification of the technique of Perry and Cumming ('52) was used to measure levels of activity of this enzyme in tissue homogenates of different regions of the heart at varying stages of development. The localization of this enzyme in tissue sections of the heart has been carried out according to the method of Rutenberg, Wolman and Seligman ('53). These parallel studies were undertaken to ascertain whether (1) there exists a difference in the intracellular succinic dehydrogenase activity of the cardiac muscle fibers of the atria and ventricles and (2) whether this differential enzyme concentration varies in pre- and post-natal life. The differences observed are discussed with regard to the possibility of the presence of other variations in the cytological components of atrial and ventricular cardiac muscle fibers.

MATERIALS AND METHODS

Portions of the atria and ventricles from fetal, newborn, young and adult rat hearts of a Long-Evans strain were analyzed by methods employing tetrazolium salts to visualize the sites and levels of succinic dehydrogenase activity.

In order to obtain a close estimate of the age of the fetuses and the approximate time of delivery of the newborn animals it was necessary to use timed matings. Day I was taken as beginning at midnight preceding the observation of sperm in the morning vaginal smear. Fetuses in the 20th and 21st day of development were used in the pre-natal phase of this study. The fetus was delivered with its membranes intact and placed immediately in warm Ringer's solution. During the subsequent removal of the heart the fetus was continuously submerged in the Ringer's solution and hence restrained from breathing. For the newborn determinations the litter was

delivered by Caeserian section at noon on the 22nd day of development (full term) and allowed to breathe for periods from 15 minutes to 12 hours after which they were then sacrificed. Newborn, young and adult rats were sacrificed with chloroform immediately before the determinations were carried out.

Tissue homogenates were analyzed by a modification of the method of Perry and Cumming ('52) utilizing triphenyl tetrazolium chloride as an indicator of succinic dehydrogenase activity. In each adult determination similar representative samples of the atria, right and left ventricles were homogenized with Berkshire sand in a buffered (pH 7.6) solution of 0.2 M. sodium succinate containing an excess of triphenyl tetrazolium chloride. For the embryonic and newborn determinations it was necessary to pool the respective samples taken from three animals in order to obtain a sufficient quantity of tissue. Incubations were carried out anaerobically for two hours at 37° C. The resultant formazan was extracted with acetone and dried with anhydrous sodium sulfate. The optical density of the solution was determined by a Coleman-Universal spectrophotometer at 485 mμ. Concentration of the reduced dye (formazan) was calculated by comparing the optical density of the solution being tested with a standard curve. Succinic dehydrogenase activity was expressed as micrograms of reduced tetrazolium per 100 mg of cardiac tissue. Control determinations were carried out on homogenates from which sodium succinate had been omitted from the incubation medium. In order to ascertain the effects of incubation time on the determination of concentration of formazan-reducible substances, a series of experiments were carried out whereby both atrial and ventricular homogenates were incubated for periods ranging from one-half to 4 hours.

Histochemical localization of succinic dehydrogenase activity in tissue sections was carried out according to the technique of Rutenberg, Wolman and Seligman ('53). Entire hearts (fetal and newborn) or blocks of cardiac tissue (adult) taken from the atrio-ventricular junction were removed from

the rats immediately after death and placed in chilled Ringer's solution. Sagittal sections cut at 10 μ and containing both atrial and ventricular tissue were affixed to cover slips and allowed to thaw momentarily. They were then placed in the incubating solution containing 0.2% blue tetrazolium, 0.2 M. sodium succinate plus magnesium, calcium, aluminum and bicarbonate ions in a phosphate buffer of pH 7.6. Anaerobic incubation was carried out for two hours at 37° C. Nitrogen gas was bubbled through the solution one hour prior to and continuously during the incubation in order to maintain anaerobic conditions. Sections were then washed briefly in distilled water, fixed in 10% neutral buffered formalin and mounted in glychrogel. Control preparations were obtained by incubating sections in a solution from which sodium succinate had been omitted. Neotetrazolium chloride was used as the indicator dye in the latter phase of this study.

OBSERVATIONS

The results obtained in determining the levels of succinic dehydrogenase activity in different parts of the heart at various stages of development both by the analysis of tissue homogenates and localization of activity in tissue sections are in close agreement. The activity of this enzyme as expressed by the reduction of the tetrazolium salt in the ventricles is of a higher level than that found in the atria. The ratio of ventricular to atrial succinic dehydrogenase activity (V/A ratio) increases with the age of the animal.

Homogenate studies

The variation of succinic dehydrogenase activity existing in embryonic, newborn and adult rat hearts is shown in figure 1. In all age groups the differential concentration of the enzyme in the atrium is lower than that in right and left ventricles. This difference becomes statistically significant from the 6th hour of post-natal life through adulthood.

A relatively constant level of enzyme activity is maintained throughout the latter part of pre-natal life covered in this study. Mean values for both atrial and ventricular succinic dehydrogenase in this period are given in table 1. The ratio of ventricular to atrial succinic dehydrogenase (V/A ratio) is 1.4. Since it was found that the ventricular succinic dehydrogenase concentration rises within the first day of

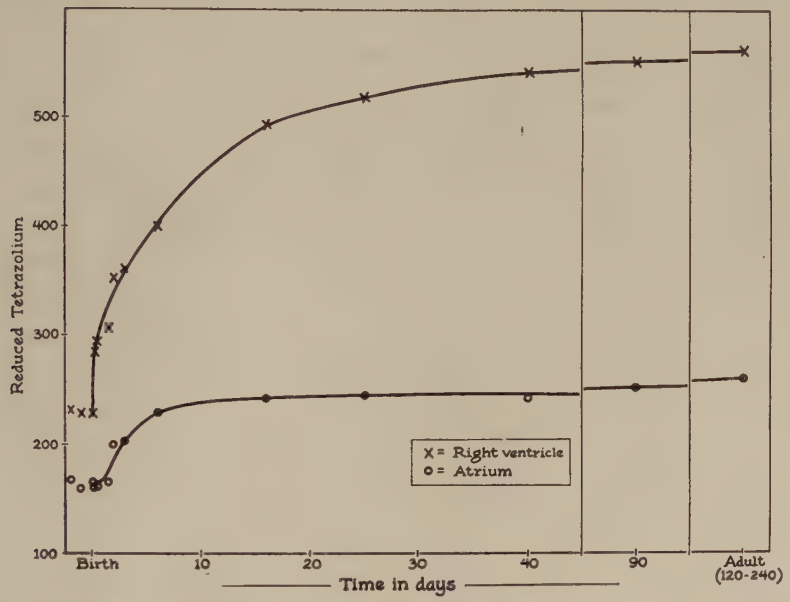

Fig. 1 Reduction of tetrazolium by pre- and post-natal cardiac tissue in a sodium succinate substrate at pH 7.6. Concentration of reduced tetrazolium expressed in micrograms per 100 milligrams of cardiac tissue per two hours of incubation.

post-natal life it was necessary to deliver the full-term litter by Caesarian section in order to definitely establish the exact age of the newborn. By so doing it was found that the first alteration of succinic dehydrogenase activity takes place about 6 hours after birth (table 1). At this time the ventricular concentration rises while the atrial concentration remains relatively constant. This accounts for the elevation of the R.V./A. ratio to 1.7 and the L.V./A. ratio to 2.0. Succinic

dehydrogenase activity in both ventricle and atrium increases gradually from 6 to 36 hours of post-natal life with the V/A ratio changing from 1.7 to 1.8 for the right ventricle and 2.0 to 2.1 in the left ventricle. Between the 36th and the 48th hour there is an increase in both atrial and ventricular succinic dehydrogenase activity. Although the absolute values for both chambers increase at this time, the proportion of

TABLE 1

Succinic dehydrogenase activity in the pre-natal and early post-natal rat heart

AGE IN HOURS	BODY WT. (GM)	NO. DETERM.[1]	MEAN ATRIAL CONCENT.[2]	MEAN RIGHT VENTRICULAR CONCENT.	MEAN LEFT VENTRICULAR CONCENT.	R.V./A. RATIO	L.V./A. RATIO
Pre-natal							
—48	..	4	168 ± 24	233 ± 23	236 ± 13	1.4	1.4
—24	..	8	160 ± 14	229 ± 16	238 ± 11	1.4	1.5
Post-natal							
1	5	5	169 ± 2	228 ± 8	230 ± 12	1.4	1.4
2	5	2	159 ± 2	223 ± 7	235 ± 15	1.4	1.5
3	5	2	166 ± 2	234 ± 20	..	1.4	..
6	6	3	163 ± 6	285 ± 5	334 ± 19	1.7	2.0
12	6	3	163 ± 7	296 ± 2	350 ± 10	1.8	2.1
36	7	4	166 ± 11	308 ± 17	355 ± 22	1.8	2.1
48	8	3	200 ± 25	353 ± 18	..	1.8	..
72	8	4	203 ± 3	361 ± 8	429 ± 8	1.8	2.1

[1] Each determination represents the pooling of cardiac tissue from three littermates.

[2] Concentrations expressed in micrograms of reduced tetrazolium/100 mg of cardiac tissue ± standard error of the mean, calculated for small samples.

ventricular to atrial succinic dehydrogenase concentration remains relatively constant as expressed by the R.V./A. ratio of 1.8 and L.V./A. ratio of 2.1 for this period. Table 2 presents the data for young rats where it can be seen that the ventricular succinic dehydrogenase gradually increases with age. The atrial succinic dehydrogenase during this period is also increasing but at a slower rate hence the reason for the increasing V/A ratio.

From three days to 6 days of post-natal life the atrial succinic dehydrogenase activity increases fairly rapidly, then levels off somewhat, and subsequently increases gradually until the adult level is reached (fig. 1). The ventricular concentration of the enzyme increases rapidly from birth to day 16 of post-natal life attaining the adult level by a more gradual increase after day 16. The rate of increase in the ventricular concentration is always of a higher magnitude than that of the atrium. The corresponding V/A ratios for this

TABLE 2

Succinic dehydrogenase activity in the young and adult rat heart

AGE IN DAYS	BODY WT. (GM)	NO. OF ANIMALS	MEAN ATRIAL CONCENT.[1]	MEAN RIGHT VENTRICULAR CONCENT.	MEAN LEFT VENTRICULAR CONCENT.	R.V./A. RATIO	L.V./A. RATIO
6	9	6	229 ± 16	400 ± 21	..	1.8	..
16	30	3	243 ± 20	494 ± 22	..	2.0	..
25	40	4	245 ± 6	517 ± 28	559 ± 38	2.1	2.3
40	70	3	242 ± 14	541 ± 18	572 ± 13	2.2	2.4
90	159	3	252 ± 16	552 ± 26	..	2.2	..
150	210	6	256 ± 14	561 ± 13	606 ± 24	2.2	2.4
240	245	4	264 ± 16	564 ± 30	607 ± 25	2.2	2.4
300	250	4	264 ± 13	622 ± 25	..	2.4	..
420	311	2	279 ± 11	655 ± 16	713 ± 13	2.4	2.6

[1] Concentrations expressed in micrograms of tetrazolium/100 mg of cardiac tissue ± standard error of the mean, calculated for small samples.

period of post-natal life are expressed in table 2. Here it can be seen that there is little change in the R.V./A. ratio from 6 hours to 6 days after birth due to the fact that both atrial and ventricular succinic dehydrogenase levels are increasing at a similar rate. As noted above the atrial concentration seems to peak at day 6, but the ventricular level continues to increase at a higher rate in attaining its adult concentration. This explains the increase in the R.V./A. ratio from 1.8 in the 6-day-old animal to 2.4 in the 14 month-old animal.

Portions of the left ventricle during similar stages of development were analyzed for succinic dehydrogenase ac-

tivity. In the pre-natal stages studied there was little difference between the values obtained for right or left ventricular samples (table 1). In the post-natal studies the left ventricular values were consistently but not significantly higher than those for the right ventricle. The relationship between the succinic dehydrogenase activity in the left ventricle and the atrium can be seen by noting the increase with

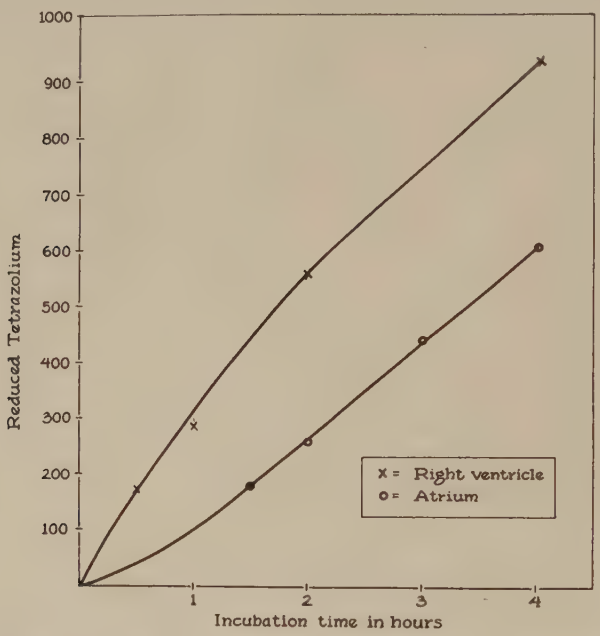

Fig. 2 Effect of incubation time on the reduction of tetrazolium by cardiac tissue in a sodium succinate substrate at pH 7.6. Concentration of reduced tetrazolium expressed in microgram per 100 mg of cardiac tissue.

time of the L.V./A. ratio in table 2. Explanation for the increasing ratio at different ages is essentially the same as that given for the R.V./A. ratio.

In the preceding determinations the concentration of reduced tetrazolium was used as an index of succinic dehydrogenase activity. A series of experiments was carried out in which the concentrations of tetrazolium reduced by both atrial and ventricular tissue homogenates were deter-

mined after periods of incubation ranging from one-half to 4 hours. The results indicate that the concentration of reduced tetrazolium (succinic dehydrogenase activity) increases as a function of incubation time (fig. 2). All comparisons of atrium and ventricle were done on tissue homogenates which had been incubated for a two hour period.

Histochemical localization in tissue sections

Succinic dehydrogenase activity was revealed in tissue sections by the presence of dark blue granules within the cardiac muscle fibers. These blue granules represent the completely reduced form (diformazan) of the blue tetrazolium salt. In addition to the granules there was noted a diffuse red color in most fibers which probably represents the partially reduced form of the dye (monoformazan).

A comparison of a low power view of a section of a fetal heart with that of the adult shows the great difference which occurs in the ratio of ventricular to atrial succinic dehydrogenase in these two age groups. In the fetal heart (fig. 3) there is only a slight difference in the succinic dehydrogenase activity of the cardiac muscle fibers in the atrium and ventricle, with the greatest number of blue granules present in the ventricular fibers. The higher enzyme content of the adult ventricle contrasted to that of the atrium is well shown in figure 5 where the abundance of the diformazan granules can readily be observed within the ventricular fibers. In this figure the connective tissue separating the walls of the two chambers is devoid of any succinic dehydrogenase activity. Examination of similar sections taken from the atrio-ventricular junction of the hearts of animals from one day to 4 months of age showed a gradual increase in the histologically visable V/A ratio of succinic dehydrogenase activity. Except for these differences in the relative concentrations of the two chambers, the intracellular arrangement of the diformazan granules was similar in all age groups studied.

The intracellular distribution of these granules can be studied in figures 7–10. Generally speaking the granules of dye were of various sizes and shapes, often appearing clumped together. The most consistent arrangement of the granules is shown in figure 9 where they can be seen to be arranged in rows lying within the sarcoplasm between the unstained myofibrils. Very frequently the particles of dye took the form of rod-shaped structures lying between the myofibrils. Since the ventricular fibers contained the greater concentration of the formazan there was a marked tendency for these granules to clump together. This was not observed to the same extent in the atrial fibers due to their relatively low concentration of the enzyme. Although some diffuse red staining (monoformazan) was noted in the ventricular fibers, this was generally more pronounced in the atrium. In some instances there was a tendency for the diformazan granules to be more numerous in the portion of the sarcoplasm surrounding the nucleus. The arrangement of the diformazan granules on the isotropic discs of the muscle fiber as described by Rutenberg et al. ('53) was not observed consistently.

In many of the hearts studied there appeared to be a site of high enzyme activity located within the ventricular myocardium surrounding a branch of the coronary artery near the right atrio-ventricular junction. The significance of this is not known.

Connective tissue and smooth muscle located in the endocardium, epicardium and blood vessels gave a negative reaction as shown in figure 5.

Sections incubated aerobically gave a less intense reaction than those incubated under anaerobic conditions. Control sections incubated in a substrate devoid of sodium succinate or tetrazolium salt were negative. The omission of activating ions from the substrate solution brought about a decrease in succinic dehydrogenase activity of the tissue sections.

In some of the latter phases of this study neotetrazolium chloride was used as an indicator of succinic dehydrogenase

activity. Results obtained were identical to those obtained with blue tetrazolium chloride as the indicator.

DISCUSSION

Chemical analyses of different parts of the heart have been carried out on amphibians, birds and mammals by numerous investigators in an attempt to explain some of the functional differences observed between the various regions.

Davies, Francis and Stoner ('47) have shown that in the rabbit, the ventricles contain a greater concentration of nucleotides than do the atria, with the left ventricle containing more than the right ventricle. Similarly, Kováts ('49) analyzed the atria, right and left ventricles for their myosin content and found that the concentration of this substance in different parts of the heart was proportional to their mechanical activity. The left ventricle contained slightly more than the right and much more than the atrium. Both these findings tend to indicate that the increased functional requirements which the ventricle has been called upon to fulfill has been accompanied by a corresponding increase in the essential metabolites necessary to maintain its added responsibility.

It seems logical therefore that the enzyme systems present within the respective cardiac muscle fibers should also show either qualitative or quantitative differences. Since succinic dehydrogenase is one of the key enzymes involved in the metabolism of muscle fibers it was chosen as the enzyme to be studied in this series of experiments.

The results indicate that there exists a significant difference between the succinic dehydrogenase concentration of the cardiac muscle fibers of the atria and ventricles with the highest concentration being present in the left ventricle. This difference cannot be explained as being due merely to the difference in the number of fibers within each chamber since the localization of the enzyme in tissue sections has shown that the individual ventricular fibers contain more succinic

dehydrogenase than those of the atrium. Since the ventricular fibers are called upon to carry out more work than are those of the atrium, it is suggested that this difference in functional requirements is paralleled with the observed difference in succinic dehydrogenase concentration. With the increased post-natal growth of the animal and subsequent increase in functional requirements for the heart, the enzyme systems involved in maintaining the efficiency of contraction should also increase in concentration. Both of these requisites hold true for succinic dehydrogenase as the present study indicates.

Moog ('47) in a study of the adenylpyrophosphatase content of pre- and post-natal chick hearts points out that, in the case of the chick heart, the enzyme accumulation is not dependent merely on tissue increase, but that "the basis for the increase of the enzyme must be sought in differentiation and in function rather than in growth." The present study supports Moog's conclusion that enzyme accumulation is not dependent merely on tissue increase, but it does not attempt to answer the question whether cardiac succinic dehydrogenase accumulates rapidly during embryonic differentiation. Additional pre-natal stages are now being studied and will be reported in a future survey of enzyme systems in the embryonic rat heart.

Sippel ('54) in his study of succinoxidase activity in the ventricle of the developing chick and rat heart found a close parallel between succinoxidase activity and the development of "cardiac effectiveness". His results indicate that succinic dehydrogenase activity of the rat ventricle increases in two phases during pre-natal development. The attainment of the adult level of enzyme activity is then accomplished by a more gradual increase beginning during late fetal life (day 18). The present study differs from Sippel's findings in that our results indicate a rise in the succinic dehydrogenase activity with the onset of post-natal life. Subsequent increase in enzyme activity follows a more gradual course from 8 days of post-natal life until the adult level is attained (fig. 1).

The elevation of succinic dehydrogenase activity in both atria and ventricles soon after birth is of particular interest. With the advent of post-natal life and its establishment of a new type of circulation there is an additional functional load placed upon the heart. In order to maintain the proper functioning of the contractile apparatus of the respective chambers there must be need for a corresponding increase in concentration of those enzymes involved in the turnover of the citric acid cycle. The fact that the early post-natal rise in ventricular concentration of succinic dehydrogenase is more pronounced than the atrial level is understandable since the work done by the ventricle is of a greater magnitude than that required for the atrium.

Potter, Schneider and Liebl ('45) in their study of succinic dehydrogenase activity in the brain of the fetal and newborn rat noted that there was a close correlation in the concentration of succinic dehydrogenase and the neural functioning of the animal. Throughout the last three days of fetal life and the first 6 days of post-natal life the succinic dehydrogenase concentration of the brain remained constant. After this time there was a marked increase in concentration of the enzyme which was closely correlated with the increased neural functioning of the animal. They concluded from their study that during the period of increased functional load and increased differentiation there is an increase in both the energy-yielding (respiratory type) and energy-depleting (adenosine triphosphatase) enzymes.

The localization of succinic dehydrogenase in cardiac muscle fibers has been described by Padykula ('52), Rutenberg, Wolman and Seligman ('53) and Malaty and Bourne ('53). Our findings are in close agreement as to the intracellular localization of the enzyme. We have observed numerous areas of formazan deposition which resemble mitochondria in size and shape (figure 9). However, the abundance of the enzyme within the fibers in addition to the excess of the tetrazolium frequently produces amorphous granules larger

than mitochondria. These probably represent the accumulation of formazan crystals on the surface of the mitochondria.

Padykula ('52) carried out a comprehensive study of the succinic dehydrogenase activity in sections of many tissues of the rat. Her observations on the intracellular distribution of the enzyme in cardiac muscle fibers were similar to the findings reported here, but she made no mention of a difference between the chambers. In her comprehensive survey of this oxidative enxyme she concluded that it was found in highest concentration within those portions of tissues and organs which possess high metabolic activity. The results of her analysis of skeletal muscle are interesting in that she found that the small skeletal muscle fibers contained a greater concentration of succinic dehydrogenase than did those of a larger diameter. If it is possible to draw an analogy between skeletal muscle and cardiac muscle in comparing fiber size with succinic dehydrogenase activity then the differences between the atrial fibers and ventricular fibers observed in the present study are similar to those differences observed by Padykula for skeletal muscle fibers of different size. The ventricular fibers which are of a smaller diameter contain more succinic dehydrogenase than do the larger atrial fibers.

Shelton and Schneider ('52) studied the intracellular distribution of succinic dehydrogenase utilizing tetrazolium salts in the presence of sodium succinate to ascertain the localization of the enzyme in fractions of cells obtained by centrifugation. In their study they found that isolated mitochondria were capable of reducing neotetrazolium to its formazan while nuclear and supernatant fractions could produce only a small quantity of formazan and only after prolonged incubation. They concluded that the precipitation of formazan took place in the vicinity of the mitochondria.

In a series of studies on mitochondria in cardiac muscle Harman and Feigelson ('52a,b,c,) have described the morphology and enzyme relationships of these important cytoplasmic structures. Their description of the localization of the rod-shaped or beaded mitochondria between the myofibrils

and lying in parallel rows coincides with the intracellular localization of succinic dehydrogenase activity observed in this study. They suggest that the intimate relation of the mitochondria to the myofibrils indicates an active contribution to the contractile process.

Schneider et al. ('53) in a study of succinic dehydrogenase activity in relation to mitochondria in normal and pathological livers have shown that the activity of this enzyme varies directly with the number of mitochondria present.

Shelton ('53) offered an interesting correlation when she stated that "since evidence to date indicates that the succinoxidase activity per mitochondrion is constant, one is tempted to say that those cells whose function demands a greater output of energy should be endowed with a large number of mitochondria."

Whether or not the increase in cardiac succinic dehydrogenase reported here is due to an actual increase in number of mitochondria or whether it is due merely to an increase in enzyme activity per mitochondrion remains to be established. It is difficult to visualize that the sudden increase in enzyme activity which occcurs over such a short period of time following birth could be the result of an increase in number of mitochondria alone. It seems logical that both the activity per mitochondrion as well as the total number of mitochondria per fiber may be increased to fulfill the increased functional requirements of the heart. Studies are in progress to ascertain whether the differential concentration of succinic dehydrogenase observed in atrial and ventricular fibers is paralleled by differences in cytochrome oxidase concentration and number of mitochondria present within the individual fibers during different stages of development.

SUMMARY

1. Portions of the ventricles and atria from fetal, newborn and adult rat hearts were analyzed by methods employing tetrazolium salts to visualize sites and levels of succinic dehydrogenase activity.

2. In all age groups studied the ventricles were found to have a higher concentration of succinic dehydrogenase than the atria in both tissue homogenates and tissue sections.

3. The ratio of ventricular to atrial succinic dehydrogenase increased with the age of the animal.

4. The correlation between the intracellular localization of this enzyme in the different chambers of the heart at different ages is discussed with respect to its possible association with mitochondrial number and function.

LITERATURE CITED

DAVIES, F., E. T. B. FRANCIS AND H. B. STONER 1947 The distribution of nucleotide, phosphocreatine and glycogen in the heart. J. Physiol., *106:* 154–166.

HARMAN, J. W. 1950 Studies on mitochondria. I. The association of cyclophorase with mitochondria. Exptl. Cell. Res., *1:* 382–393.

HARMAN, J. W., AND M. FEIGELSON 1952a Studies on mitochondria. III. The relationship of structure and function of mitochondria from heart muscle. Exptl. Cell Res., *3:* 47–58.

———— 1952b Studies on mitochondria. IV. The cytological localization of mitochondria in heart muscle. Exptl. Cell Res., *3:* 58–64.

———— 1952c Studies on mitochondria. V. The relationship of structure and oxidative phosphorylation in mitochondria of heart muscle. Exptl. Cell Res., *3:* 509–525.

HOGEBOOM, G. M., W. C. SCHNEIDER AND G. E. PALLADE 1948 Cytochemical studies of mammalian tissues. I. Isolation of intact mitochondria from rat liver; some biochemical properties of mitochondria and submicroscopic particulate material. J. Biol. Chem., *172:* 619–636.

KOVÁTS, J. 1949 Myosin and actomyosin content of the heart-muscle. Nature, *163:* 606–607.

MALATY, H. A., AND G. H. BOURNE 1953 Histochemistry of succinic dehydrogenase. Nature, *171:* 295–297.

MOOG, F. 1947 Adenylpyrophosphatase in brain, liver, heart and muscle of chick embryos and hatched chicks. J. Exp. Zool., *105:* 209–220.

PADYKULA, H. A. 1952 The localization of succinic dehydrogenase in tissue sections of the rat. Am. J. Anat., *91:* 107–145.

PERRY, W. F., AND G. R. CUMMING 1952 Adrenal succinic dehydrogenase activity determined by the reduction of tetrazolium salt by adrenal homogenate. Endocrin., *50:* 385–387.

POTTER, V. R., W. C. SCHNEIDER AND G. J. LIEBL 1945 Enzyme changes during growth and differentiation in the tissues of the newborn rat. Cancer Res., *5:* 21–24.

RUTENBERG, A. M., M. WOLMAN AND A. M. SELIGMAN 1953 Comparative distribution of succinic dehydrogenase in six mammals and modification in the histochemical technique. J. Histo. and Cyto., *1:* 66–81.

SCHNEIDER, W. C., G. H. HOGEBOOM, E. SHELTON AND M. J. STRIEBICH 1953 Enzymatic and chemical studies on the livers and liver mitochondria of rats fed 2-methyl- or 3'-methyl-4-dimethylaminoazobenzene. Cancer Res., *13:* 285–288.

SHELTON, E. 1953 In "Discussion" of symposium: The structure and biochemistry of mitochondria. J. Histo. and Cyto., *1:* 274.

SHELTON, E., AND W. C. SCHNEIDER 1952 On the usefulness of tetrazolium salts as histochemical indicators of dehydrogenase activity. Anat. Rec., *112:* 61–81.

SIPPEL, T. O. 1954 The growth of succinoxidase activity in the hearts of rat and chick embryos. J. Exp. Zool., *126:* 205–222.

PLATE 1

EXPLANATION OF FIGURES

All figures are from fresh frozen sections cut at 10 μ and incubated anaerobically in a sodium succinate substrate at pH 7.6 with blue tetrazolium as the indicator of succinic dehydrogenase activity.

3 Fetal rat heart (— 1 day). Only a slight difference is observable between the concentration of diformazan granules in the atrium (A) and ventricle (V). × 200.

4 Early post-natal heart (two days old). Ventricle (V) contains a higher concentration of diformazan granules than does the atrium (A). × 166.

5 Adult rat heart. Section taken through atrio-ventricular junction. Intense succinic dehydrogenase activity of ventricle (V) indicated by large concentration of diformazan granules. Atrium (A) contains fewer granules. Note negative reaction of connective tissue separating the atrium and ventricle. × 166.

6 Adult rat heart. High power view of section taken through atrio-ventricular junction. Cardiac muscle fibers in both chambers are oriented longitudinally. Atrial fibers (A) contain fewer diformazan granules which tend to be of a finer calibre than those found in the ventricle. Ventricular fibers (V) contain a much greater number of diformazan granules which vary from a granular form to the more prevalent rod-shaped structures. Connective tissue between atrium and ventricle gives a negative reaction. × 980.

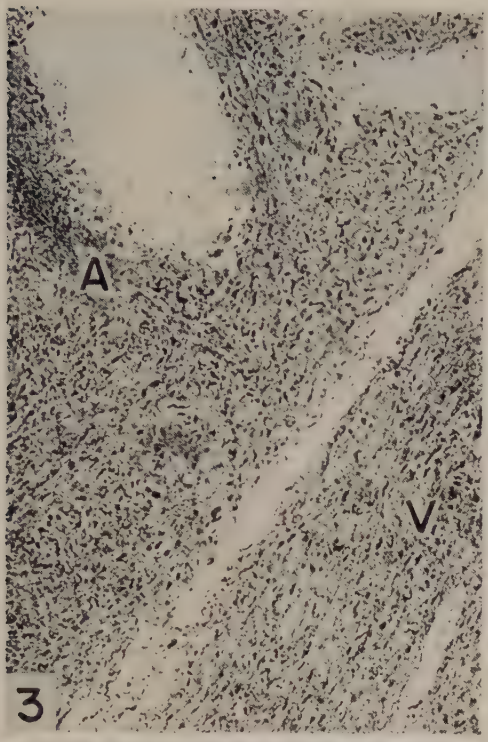
A
V
3

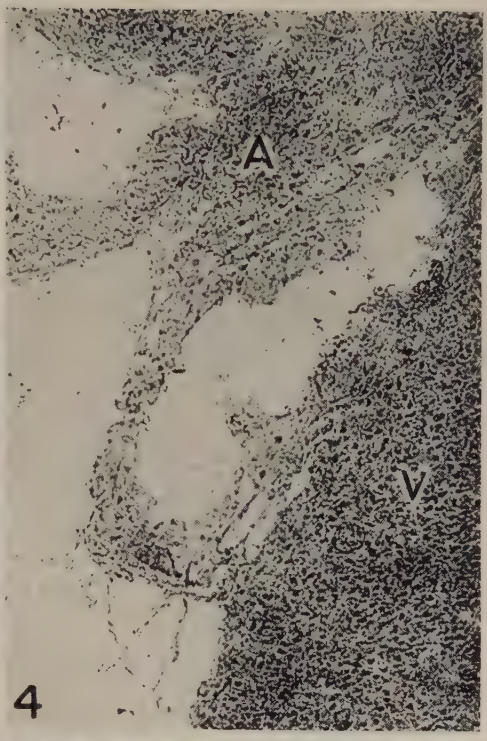
A
V
4

A
V
5

A
V
6

PLATE 2

EXPLANATION OF FIGURES

7 Adult atrium. Fibers running longitudinally from above to below. Diformazan granules are finer and less numerous here than in ventricle (fig. 8). Note longitudinal orientation of granules. × 980.

8 Adult ventricle. Longitudinal section of fibers. Much higher concentration of diformazan present here than in atrial fibers. Rod-shaped forms are more numerous. There is a greater tendency for the diformazan particles to clump due to the high concentration of the enzyme. × 980.

9 Adult ventricle. Note preponderance of rod-shaped form of diformazan granules. Longitudinal arrangement of these granules within the fibers and parallel to the myofibrils is apparent. × 980.

10 Adult ventricle. Enlarged to show intracellular orientation of diformazan granules in a longitudinal fashion parallel to unstained myofibrils. × 2550.

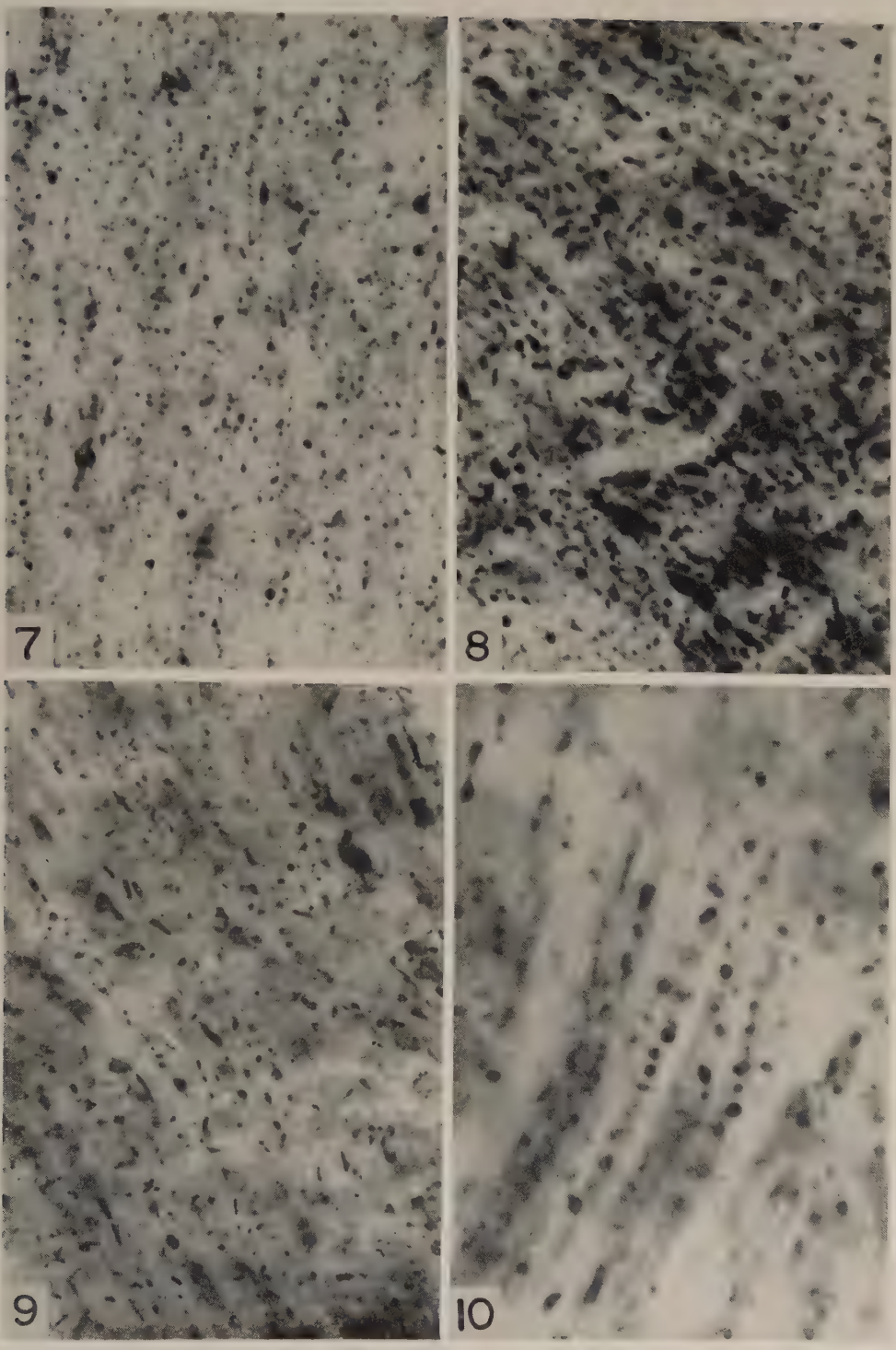
7
8
9
10

CECAL VILLI IN DICROSTONYX TORQUATUS (RODENTIA: MICROTINAE)

MARIETTA VOGE AND HOWARD A. BERN

Department of Infectious Diseases, School of Medicine, University of California, Los Angeles, and Department of Zoology, University of California, Berkeley

FOUR FIGURES

Examination of the ceca of 6 *Dicrostonyx torquatus* collected at Tulugak Lake, Brooks Range, Alaska, revealed villi similar to those described by Voge and Bern ('49) from the Red Tree Mouse, *Phenacomys longicaudus*. In view of the rare occurrence of cecal villi in mammals, further description of such structures in a genus related to *Phenacomys* seems desirable.

Intestinal tracts were fixed in Bouin's fluid, formalin, and acetone. Whole mounts of villi were stained with dilute Ehrlich's hematoxylin. Routine histologic sections were stained with Ehrlich's hematoxylin and eosin. Acetone-fixed material was prepared for the demonstration of alkaline phosphatase according to the Barger ('47) modification of the Gomori method. All measurements were obtained from fixed material.

DESCRIPTION

As in *Phenacomys longicaudus,* the entire inside surface of the cecal wall of *Dicrostonyx torquatus* bears long, filamentous villi (fig. 1) which extend into the first coil of the postcecal spiral. The length of these villi ranges from 4.7 mm to 14 mm; their width (taken approximately halfway between tip and base) ranges from 0.21 mm to 0.62 mm with the distal ends somewhat narrower. Some of the villi in *Dicrostonyx* differ from those in *Phenacomys* in the possession of side

branches (fig. 3). Branching was observed in about 10% of the villi and may occur anywhere along the villus except at the proximal and distal ends. In our material, the number of branches varies from one to 4 per villus. The branches are always shorter than the villus from which they originate. They may appear as small buds on the surface of the villi, or they may be one-third as long as the main stem. Their width is frequently less than that of the main stem.

The villi are covered by a tall columnar epithelium of the same type as lines the cecal wall. Both the villi and the cecal wall are equipped with acinar glands similar to those found in *Phenacomys*. The internal structure of the villi includes considerable smooth muscle, arterioles, venules, capillaries and lymph vessels. An occasional cecal villus in *Dicrostonyx* is rusty red in color; rarely a "giant" villus may be observed.

The lining and villus epithelium of the small intestine, the lining and villus epithelium (fig. 4) of the cecum, and the lining epithelium of the colon are all alkaline phosphatase-positive. In all the surface epithelia, the reaction is most intense in the apical ends of the cells. The acinar glands of the cecal wall and of the villi also show considerable cytoplasmic phosphatase activity, considerably more than do the glands of the cecal villi in *Phenacomys*.

DISCUSSION

To date, cecal villi have been reported from three genera of mammals. Two of these *(Phenacomys* and *Dicrostonyx)* are rodents belonging to the subfamily Microtinae. The third genus, *Ochotona,* (Voge and Bern, '52) is a lagomorph. The cecal villi in these mammals differ to some extent in general appearance and structure. In external and internal morphology, the villi of *Dicrostonyx* and *Phenacomys* are very similar; the villi of *Dicrostonyx,* however, are on the average longer and wider than those of *Phenacomys*. In addition, branching villi were not observed in *Phenacomys*. Judging from published reports, branching of intestinal villi is rarely

seen. Tullberg (1899) reported branched villi in the cecum of the lagomorph, *Lagomys alpinus* (=*Ochotona*?), without adding any precise description. Lobes occur occasionally on the tips of human duodenal villi (Maximow and Bloom, '52). The leaf-like cecal villi in *Ochotona* (fig. 2) are confined to the "spiral valve." They are much shorter, wider and flatter than those seen in the two microtines. However, their basic microanatomic organization is similar to that of the cecal villi from the two rodents.

TABLE 1

Alkaline phosphatase activity in various regions of the intestinal tract

	PHENACOMYS	DICROSTONYX	OCHOTONA
Small intestine: villi	+	+	+
Cecum: lining epithelium	+	+	—
Cecum: villus epithelium	+	+	—
Cecum: villus glands	±	+	—
Colon: lining epithelium	—	+	—
Colon: glands	—	—	—

Table 1 illustrates the differences in alkaline phosphatase activity observed in the three mammals under discussion. Contrary to the situation in *Phenacomys* and *Dicrostonyx,* the epithelium, as well as the glands, of the cecal villi in *Ochotona* is negative for alkaline phosphatase activity. This enzyme activity is present in surface epithelia which have absorptive functions and is presumably related to transport mechanisms (Moog, '46). Hence, it is suggested that the cecal villi in *Ochotona* do not have the same function as do the villi in the cecum of microtines.

The taxonomic status of *Phenacomys* and *Dicrostonyx* deserves some attention herein. Although both genera belong to the same subfamily, Microtinae, they are placed in dif-

ferent tribes (Miller, 1896) because of differences in tooth and external structure. However, of 7 genera of the tribe Microtini examined, *Phenacomys* is the only one possessing cecal villi. Similarly, of three genera of the tribe Lemmini examined, *Dicrostonyx* is the only one with cecal villi.

The infrequent occurrence of cecal villi in mammals generally, and their limited occurrence in microtines specifically, suggest the need for re-evaluating taxonomic criteria such as differences in tooth structure where other structural similarities exist. Although it is difficult to interpret the significance of specialized features of the soft parts in terms of evolutionary relationships, it certainly seems desirable to consider such characters in addition to those commonly used in the differentiation of species or groups of species. With regard to the two rodent genera discussed herein, the evidence derived from tooth and external morphology conflicts with that obtained from the study of the digestive tract. Whether or not structures such as cecal villi are the result of secondary adaptation and convergence, rather than indicative of a primitive relationship between the two genera, remains undetermined.

SUMMARY

Cecal villi are described from the microtine *Dicrostonyx torquatus*. They resemble those previously described from *Phenacomys* in basic structure and in epithelial alkaline phosphatase activity, indicative of an absorptive function. They differ from the latter in their larger size and in the occasional occurrence of branching. The cecal villi from the two microtines are also compared with those from the lagomorph *Ochotona*.

ACKNOWLEDGMENTS

We wish to thank Dr. Robert Rausch, Arctic Health Research Center, Anchorage, Alaska, for sending us specimens of *Dicrostonyx;* and Mr. Zane Price and Mr. Victor Duran for preparing the photographs included herein.

LITERATURE CITED

BARGER, J. D. 1947 A simplification of the technic for demonstrating alkaline and acid phosphatase in tissue. Arch. Path., *43:* 620–623.

MAXIMOW, A. A., AND W. BLOOM 1952 A Textbook of Histology. W. B. Saunders Co., Philadelphia and London. Sixth Ed. p. 373.

MILLER, G. S. 1896 The genera and subgenera of voles and lemmings. U. S. Dept. Agriculture, N. A. Fauna no. 12, pp. 1–85.

MOOG, F. 1946 The physiological significance of the phosphomonoesterases. Biol. Revs., *21:* 41–59.

TULLBERG, T. 1899 Ueber das System der Nagethiere. Eine phylogenetische Studie. Nova Acta Soc. Sci. Upsal., Ser. III, *18:* 1–514.

VOGE, M., AND H. A. BERN 1949 Cecal villi in the red tree mouse, *Phenacomys longicaudus.* Anat. Rec., *104:* 477–485.

VOGE, M., AND H. A. BERN 1952 Cecal villi in a Pika (*Ochotona princeps*). J. Mammal., *33:* 104–105.

PLATE 1

EXPLANATION OF FIGURES

1 Portion of internal surface of cecum of *Dicrostonyx* showing numerous thread-like villi. × 3 (approx.).

2 Portion of internal surface of cecum of *Ochotona* showing leaf-like villi on "spiral valve." × 2.5 (approx.).

3 Whole mount of branching villus from cecum of *Dicrostonyx*. Hematoxylin. × 32.

4 Transverse section of villus from cecum of *Dicrostonyx* showing alkaline phosphatase activity of surface epithelium and of acinar gland cytoplasm. Nuclei are lightly stained with hematoxylin. × 260.

1

2

3

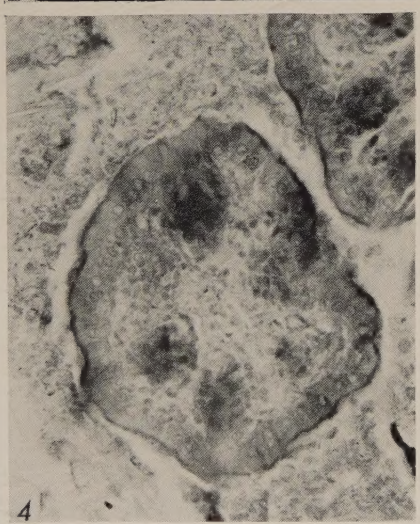
4